

Role of the Hedgehog receptor Patched1 in the development and function of T lymphocytes

Dissertation

for the award of the degree
“Doctor rerum naturalium”
of the Georg-August-University Göttingen

within the doctoral program “Molecular Biology of Cells”
of the Georg-August University School of Science (GAUSS)

submitted by
Kai-David Michel

from
Bad Kreuznach, Germany

Göttingen, 2013

Thesis Committee

Prof. Dr. Holger Reichardt (First Referee)

Department of Cellular and Molecular Immunology
University of Göttingen Medical School

Prof. Dr. Heidi Hahn (Second Referee)

Institute of Human Genetics
University of Göttingen Medical School

Prof. Dr. Matthias Dobbelstein

Department of Molecular Oncology
University of Göttingen Medical School

Additional members of the Examination Board

Prof. Dr. Frauke Alves

Department of Hematology and Oncology
University of Göttingen Medical School

Prof. Dr. Hubertus Jarry

Department of Clinical and Experimental Endocrinology
University of Göttingen Medical School

Prof. Dr. Lutz Walter

Department of Primate Genetics
German Primate Center, Göttingen

Day of oral examination: June 5th 2013

Declaration

The work presented in this thesis represents original work carried out by the author and has not been submitted in any form to any other university. It was written independently and with no other sources and aids than quoted.

June 2013
Göttingen, Germany

Kai-David Michel

Parts of this work have been published in the following article:

Michel KD, Uhmman A, Dressel R, van den Brandt J, Hahn H, et al. (2013)
The Hedgehog Receptor Patched1 in T Cells Is Dispensable for Adaptive Immunity in
Mice. PLoS ONE 8(4): e61034.

1	Introduction	1
1.1	T lymphocytes	1
1.1.1	The immune system	1
1.1.2	Thymocyte development	2
1.1.3	T cell activation	3
1.1.4	T cell subtypes	5
1.1.4.1	T Helper cells	5
1.1.4.2	Regulatory T cells	7
1.1.4.3	Cytotoxic T cells	7
1.2	The hedgehog signalling pathway	8
1.2.1	Basic concepts	8
1.2.2	Major pathway components	9
1.2.3	Signal transduction	12
1.2.3.1	Canonical signalling	13
1.2.3.2	Non-canonical signalling	15
1.2.3.2.1	Type I	15
1.2.3.2.2	Type II	16
1.2.4	Role of hedgehog signalling in haematopoiesis	17
1.3	Disease models employed in this study	20
1.3.1	Allergic airway inflammation	20
1.3.2	Acute Graft-versus-Host disease	21
1.3.3	B16 melanoma model	21
1.4	Aim of the thesis	22
2	Material and Methods	24
2.1	Material	24
2.1.1	General Laboratory equipment	24
2.1.2	Consumables	27
2.1.3	Chemicals and Reagents	29
2.1.4	Media, Buffer and Solutions	30
2.1.4.1	Media	30
2.1.4.2	Buffers and solutions	31
2.1.5	Enzymes	32
2.1.6	Antibodies for flow cytometry, cell separation and stimulation	32
2.1.7	Commercial Assays	34
2.1.8	Oligonucleotides	34
2.1.8.1	Oligonucleotides for genotyping	35
2.1.8.2	Oligonucleotides for qRT-PCR	35
2.1.9	Cell lines	36
2.1.10	Mice	36
2.1.11	Software	37
2.2	Methods	37
2.2.1	General animal work	37
2.2.1.1	Mouse husbandry	37
2.2.1.2	Identification and genotyping of $CD4Cre^{+/-} Ptch^{flox/flox}$ mice	37
2.2.1.3	Tissue preparation and isolation of cells	38
2.2.1.3.1	Lymphocytes	38
2.2.1.3.2	Thymocytes	38
2.2.1.3.3	Bone Marrow	38
2.2.1.4	Anaesthesia	39
2.2.1.4.1	Short-term anaesthesia	39
2.2.1.4.2	Extended anaesthesia	39
2.2.1.5	Irradiation	39
2.2.2	<i>In vitro</i> methods	39

TABLE OF CONTENTS

2.2.2.1	Cell culture	39
2.2.2.1.1	Cell counting	40
2.2.2.1.2	Haemolysis	40
2.2.2.1.3	Thawing of cryopreserved cells	40
2.2.2.1.4	Detachment of adherent cells	40
2.2.2.1.5	Generation of bone marrow-derived macrophages	41
2.2.2.1.5.1	Preparation of L cell conditioned medium	41
2.2.2.1.5.2	<i>In vitro</i> differentiation of macrophages	41
2.2.2.1.6	Cultivation of B16F10 melanoma cells	42
2.2.2.2	Cell purification and depletion	42
2.2.2.2.1	Isolation of conventional T cells	42
2.2.2.2.2	Isolation of regulatory T cells	42
2.2.2.2.3	Generation of T cell depleted bone marrow	43
2.2.2.3	Proliferation assays	43
2.2.2.3.1	Allogenic stimulation of T cells	43
2.2.2.3.2	Polyclonal stimulation of T cells	44
2.2.2.3.3	Suppression assays	44
2.2.2.3.4	<i>Ex vivo</i> restimulation of T cells with Ovalbumin	44
2.2.2.3.5	Solid scintillation counting	45
2.2.2.4	Enzyme-linked Immunosorbent Assay	45
2.2.2.4.1	Detection of Cytokines	45
2.2.2.4.2	Detection of Ovalbumin-specific Immunoglobulins	46
2.2.2.5	Flow cytometry	46
2.2.2.5.1	Analysis of extracellular antigens	46
2.2.2.5.2	Analysis of intracellular antigens	47
2.2.2.5.3	Apoptosis staining	47
2.2.2.6	Histology	47
2.2.2.6.1	Tissue fixation	47
2.2.2.6.2	Preparation and sectioning of paraffin blocks	48
2.2.2.6.3	Hematoxylin and eosin stain	48
2.2.3	Molecular biological methods	49
2.2.3.1	Isolation of genomic DNA from biopsies	49
2.2.3.2	Isolation of total RNA from cells	50
2.2.3.3	Measurement of nucleic acid concentration	50
2.2.3.4	Reverse Transcription	50
2.2.3.5	Polymerase Chain Reaction	50
2.2.3.6	Real Time Quantitative Reverse Transcription PCR	51
2.2.3.7	Agarose Gel Electrophoresis	52
2.2.4	Disease models	52
2.2.4.1	Allergic airway inflammation	52
2.2.4.1.1	Induction	52
2.2.4.1.2	Analysis	53
2.2.4.2	Acute Graft-versus-Host disease	53
2.2.4.2.1	Induction	53
2.2.4.2.2	Monitoring of disease progression	54
2.2.4.3	B16 Melanoma model	55
2.2.4.3.1	Induction of subcutaneous tumour development	55
2.2.4.3.2	Anti-tumour immunisation	55
2.2.4.3.3	Monitoring of disease progression	55
2.2.5	Statistical analysis	55

3	Results	56
3.1	Investigation of thymocyte development	56
3.2	Characterisation of peripheral T cells	59
3.2.1	Efficiency and molecular effects of Ptch inactivation	59
3.2.2	T cell populations and their activation state in the periphery	60
3.3	Functional analysis of conventional T cells <i>in vitro</i>	65
3.4	Analysis of naturally occurring regulatory T cells	69
3.5	Susceptibility of T cells to apoptosis	71
3.6	<i>In vivo</i> analysis of Ptch-deficient T cells	74
3.6.1	Allergic airway inflammation	74
3.6.2	Acute Graft-versus-Host disease	78
3.6.3	B16 Melanoma model	80
4	Discussion	83
4.1	Thymocyte development is marginally affected by the Ptch ablation while numbers, distribution and activation states of peripheral T cells remain unaltered	83
4.2	Ptch does not impact on functional characteristics of T cells <i>in vitro</i>	85
4.3	Expression of Ptch in T cells is dispensable for adaptive immunity	88
4.4	Absence of Ptch in T cells does not lead to the activation of canonical Hh signalling	90
4.5	Investigations on the role of Hh signalling in the development and function of T cells	92
5	Summary	96
6	References	97
7	Appendix	125
7.1	List of abbreviations	125
7.2	List of figures	129
7.3	Acknowledgements	130
7.4	Curriculum vitae	131

1 Introduction

1.1 T lymphocytes

1.1.1 The immune system

Pathogenic microorganisms such as bacteria, viruses, fungi, protozoan- and multicellular parasites pose a constant threat to higher developed organisms. They can invade the body through different routes with most pathogens entering via mucosal surfaces of the urogenital, digestive and respiratory tracts. Once an organism is successfully colonised, pathogens can harm the host in several ways ranging from the competition for nutrients over the production of poisonous metabolic products to the direct induction of cytopathic effects. This may damage or destroy vital tissues and organs and eventually cause death of the host. In order to defend the organism against pathogens but also to remove malignant host cells, a multi-faceted array of cells and molecules has evolved which is referred to as the immune system. It consists of two distinct but intertwined arms which fulfil different but equally important tasks in providing effective resistance against various threats.

The innate immune system represents the front line of host defence and has a wide variety of mechanisms at its disposal for combating infections. Those include physical barriers presented by epithelial tissues which line body surfaces, physiological barriers such as antibacterial peptides and the complement system as well as numerous innate immune cells which patrol the periphery. These cells are equipped with a set of germline encoded receptors, so-called pattern recognition receptors (PRR), that recognise conserved and ubiquitously expressed structures found on many pathogens. Using these receptors, innate immune cells can instantly engage invading microorganisms and frequently prevent the establishment of an infectious focus. The downside of innate immune responses is that they are neither specific for a particular pathogen nor do they lead to the development of an immunological memory. Once pathogens manage to overcome innate immunity and establish a focus of infection, different and more sophisticated mechanisms are required in order to protect the host.

The adaptive immune system which is unique to vertebrates provides such improved protection by employing mechanisms of its humoral and cell-mediated branches. A hallmark of the adaptive immune system is its inherent flexibility which allows the recognition of virtually unlimited numbers of different antigens. This is achieved by employing specialised receptors on the surface of lymphocytes which are generated by highly diverse and variable

recombination events on the DNA level. The generation of sufficient amounts of lymphocytes that bear highly antigen-specific receptors is a rather slow process that requires interactions between cells of the innate and the adaptive immune system. However, this process also leads to the generation of long-lived memory cells which trigger stronger and more immediate responses upon subsequent infections with the same pathogen. While B lymphocytes provide humoral immunity by secreting antigen-specific antibodies into the body fluids, T lymphocytes or T cells are not only implicated in this process as well but they are also the principal mediators of cell-mediated adaptive immunity.

1.1.2 Thymocyte development

The development of T cell precursors or thymocytes is a highly ordered process that takes place in the thymus. Together with the bone marrow (BM), the thymus belongs to the primary lymphoid organs and is essential for the development of prospective T cells (van Ewijk, 1991; Carlyle and Zúñiga-Pflücker, 1996). It consists of numerous lobules each divided into an outer cortex where most stages of thymocyte development occur and an inner medulla region. Thymocyte development begins with the entry of common lymphoid progenitors (CLP) into the thymus via blood vessels located in the corticomedullary junction (Cantor & Weissmann 1976; Kondo et al., 1997). These cells lack expression of characteristic T cell surface molecules including the T cell receptor (TCR), the CD3-complex which is necessary for TCR-dependent signalling and the TCR co-receptors CD4 and CD8. Due to lack of the latter two, these cells are referred to as CD4 and CD8 double negative (DN) cells. Initial interaction with the thymic stroma in the subcapsular region of the cortex triggers a differentiation process which leads to the expression of first T cell-specific surface markers such as CD2. While these cells can give rise to different T cell populations including the minority lineages of the NKT cells and $\gamma\delta$ T cells, the majority develops into the dominating population of $\alpha\beta$ T cells (Fehling et al., 1999). DN cells can be further subdivided according to surface expression of the adhesion molecule CD44 and the IL-2 receptor α -chain CD25 (Godfrey et al., 1993). Cells of the DN1 stage (CD25⁻ CD44⁺) have recently entered the thymus and their TCR-encoding genes are still in the germline configuration. These cells progress via the DN2 stage (CD25⁺ CD44⁺) to the DN3 stage (CD25⁺ CD44⁻) where rearrangement of the TCR β -chain locus occurs through the process of VDJ recombination (Bonati et al., 1992). Upon successful rearrangement of this locus, the cells start expressing the pre-TCR which consists of the β -chain and a surrogate α -chain (von Böhmer and Fehling, 1997). This receptor associates with CD3 molecules and transduces signals into the cell leading to the arrest of further β -chain rearrangement and promoting differentiation into

the DN4 stage (CD25⁻ CD44⁻) after several rounds of proliferation. Soon after, cells migrate to the cortex and start with the expression of CD4 and CD8 co-receptors which defines them as CD4 and CD8 double positive (DP) cells. At this stage, multiple rearrangement attempts can be made at the α locus after which most cells succeed to produce a functional α -chain that replaces the pre α -chain thus generating a functional $\alpha\beta$ TCR (Thompson et al., 1990). Although $\alpha\beta$ TCRs are highly variable and allow the generation of immune responses to a wide array of pathogens, they are subject to major histocompatibility complex (MHC) restriction meaning that they can only recognise peptides that are presented on MHC molecules. This important aspect of TCR-mediated antigen recognition forms the basis of subsequent stages in thymocyte development which are positive selection, negative selection and lineage commitment. Positive selection occurs in the cortex and is mediated by specialised thymic epithelial cells (cTEC) which present self antigen on MHC class I and MHC class II molecules to DP cells (Marrack and Kappler, 1997). Only thymocytes which successfully recognize peptide:MHC complexes survive while those that fail die by neglect. In addition to positively selecting cells that recognise self antigens with a low avidity, the TCR-intrinsic specificity for molecules of either MHC class also determines which co-receptor a mature T cells will express. While TCR and CD8 engagement with MHC class I commits the thymocyte to develop into a CD8 single positive (SP) cell, interaction with MHC class II leads to a loss of CD8 expression and destines the DP thymocyte to become a CD4 SP T cell (von Böhmer et al., 1989). However, cells which display a high avidity for self antigens pose a threat to the organism and are removed in the process of negative selection (Punt et al., 1994). This process is mediated by BM-derived cells such as macrophages and dendritic cells (DC) and also by medullary thymic epithelial cells (mTEC) (Hoffmann et al., 1992). Eventually, naïve self-tolerant SP T cells leave the thymus via the medulla and begin to circulate between blood and lymphoid tissues until they encounter their specific antigen.

1.1.3 T cell activation

In order to become activated and differentiate into effector cells, naïve T cells require at least two separate signals for their activation (Bretscher and Cohn, 1970). The first one is transmitted through the TCR upon recognition of a foreign antigen. Since T cells are not able to recognise their specific antigen directly due to MHC restriction of the TCR, they require accessory cells to process and present antigens in the form of small peptides bound to MHC molecules. In addition to the presented antigen, T cells also depend on co-stimulatory signals delivered through distinct surface receptors which are essential for their proper activation. These tasks are performed by a specialised subset of cells which are the so-called professional antigen-presenting cells (APC). These include DCs which are the main

mediators of T cell activation but also macrophages and B cells. APCs reside as immature cells in peripheral non-lymphoid tissues and act as sentinels patrolling for foreign antigens. In this state, they are characterised by a high endocytic activity but only a weak expression of MHC and co-stimulatory molecules. On their surface, APCs bear an array of conserved receptors such as Toll-like receptors (TLR) and C-type lectin receptors (CLR) that are able to recognise pathogen-associated molecular patterns (PAMP). Recognition of pathogens leads to their ingestion by receptor-mediated endocytosis which has several consequences. Firstly, the engulfed pathogen is degraded and its peptides are presented on MHC molecules whose expressions are drastically upregulated. Secondly, the APCs become activated and begin to express high levels of cell-adhesion and co-stimulatory molecules such as those of the B7 family which are pivotal for T cell activation (Greenwald et al., 2005). Thirdly, activated APCs rapidly lose their ability for endocytosis and migrate to draining lymphoid tissues where they act as potent initiators and modulators of an adaptive immune response (Steinmann et al., 1997).

Naïve T cells that circulate through the periphery enter secondary lymphoid organs via high endothelial venules through a process which requires interaction of adhesion molecules on T cells and endothelial cells. Upon entry into lymphoid organs, T cells begin to sample MHC:peptide complexes presented on APCs until they recognise a complex with high avidity on activated cells. This induces conformational changes in T cell adhesion molecules that stabilises the T cell-APC interaction (Lebedeva et al., 2005). In addition, T cells receive activation signals both through the TCR and through several co-stimulatory receptors which belong to the immunoglobulin- and tumour necrosis factor receptor (TNFR) superfamilies. These include activating receptors such as CD28, CD40L and the inducible T cell co-stimulator (ICOS) whose ligands are expressed on activated APCs but also negative regulators like cytotoxic T lymphocyte antigen 4 (CTLA-4), programmed cell death 1 (PD-1) and B- and T-lymphocyte attenuator (BTLA) which compete for ligand binding thus limiting T cell activation (Rudd and Schneider 2003; Watanabe et al., 2003). Supply of co-stimulatory signals is essential for T cell activation as antigen recognition in their absence can cause apoptosis or lead to anergy (Kroczek et al., 2004). In contrast, the availability of both signals triggers the proliferation and differentiation of naïve T cells into effector T cells, a process which is largely driven by the cytokine Interleukin (IL)-2 and accompanied by the expression of activation markers such as CD69 and CD25 (Parry et al., 2003; Caruso et al., 1997). Importantly, the differentiation process can be influenced by cytokines which are differentially secreted mainly by APCs and other T cells depending on the encountered pathogen. Naïve CD4⁺ T cells differentiate into T helper (T_H) cells which can participate in both humoral and cell-mediated immunity whereas CD8⁺ T cells differentiate into cytotoxic T lymphocytes (CTL)

that mediate killing of virally infected and tumourigenic cells. A common feature of all effector T cells is that they can act independently of further costimulation upon encounter with their antigen in the periphery.

1.1.4 T cell subtypes

1.1.4.1 T Helper cells

The process of antigen-specific T cell activation serves several purposes. One of them is that it facilitates the generation of sufficient amounts of T cells which are specific for a given antigen through the process of clonal expansion. Another important aspect is that it allows tailoring the upcoming immune response specifically to the ongoing immune challenge. The polarisation of naïve CD4⁺ T_h (T_h0) cells into specialised subsets is therefore pivotal for mounting an effective response to diverse types of pathogens. Originally, two distinct subsets of T_h cells were defined according to their cytokine secretion patterns and functions: The T helper cell 1 (T_h1) and the T helper cell 2 (T_h2) (Mosmann et al., 1986; Mosmann and Coffman, 1989). More recent studies have indicated that T_h0 cells can also differentiate into a different lineage which was termed T helper cell 17 (T_h17) due to their ability to produce the pro-inflammatory cytokine IL-17A and other molecules of this family (Harrington et al., 2005). The differentiation of T_h0 cells into different subtypes depends on the conditions under which the cells are activated. It has been shown that the amount of antigen, the presenting APC type and the cytokine milieu affect this decision process (Croft et al., 1992; Constant and Bottomly, 1997; Rothöft et al., 2003).

In the presence of intracellular pathogens or engulfed fungi, professional APCs begin to secrete the cytokine IL-12 to which T_h0 cells respond with the transcription of the master regulators T-box expressed in T cells (T-bet) and signal transducer and activator of transcription 4 (STAT4) (Szabo et al., 2000). This in turn promotes the development of T_h1 effector cells which are crucial for immune responses against intracellular pathogens such as bacteria, viruses and fungi. T_h1 cells exert their function by secreting Interferon gamma (IFN- γ) and several other pro-inflammatory cytokines such as tumour necrosis factor alpha (TNF- α), lymphotoxin alpha, IL-2 and IL-3. These act by enhancing the antimicrobial activity of innate immune cells, promote the production of immunoglobulin (Ig) G2a antibodies and lead to the recruitment of other lymphocytes and NK cells (Zhu and Paul, 2008). Furthermore, IFN- γ augments the production of IL-12 by APCs which promotes the differentiation of additional T_h1 cells while the development of T_h2 cells is blocked (So et al.,

2000). In addition to serving as a growth factor, IL-2 also stimulates the proliferation of CTL and promotes the formation of T_h1 memory cells (Darrah et al., 2007). Thus, T_h1 cells are important contributors to cell-mediated immune responses against intracellular pathogens and fungi.

Contrariwise, extracellular bacteria and parasites trigger the production of IL-4 which largely derives from NKT cells and polarises naïve $CD4^+$ T cells to differentiate towards the T_h2 lineage. In addition, low levels of antigen presented on APCs also favour the development of this lineage. The differentiation process is regulated by the master transcription factors GATA binding protein 3 (GATA3) and STAT6 (Yamashita et al., 2004). T_h2 cells are characterised by a cytokine expression pattern which differs from that of T_h1 cells and includes IL-4, IL-5, IL-6, IL-10 and IL-13 (Zheng and Flavell, 1997). These skew adaptive immunity towards a humoral immune response by stimulating B cell proliferation, promoting the generation of IgG1 and IgE antibodies and by affecting innate immune cells in several ways. IgE binds to receptors on eosinophil granulocytes and mast cells which leads to the release of inflammatory mediators such as histamine and leukotrienes that play important roles in the resistance to parasite infections (Wedemeyer et al., 2000). T_h2 cytokines also have profound effects on non-immune cells and cause goblet cell hyperplasia, muscle hyper-contractility and excessive mucus production in the airways during allergic responses (Venkayya et al., 2002). Furthermore, IL-4 stimulates the differentiation of additional T_h2 cells from naïve $CD4^+$ T cells whereas IL-10 inhibits the production of IL-2, IL-12 and IFN- γ from T cells and APCs thus further stabilising the T_h2 response.

In addition to the T_h1 and T_h2 lineages, it has been found more recently that T_h17 cells form a third important subpopulation of T_h cells. Polarization of these cells is triggered in the presence of IL-6 and transforming growth factor beta (TGF- β) which activate the transcription factors retinoic-acid-receptor-related orphan receptor alpha (ROR α) and gamma t (ROR γ t) as well as STAT3 (Weaver et al., 2006; Iwanov et al., 2006; Yang et al., 2007; Yang et al., 2008). Upon activation, T_h17 cells secrete the cytokines IL-17A, IL-17F, IL-21, IL-22 and granulocyte macrophage colony-stimulating factor (GM-CSF) (Ouyang et al., 2008). Although the precise role of this population is yet to be established, it is believed that T_h17 cells play a critical role in mucosal immunity and the defence against certain microbial pathogens, such as extracellular bacteria and fungi but also in tumour regression (Weaver et al., 2006; Martin-Orozco et al., 2009). In this context, the recruitment and activation of innate immune cells such as neutrophil granulocytes and macrophages appears to be a central mode of action employed by T_h17 cells (Martin-Orozco et al., 2009; Pelletier et al., 2010).

1.1.4.2 Regulatory T cells

In addition to protecting the host from infections, one important task of the immune system is to maintain tolerance to self. The vast majority of potentially autoreactive cells are removed in the thymus by mechanisms of central tolerance but some avoid detection and escape into the periphery. Regulatory T (T_{reg}) cells are essential for the maintenance of peripheral tolerance by preventing the activation of autoreactive cells. In addition, they are also important for protecting the host from overshooting immune responses against pathogens which could cause additional tissue damage. T_{reg} cells can be classified into naturally occurring (nT_{reg}) and inducible (iT_{reg}) cells. The former constitutively express CD25 and the transcription factor forkhead box P3 (FoxP3) which is essential for their development and function (Fontenot et al., 2003). They arise from DP cells in the thymus which show an intermediate affinity for self antigen and are thus potentially autoreactive (Itoh et al., 1999; Jordan et al., 2001). On the other hand, iT_{reg} cells develop from naïve T cells in the periphery which are activated under sub-immunogenic or non-inflammatory conditions and can be further subdivided into several populations (Dons et al., 2012). A common feature of all T_{reg} cells is that they are hypoproliferative upon stimulation and can suppress the activation, proliferation and cytokine secretion of conventional T cells (Shevach, 2009). This is achieved by different means such as the induction of apoptosis in effector T cells, the modulation of the environment through anti-inflammatory cytokines or the competition for survival- and activation signals (Sakaguchi et al., 2009). Hence T_{reg} cells are an important subset of T cells which is critical for the control of normal immune responses and for self-tolerance.

1.1.4.3 Cytotoxic T cells

CTLs are the main antigen-specific effector cells of cell-mediated immune responses. They are crucial for controlling infections by cytoplasmic bacteria, viruses and some intracellular protozoan parasites which are beyond the reach of the humoral immune system. In addition, they have also proven to be the most important effector T cells in immune responses against tumours. Once activated, CTLs can rapidly and selectively kill infected cells with high efficiency by two different means (Henkart et al., 1994). The first mechanism is based on preformed effector molecules which are stored in lytic granules and are released upon TCR cross-linking. These vesicles contain perforin which polymerises to form transmembrane pores in the target cells membrane and a set of serine proteases called granzymes that move through these pores into the target cells and induce apoptosis via caspase activation (Kuppers and Henney, 1977). In the course of apoptosis, viral DNA as well as non-viral cytosolic pathogens are destroyed which prevents the infection of adjacent cells. A second mode of action involves surface expression of Fas ligands which also cause apoptosis in

target cells that bear the appropriate receptor (Suda et al., 1993). Finally, CTLs can act via the secretion of cytokines. IFN- γ , which is produced in large quantities, inhibits viral replication, promotes increased expression of MHC class I molecules on target cells and causes recruitment and activation of macrophages. In addition, CTLs secrete TNF- α and TNF- β which synergise with IFN- γ in macrophage activation and can kill cells through interaction with TNFR-1.

1.2 The hedgehog signalling pathway

1.2.1 Basic concepts

One decisive step during the evolution of life was the emergence of multicellular organisms which appeared approximately 1,2 billion years ago. Multicellularity however required the development and refinement of mechanisms that allowed interaction and communication between adjacent and distant cells. During the last decades, extensive research has unveiled many key molecular players in this context which led to the surprising finding that evolution has been working with a rather limited number of signalling pathways to generate the tremendous diversity and complexity of multicellular life. These include the TGF- β , the Janus kinase (JAK) and signal transducer and activator of transcription (STAT), the epidermal growth factor receptor (EGFR), the fibroblast growth factor (FGF) as well as the Notch, Wnt and Hedgehog (Hh) signalling pathways. Early studies of Hh signalling were exclusively based on genetic analysis in the fruit fly *Drosophila melanogaster* where it was originally identified and recognised as an important factor for proper segmental patterning during embryogenesis (Nüsslein-Volhard and Wieschaus, 1980; Forbes et al., 1993). Further investigations revealed that this pathway is not only implicated in the embryonic development of both invertebrates and vertebrates but also plays an important role in the maintenance of many adult structures. It has been shown to regulate proliferation, differentiation and cell fate determination of progenitor cells that give rise to various tissues such as epithelia, neuronal structures and others (Beachy et al., 2004; Watkins et al., 2003; Machold et al., 2003; Palma and Ruiz i Altaba, 2004). The central importance of this pathway for tissue development and homeostasis is clearly demonstrated by the fact that aberrant signalling contributes to severe developmental abnormalities such as Gorlin syndrome, holoprosencephaly and cyclopia (Hahn et al., 1996; Chiang et al., 1996; Rössler et al., 1996; Nieuwenhuis & Hui, 2005) while complete loss of Hh signalling is embryonically lethal (Goodrich et al., 1997; Hahn et al., 1998). Importantly, mutations in Hh signalling components that lead to constitutive pathway activation are also associated with oncogenesis and can cause basal cell carcinoma (BCC),

medulloblastoma (MB) and rhabdomyosarcoma (RMS) (Hahn et al., 1996; Goodrich et al., 1997; Hahn et al., 1998). A detailed understanding of Hh signalling function and its beneficial or adverse effects on the organism requires knowledge of the different pathway components and how they interact with each other.

1.2.2 Major pathway components

A hallmark of Hh signalling is its ability to act over a long range and control distinct cell fates as a function of Hh concentration. The principal mediators of this long range communication are proteins of the Hh family. While there is only one *Hh* gene in *Drosophila* and other invertebrates, three homologues have been identified in birds and mammals which were called Sonic hedgehog (Shh), Desert hedgehog (Dhh) and Indian hedgehog (Ihh) (Krauss et al., 1993). Other vertebrates may have additional family members such as the zebrafish which harbours six *Hh* genes following gene duplication (Avaron et al., 2006). The various Hh proteins are believed to mainly differ in their tissue distribution with Shh being the most widely expressed family member (Ingham & McMahon, 2001). Hh proteins are synthesised as precursor proteins with a size of approximately 45 kDa. Following translation, they undergo autocatalytic cleavage which yields two fragments of almost identical size. The C-terminal fragment contains a highly conserved 'Hog' domain that catalyses the autocleavage reaction and is quickly degraded. The 'Hedge' domain carrying N-terminal fragment (Hh-N) however is covalently bound to cholesterol, a modification which is essential for its signalling activity (Porter et al., 1996). Subsequently, Hh-N is subject to another modification mediated by Hh acetyltransferase (Hhat) which catalyses the attachment of palmitate, a derivative of palmitic acid (Chamoun et al., 2001). The addition of this second lipid moiety is believed to further enhance activity and tissue distribution of the protein by promoting the formation of freely diffusible multimeric complexes (Zeng et al., 2001; Vyas et al., 2008). Finally, release of the modified Hh-N from the signal-sending cell requires the activity of a 12-pass transmembrane protein called Dispatched (Disp) which shows homology to the resistance-nodulation-division (RND) family of bacterial transporters (Burke et al., 1999). Both the exact mechanism of Hh-N secretion and the process that leads to the formation of multimeric complexes at the surface of vertebrate cells remain uncertain. Once released into the intercellular space, Hh-N complexes can bind to receptors on signal-receiving cells.

The main receptor for Hh is Patched1 (hereinafter referred to as Ptch) which, like Disp, also shows homology to the RND family of bacterial transporter proteins and has a high affinity for Hh ligands (Goodrich et al., 1997; Marigo et al., 1996). In mammals, the receptor has a

length of approximately 1.500 amino acids and contains 12 hydrophobic membrane-spanning domains, a sterol-sensing domain (SSD) which can also be found in many cholesterol-binding proteins, two large extracellular loops where binding of the Hh ligands occurs, a central intracellular loop that mediates interaction with cyclin B1 and a C-terminal cytoplasmic tail (Figure 1) (Hooper and Scott, 1989; Marigo et al., 1996; Barnes et al., 2001; Strutt et al., 2001; Martín et al., 2001). RND-type transporters are almost exclusively found in bacteria where they pump lipophilic toxins and heavy metals out of the cell. The finding that mutations of amino acids which are crucial for transporter activity negatively affects Ptch function suggests that it might perform a similar task in eukaryotic cells (Taipale et al., 2002). Mammals also have a second Ptch receptor (Ptch2) which is structurally similar to Ptch and Disp (Zaphiropoulos et al., 1999). It is however somewhat smaller in size and lacks a C-terminal cytoplasmic extension which is present in Ptch. Both are differentially expressed during mouse development but while Ptch2 is also fully capable of binding Hh ligands, the finding that it cannot compensate for lacking Ptch in BCCs suggests that it may have related, yet distinct functions when compared with Ptch (Motoyama et al., 1998; Carpenter et al., 1998; Zaphiropoulos et al., 1998).

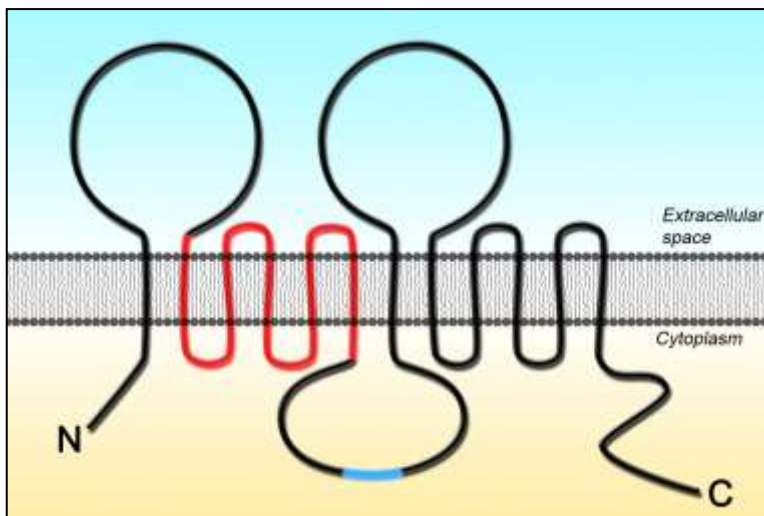


Figure 1. Schematic view of Ptch
Ptch is a 12-pass transmembrane protein with two characteristic extracellular loops that mediate ligand binding, a central intracellular loop that contains a cyclin B1 interaction domain (blue), a sterol-sensing domain that spans over transmembrane domains 2-6 (red) and a C-terminal cytoplasmic tail.

Reception of Hh ligands by Ptch is supported by several surface proteins that act as presumptive co-receptors. These include the single-pass transmembrane proteins cell adhesion molecule down-regulated by oncogenes (CDO) and brother of CDO (BOC) which belong to the family of immunoglobulin- and fibronectin type III (FnIII)-containing membrane proteins (Lum et al., 2003; Tenzen et al., 2006). Mice lacking either one of these proteins are viable but display signs of disturbed Hh signalling while those deficient for both co-receptors exhibit more severe signalling defects (Zhang et al., 2006; Zhang et al., 2011). Thus, both proteins are not mandatory for signal transduction but act in a redundant fashion to enhance Ptch-mediated signalling. While both co-receptors are orthologues of *Drosophila* proteins,

vertebrates harbour additional and structurally distinct Hh-binding proteins with one of them being growth arrest-specific gene 1 (GAS1) (Del Sal et al., 1992; Allen et al., 2007). Interestingly, it has been shown that inactivation of GAS1 in mice that already lack CDO and BOC leads to a complete loss of Hh signalling thus emphasizing the requirement for co-receptors during Hh ligand reception (Allen et al., 2011). Analogous to *Drosophila* where the interaction of co-receptors with Hh ligands is only possible in the presence of heparin, it was found that mammalian orthologues require high concentrations of calcium ions to mediate ligand binding showing that co-receptor requirement but not the mode of Hh binding is conserved across different phyla (McLellan et al., 2008). Finally, with Hedgehog-interacting protein (HIP) vertebrates possess a fourth protein that is capable of binding Hh ligands. HIP has no downstream signalling function and is believed to modulate signalling by directly competing with Ptch for Hh binding and by ligand sequestration (Chuang et al., 1999).

The major pathway component that acts downstream of Ptch is Smoothed (Smo) which belongs to the seven-transmembrane G protein-coupled receptor (GPCR) superfamily and is indispensable for Hh signalling both in *Drosophila* and in vertebrates (Alcedo et al., 1996; van den Heuvel et al., 1996; Kristiansen, 2004). Unlike most other members of this family, Smo possesses a long C-terminal domain that contains several conserved phosphorylation sites which are required for Hh-dependant signalling (Apionishev et al., 2005). Indeed, phosphorylation is the crucial step that leads to a conformational change which causes recruitment and activation of Smo. Phosphorylation is mediated by the 3',5'-cyclic adenosine monophosphate (cAMP)-dependent G protein-coupled receptor kinase 2 (GRK2) and casein kinase 1 alpha (CK1 α) in the presence of Hh ligand (Phillipp et al., 2008; Chen et al., 2011). Consistent with its GPCR-like topology, Smo has also been shown to regulate Hh signalling through the direct interaction with a specific family of heterotrimeric GTP-binding proteins (Riobo et al., 2006; Ogden et al., 2008).

Ultimately, Smo modulates abundance and activity of the glioma-associated oncogene (Gli) family of zinc finger transcription factors. Mammals possess three Gli proteins (Gli1-3) which constitute the principal effectors of canonical Hh signalling (Aza-Blanc and Kornberg, 1999; Alexandre et al., 1996). They consist of a N-terminal transcriptional repressor domain and a C-terminal transcriptional activator domain. In the absence of Hh ligand, Gli proteins exist in both the full-length form (Gli-FL) and the proteolytically processed form that lacks the C-terminal activator domain and therefore acts as a transcriptional repressor (Gli-R). Upon Hh stimulation, processing into the repressor form is largely inhibited and the Gli proteins accumulate in the nucleus where they are modified to become transcriptional activators (Gli-A). Both the processing into transcriptional repressors and the rapid removal of

transcriptional activators is controlled by the ubiquitin-proteasome system (Jiang, 2006). Gli2 and Gli3 are principally bi-functional transcription factors and can act both as an activator or a repressor form with Gli3 mainly acting as a transcriptional repressor (Person et al., 2002). In contrast, Gli1 lacks the N-terminal repressor domain and functions exclusively as a transcriptional activator (Bai et al., 2004). Its transcription is largely increased during a positive feedback-loop in response to active signalling and thus it is widely used as a biomarker for increased canonical signalling activity (Park et al., 2000). Both repressor and activator forms of Gli largely bind to the same sites in the promoters of Hh target genes and regulate the expression of hundreds of genes in response to Hh ligands (Müller and Basler, 2000; Hallilas et al., 2006; Vokes et al., 2008).

1.2.3 Signal transduction

Although many aspects of Hh signalling are conserved across metazoans, it has become evident in recent years that this pathway is coupled to a specific cellular organelle in mammals, the primary cilium (Oro, 2007). Interestingly, this requirement has not only been demonstrated for mammals but also for amphibians (Park et al., 2006), birds (Yin et al., 2009) and fish (Huang and Schier, 2009) suggesting that it is a common feature of Hh signalling in vertebrates. This is different from *Drosophila* where primary cilia are dispensable for Hh signalling activity which can be explained by the absence of these structures in most cell types (Götz et al., 2009). Primary cilia are cellular organelles which protrude from the surface of most vertebrate cells (Bettencourt-Dias et al., 2011). Similar to conventional cilia, the axoneme of primary cilia is made up of microtubule pairs in a characteristic 9-fold symmetric organisation and is anchored to the plasma membrane through the basal body. Due to the lack of key elements involved in ciliary motility including the central pair of microtubules, primary cilia are immotile structures. Thus they have been regarded as vestigial organelles without important function until they have recently emerged as important regulators of several developmental signalling pathways including the Hh signalling pathway (Huangfu et al., 2003, May et al., 2005). Different studies have shown that components of the Hh pathway including Ptch (Rohatgi et al., 2007), Smo (Corbit et al., 2005), Sufu (Zeng et al., 2010) and the Gli transcription factors (Haycraft et al., 2005) are enriched in primary cilia. Notably, localisation of Hh signalling components in motile cilia could not be demonstrated and Hh signalling was not affected when the formation of these organelles was disrupted either (Wilson et al., 2009; Fliegauf et al., 2007). Although the precise interaction between Hh signalling and primary cilia is not fully understood, recent investigations have identified the kinesin Kif7, a component of the intraflagellar transport machinery, as a major factor which tethers the Hh signalling pathway to the primary cilium by directly interacting with Hh

components (Cheung et al., 2009; Endoh-Yamagami et al., 2009; Liem et al., 2009). A second finding which has been made during the past few years and which has expanded the understanding of the Hh signalling pathway is that Hh proteins can transduce signals into the cell by different means. A signal transduction that involves the Gli transcription factors and follows the central Ptch-Smo-Gli axis is classically referred to as canonical signalling while Gli-independent mechanisms are summarised under the term “non-canonical signalling”.

1.2.3.1 Canonical signalling

In the absence of a ligand, the Hh receptor Ptch localises to the base of the primary cilium and prevents Smo from entering the organelle by maintaining it in an inactive conformation (Figure 2) (Hammerschmidt et al., 1997; Goodrich et al., 1999; Rohatgi et al., 2007). The precise mechanism by which Smo repression occurs is not well understood. Although initial studies proposed that a direct interaction between both transmembrane proteins takes place (Murone et al., 1999), the finding that Ptch-mediated inhibition occurs non-stoichiometrically suggested that an indirect mechanism is employed instead (Taipale et al., 2002). Concerning the sequence similarities between Ptch and the RND family of bacterial transporters and the presence of its sterol-sensing domain, it has thus been hypothesised that Ptch regulates Smo catalytically through local changes in the concentration of small molecules such as sterols or lipids (Taipale et al., 2002; Chen et al., 2002). Different classes of oxidised derivatives of cholesterol (oxysterols) and phosphatidylinositol-4-phosphate (PI4P) have been proposed as mediators of Ptch-mediated repression (Billsma et al., 2006; Corcoran and Scott, 2006; Yavari et al., 2010). While Smo is retained in an inactive conformation, Gli2-FL and Gli3-FL form a complex with suppressor of fused (Sufu) at the base of the primary cilium. This interaction stabilises and sequesters the transcription factors in the cytosol thus preventing their nuclear translocation (Humke et al., 2010; Wang et al., 2010). In addition, Sufu promotes the phosphorylation of C-terminal amino acid residues in Gli-FL by protein kinase A (PKA). This allows further phosphorylation by glycogen synthase kinase 3 beta (GSK-3 β) and CK1 α (Tempé et al., 2006; Kise et al., 2009). The kinesin-4 family member Kif7 which acts as a scaffold-protein and binds to the Sufu-Gli complex is thought to facilitate the phosphorylation process (Liem et al., 2009, Cheung et al., 2009; Endoh-Yamagami et al., 2009). Fully phosphorylated Gli-FL is subsequently recognised by the E3 ubiquitin ligase beta-transducin repeat containing protein (β -TrCP) which leads to the ubiquitylation of Gli-FL. The full length transcription factors are then partially proteolysed in a manner that degrades only the C-terminal activation domain, yielding the transcriptional repressors form (Gli-R) of the proteins (Humke et al., 2010). The truncated Gli-R proteins then translocate into the nucleus where they inhibit the expression of Hh target genes.

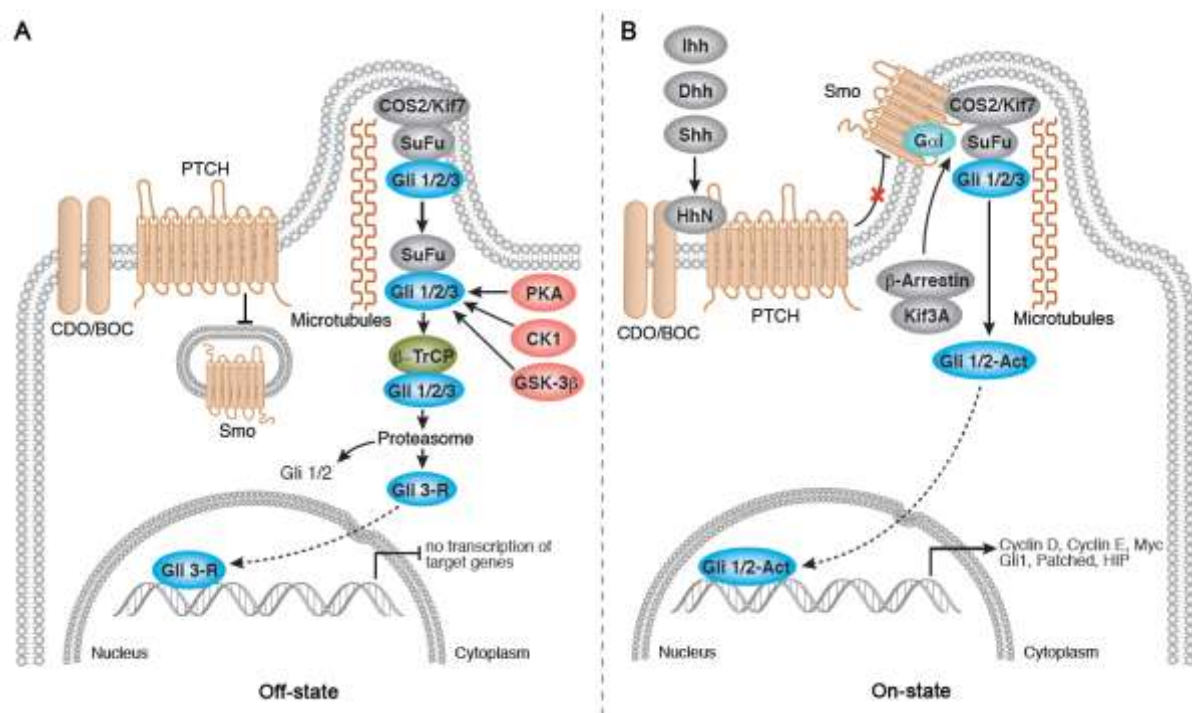


Figure 2. The canonical hedgehog signalling pathway

(A) In the absence of Hh ligands, Ptch localises to the base of the primary cilium from where it maintains Smo in an inactive conformation. Gli-FL then forms a complex with Kif7 and SuFu which prevents its nuclear translocation and promotes the phosphorylation of C-terminal residues by PKA, CK1 α and GSK-3 β . This results in partial proteasomal degradation which generates truncated transcriptional repressors that inhibit target gene expression. (B) Upon ligand binding, Ptch exits the primary cilium and its inhibition of Smo is abrogated. Phosphorylation of Smo by CK1 α and GRK2 leads to its activation and translocation into the primary cilium where it promotes the disassembly of SuFu-Gli complexes. Gli is then transported into the nucleus where it is converted into a transcriptional activator that promotes target gene transcription. (modified from Cell Signalling Technology, www.cellsignal.com)

Canonical signalling is activated in the presence of Hh ligands. The multimeric protein complexes are recognized by the Hh receptor Ptch and binding is facilitated by the co-receptors CDO, BOC and GAS1 which interact with Hh proteins through their FnIII repeats (Beachy et al., 2010). This interaction causes Ptch to exit the primary cilium and relieves its inhibition of Smo. Subsequently, the C-terminal tail of Smo becomes phosphorylated by CK1 α and GRK2 which leads to a conformational change of the protein thus triggering its activation (Chen et al., 2011). In addition, the phosphorylation event recruits β -arrestins and the kinesin-2 motor subunit Kif3a to Smo which mediate its transport into the primary cilium (2004 Chen et al., 2008 Kovacs et al., 2009 Milenkovic et al.). Along with Smo, SuFu-Gli

complexes are also transported to the tip of the primary cilium by the kinesin Kif7. Although the exact mechanism remains poorly understood, activated Smo is likely to promote the dissociation of Sufu-Gli complexes at the cilium tip and thus inhibit Gli processing into the repressor form (Humke et al., 2010; Tukachinsky et al., 2010). Kif7 presumably assists in the disassembly of the Sufu-Gli complex (Liem et al., 2009; Endoh-Yamagami et al., 2009). Following the liberation from Sufu, Gli-FL is actively transported along microtubules into the nucleus where it is converted into its activator form (Kim et al., 2009; Tukachinsky et al., 2010). The details of this conversion process also remain uncertain but are likely to involve phosphorylation events which promote the removal of the N-terminal repressor domain (Humke et al., 2010). Eventually, Gli-A promotes transcription of genes involved in differentiation, proliferation and cell survival as well as several positive and negative regulators of the pathway such as Gli1, Ptch, and HIP (Goodrich et al., 1996; Chuang et al., 1999).

1.2.3.2 Non-canonical signalling

The components involved in canonical Hh signalling and their interactions have been intensely studied since the discovery of the pathway. In recent years however, numerous observations suggested that Hh proteins can also transduce signals into cells through different mechanisms (Jenkins et al., 2009). Cellular responses to Hh ligands which do not involve activation of the Gli transcription factors are collectively referred to as non-canonical signalling. According to current experimental evidence, two different classes of Gli-independent signalling can be defined: Type I which solely depends on Ptch and is unrelated to its repression of Smo and type II which requires Smo function.

1.2.3.2.1 Type I

Early evidence for the ability of Ptch to function independent of canonical pathway components came from observations that its overexpression induced apoptosis in different cell lines (Thibert et al., 2003). This effect was independent of Smo function and did not cause the activation of canonical signalling. In this context, Ptch has been proposed to function as a “dependence receptor” meaning that cell survival depends on the presence of Hh ligands while apoptosis is actively induced when the ligand is removed (Bredesen et al., 2004; Mehlen and Thibert, 2004). Indeed, it has been reported that the C-terminal cytoplasmic domain of Ptch is a substrate for several caspases and that it is essential for apoptosis induction (Thibert et al., 2003). Additional studies revealed that Ptch-induced apoptosis is preceded by the recruitment of caspase 9, the caspase-interacting protein

Tucan-1 and the adaptor protein Dral which form a pro-apoptotic complex at its C-terminal domain (Mille et al., 2009). Support for this hypothesis comes from observations that the C-terminal domain is not required for canonical Hh signalling but appears to be associated with the regulation of proliferation and/or apoptosis (Sweet et al., 1996; Makino et al., 2001). A different function of Ptch in cellular regulation that is independent of Hh signalling components was reported by Barnes and colleagues (2001). They showed that Ptch can bind the phosphorylated but not the unphosphorylated form of the cell cycle regulator cyclin B1 with its large intracellular loop. Overexpression of Ptch in vertebrate cell culture led to a redistribution of cyclin B1 from the nucleus to the cytoplasm and negatively affected cell proliferation. Interestingly, binding of Hh to Ptch suspended this interaction and allowed nuclear translocation of cyclin B1 thus promoting proliferation. A later study provided mechanistic insights into the interaction between Ptch and cyclin B1. It was shown that the dissociation of this complex involved interaction between Ptch and GRK2, the kinase which is also implicated in the activation of Smo during canonical pathway activation (Jiang et al., 2009). Taken together, several lines of evidence suggest that Ptch can modulate proliferation and apoptosis upon Hh binding by mechanisms that are independent of components of the canonical signalling pathway.

1.2.3.2.2 Type II

The discovery that Smo can act as a GPCR and selectively interact with inhibitory heterotrimeric G (G_i) proteins had important consequences for the understanding of Hh signalling (Riobo et al., 2006). Only recently, it was reported that Hh proteins could promote the formation of actin filaments and microtubules in endothelial cells in the absence of canonical pathway activation (Chinchilla et al., 2010). This effect was shown to be dependent on Smo and on G_i protein-mediated activation of RhoA, a member of the Rho family of small GTPases which are known to regulate cytoskeletal reorganisation (Sit and Manser, 2011). A different study demonstrated that Hh proteins could also stimulate the migration of fibroblasts by a mechanism which involved G_i proteins but was independent of Gli activation (Polizio et al., 2011). Furthermore, the requirement for Smo-mediated activation of phosphoinositide 3-kinase (PI3K) was shown which led to the activation of the Rho family members RhoA and Rac1. The exact mechanism by which Rho GTPases are activated by Smo has not yet been elucidated but a recent report suggested that Smo interaction with specific guanine nucleotide exchange factors (GEF) such as T-lymphoma invasion and metastasis 1 (Tiam-1) might also be involved (Sasaki et al., 2010). Other reports focussed on the ability of Hh proteins to guide the growth of axons in the developing nervous system. It was found that Shh could act either as an attractive or repulsive factor for different axon types. The

mechanism by which Shh directed axon growth was shown to be Smo-dependent but Gli-independent and involved activation of the Src family kinases Src and Fyn instead (Yam et al., 2009). Interestingly, it has been reported by another group that Src kinases can directly associate with the C-terminal tail of Ptch via SH3 domains (Chang et al., 2010). Yet other studies have suggested that metabolites of arachidonic acid such as leukotrienes might be involved in Smo-dependent but Gli-independent signal transduction that causes cytoskeletal remodelling. This assumption was based on the observation that addition of Shh to cultured fibroblasts promoted lamellipodia-formation and migration which could be inhibited by treatment with inhibitors of 5-lipoxygenase, a key enzyme in the biosynthesis of leukotrienes (Bijlsma et al., 2007; Polizio et al., 2011). Finally, it was also suggested that calcium ions may act as second messengers in Smo-dependent but Gli-independent responses to Hh ligands (Belgacem and Borodinsky, 2011). In the context of spinal cord development, it was speculated that G_i protein-mediated activation of phospholipase C gamma (PLC- γ) led to the release of calcium ions from the endoplasmic reticulum (ER) thereby affecting cellular behaviour. In summary, experimental data from several different studies suggest that Hh proteins can affect cellular responses by modulating cytoskeletal organisation through a variety of Gli-independent mechanisms. Although the underlying principles are far from being well understood, Smo appears to have a central role in these processes by directly interacting with specific G proteins, small GTPase-associated proteins and kinases.

1.2.4 Role of hedgehog signalling in haematopoiesis

The term haematopoiesis describes the generation of cellular blood constituents from multipotent progenitor cells. In vertebrates, this process can be broadly divided into two major phases based on the stage of development (Keller et al., 1999). Primitive haematopoiesis occurs predominantly in the yolk sac and is characterised by the commitment of embryonic mesoderm to haematopoietic precursor cells (Wong et al., 1986) while definite haematopoiesis starts with the formation of multipotent haematopoietic stem cells (HSC) later in embryonic development (Medvinsky et al., 1996). HSCs constitute a self-renewing cell population that can mature into multipotent progenitors (MPP) which in turn give rise to the two major lineages of haematopoietic cells, the myeloid and the lymphoid lineage (Lemischka et al., 1986). Early evidence that Hh signalling might play a role in haematopoiesis came from observations of Bhardwaj and colleagues who reported that all major components of the canonical Hh signalling pathway were expressed in primitive human cord blood HSCs (Bhardwaj et al., 2001). In addition, the authors reported that stimulation with exogenous Shh resulted in an increased proliferative capacity of HSCs. Similar observations were also made by another group which found that Ptch

haploinsufficiency enhanced HSC proliferation during haematopoietic recovery (Trowbridge et al., 2006). Further investigations suggested that Hh signalling may also be important in the differentiation of haematopoietic cells such as during erythropoiesis (Detmer et al., 2005; Cridland et al., 2009). While these studies proposed that Hh pathway activity was required for haematopoiesis, others reports suggested that it was dispensable. By conditional inactivation of Smo in HSCs, Dierks and colleagues found that the proliferative capacity of these cells remained unaltered (Dierks et al., 2008). This was supported by the findings of two other groups which employed different strategies to inactivate Smo in HSCs (Hofmann et al., 2009; Gao et al., 2009). Taken together, the role of Hh signalling in HSC function and haematopoietic differentiation remains controversial due to conflicting data obtained from different experimental approaches.

Several studies have also been conducted to elucidate the role of Hh signalling in the development and function of T lymphocytes. As with HSCs, major components of the canonical Hh signalling pathway including Hh, Ptch, Smo and Gli are expressed in the vertebrate thymus suggesting that this pathway might play a role in thymopoiesis (Outram et al., 2000; Sacedon et al., 2003). Indeed, early studies that investigated Hh signalling in fetal thymus organ culture (FTOC) found that Hh signals were differentially required for the development of thymocytes. It was reported that transition from DN to DP cells was enhanced in the absence of Shh signals while transition to the SP stage required Shh (Outram et al., 2000). Subsequent work which studied thymocyte development using FTOC in *Shh*^{-/-} mice however found that Shh signals were required both for the transition from DN1 to DN2 and from DN4 to DP stage (Shah et al., 2004; Hager-Theodorides et al., 2005). The work of Uhmman and colleagues supported a role for Hh signalling at these developmental stages but demonstrated that Ptch ablation blocked rather than promoted these transition events (Uhmman et al., 2007). In addition, they reported that Ptch ablation led to a severe developmental block at the stage of CLP which affected both T and B lymphocyte development. Later work revealed that T cell-intrinsic expression of Ptch was dispensable for T cell development and it was suggested that expression of Ptch in pre-thymic stromal cells was required instead (Uhmman et al., 2011). Yet, most reports focussed on the role of Hh signalling during intrathymic development. By analysing conditional or T lineage-specific Smo ablations *in vivo*, El Andaloussi and colleagues reported that Hh signalling was crucial for survival and differentiation of early thymocyte progenitors (ETP) but became dispensable after pre-TCR expression at the DN3 stage. Other groups however challenged this statement and claimed that Hh signalling was also required for thymocyte development beyond the DN3 stage. By employing a mouse model that expressed a constitutively active form of the transcription factor Gli2 (Gli2 Δ N₂) thus mimicking an active pathway, it was reported that Hh

signalling negatively affected the strength of the TCR signal (Rowbotham et al., 2007). This had implications for intrathymic selection processes since it reduced positive selection of thymocytes and allowed self-reactive cells to escape clonal deletion. Overexpression of Gli2 Δ N₂ also caused a shift in the CD4 to CD8 ratio among thymocytes by promoting the development of CD4⁺ SP cells from DN cells which affected the peripheral T cell composition as well. Importantly, not only thymocyte development and composition of peripheral T cells were affected in this model but also peripheral T cell function. Due to the attenuation in TCR signal strength, T cells responded to stimulation with reduced proliferation and expression of activation markers. When a different variant of Gli2 was expressed which lacked the C-terminal activation domain and thus acted as a constitutive transcriptional repressor (Gli2 Δ C₂), T cells were found to be hyperreactive thus supporting the notion that Hh signalling was a negative regulator of T cell function (Rowbotham et al., 2008). However, these findings were contrary to previous reports which aimed at elucidating a potential implication of the Hh signalling pathway in the function of mature T cells *in vitro*. Stewart and colleagues treated polyclonally activated human CD4⁺ T cells with recombinant Shh (rShh) and evaluated its effect on T cell activation. They found that rShh enhanced proliferation, secretion of cytokines (IL-2, IFN- γ , IL-10) and the expression of activation markers (CD25, CD69) under already optimal stimulation conditions (Stewart et al., 2002). Addition of neutralising antibodies against Shh had opposite effects which supported the previous observations and suggested that T cells secrete Shh upon activation that acts in an autocrine fashion. When the experiments were performed with murine CD4⁺ T cells, it was observed that rShh was only able to enhance the proliferation of suboptimally activated cells and had no effect on resting T cells (Lowrey et al., 2002). It was further demonstrated that Shh amplified proliferation by enhancing cell entry into the S-G₂ phase of the cell cycle and by an increased expression of the anti-apoptotic gene *B-cell lymphoma 2 (Bcl-2)*. These findings were supported by the work of another group which also studied the effect of rShh on T cells *in vitro*. Chan and colleagues reported that exogenous Shh enhanced proliferation and cytokine secretion of suboptimally stimulated T cells (Chan et al., 2006). In addition, microarray analysis revealed that Shh treatment caused the upregulation of a subset of genes which was similarly regulated by CD28 signalling. Thus the authors speculated that the Hh signalling pathway might constitute a novel costimulatory pathway in T cells.

In summary, several studies tried to elucidate the function of Hh signalling in haematopoietic cells and specifically in T cells. Although an implication of this pathway is likely, the currently available data is highly contradictory as some reports suggest that Hh signalling is a positive regulator of T cell development whereas others propose that it is a negative regulator or that it is not implicated at all. There is also disagreement whether a potential implication is limited

to the development of T cells or whether it might affect these cells beyond developmental stages as well. This demonstrates that additional investigations are required to gain further understanding of this important signalling pathway and its role in the haematopoietic system.

1.3 Disease models employed in this study

1.3.1 Allergic airway inflammation

Allergic airway inflammation represents an experimental model of human asthma which is defined as a chronic inflammatory disorder of the airways. It is characterised by reversible airflow obstruction, persistent airway hyperresponsiveness, airway inflammation and airway remodelling (Bousquet et al., 2000). Since most animals including mice do not spontaneously develop a condition with similarity to human asthma, an artificial asthma-like reaction can be induced in the airways of laboratory rodents in order to mimic and study the disease. Mouse models of acute allergic responses to inhaled foreign proteins such as Ovalbumin (Ova) are most commonly used for this purpose. Following an initial sensitisation against a protein along with a T_H2 -promoting adjuvant, mice are reexposed to the allergen by different means which typically results in an inflammatory reaction that is characterized by an eosinophil-dominated influx of inflammatory cells into the lungs, epithelial thickening, and airway hyperresponsiveness. In human asthma as well as in experimental models of airway inflammation, the observed responses involve a complex interplay between components of the innate and adaptive immune system which is still not fully understood. It is known however that T cells play a central role during this response. Exposition of sensitised mice to the allergen leads to the activation of T_H2 cells that orchestrate the following immune response in several ways (Corry et al., 1998; Hogan et al., 1998). Production of the T_H2 cytokines IL-4, IL-5, and IL-13 are known to cause many of the features of the disease by promoting isotype switching towards IgE in B cells, modulating eosinophil function and by the activation of mast cells (Georas et al., 2005). There is also evidence that other T cell subpopulations contribute to the pathogenesis of asthma including T_{reg} cells which can suppress T_H2 cell responses and T_H17 cells that seem to be associated with neutrophil activation and tissue remodelling (Lewkovich et al., 2005; Bullens et al., 2006). Hence, murine models of allergic airway inflammation provide a useful tool for the study of different T cell subsets during a T_H2 -biased immune response *in vivo*.

1.3.2 Acute Graft-versus-Host disease

Graft-versus-Host disease (GvHD) is a common clinical complication following HSC transplantation. In humans, the disease can be divided into an acute (aGvHD) and a chronic (cGvHD) form which differ in time of onset and in the underlying mechanisms. The acute form is generally observed within the first 100 days after transplantation and is characterized by selective damage to the liver, skin, mucosa and the gastrointestinal tract. Mouse models of aGvHD have provided the majority of insights into the pathophysiology of this disease. Early studies already revealed that alloreactive T cells which are contained in the graft and transferred into the recipient are the underlying cause of GvHD (Korngold and Sprent, 1978). Additional investigations in the following decades led to a much better understanding of how T cells contribute to this disease. It was found that donor T cells rapidly migrate to secondary lymphoid organs after cell transplantation where they initially become activated by host APCs due to mismatched major and minor histocompatibility antigens (Panoskaltzis-Mortari et al., 2004; Beilhack et al., 2005; van Dijk et al., 1999). This leads to the expansion and maturation of several T cells subtypes which contribute to the pathogenesis of GvHD by different means. These include T_{h1} as well as T_{h2} cells which can both cause GvHD under different conditions while aGvHD in mice has been shown to be mainly T_{h1} biased (Krenger & Ferrara, 1996). Most cytotoxic effects however are due to the activity of CTLs which cause extensive tissue damage in several organs through the induction of apoptosis and the release of inflammatory cytokines (Braun et al., 1996; Baker et al., 1996). More recently, it was reported that T_{h17} cells can also contribute to the pathogenesis especially of later stages of GvHD although a protective role has been suggested as well (Kappel et al., 2009; Yi et al., 2008). Adverse effects of effector T cell activation in GvHD may be counteracted by T_{reg} cells which can suppress a wide range of immune responses including alloreactive T cell responses (Edinger et al., 2003). Taken together, due to the involvement of various T cells subtypes in a T_{h1} -biased immune response that can easily be assessed, a murine model of aGvHD provides a platform which allows to evaluate a plethora of T cell functions in a physiologic setting.

1.3.3 B16 melanoma model

Malignant melanoma is a type of cancer which predominantly arises from melanin-producing cells (melanocytes) of the epidermis. Several murine models for malignant melanoma have been developed over time to gain insights into the mechanisms underlying tumour growth, to investigate anti-tumour immune responses and to evaluate novel drugs. These include syngeneic transplantation models, xenograft models and models involving genetically modified animals. Syngeneic transplantation models such as the B16 melanoma model (Fidler, 1973) were first established and have been used for many decades in this context.

They rely on the application of a defined number of cultured melanoma cells which are subcutaneously or intravenously injected into syngeneic recipients. Depending on the application route, these models can be used to study either the development of primary tumours under the skin or of single cell metastases in the lung (Overwijk and Restifo, 2001). CTLs represent the most effective cell type that mediates killing of neoplastic cells and thus have frequently been used as an immunotherapeutic approach in the treatment of melanoma (Jäger et al., 1996; 1997 Dufour et al., 1997). Once a tumour is sensed and engaged by the innate immune system, tumour-specific CTLs are generated in draining lymph nodes and migrate to the tumour site. Here they can successfully recognize and destroy tumour cells even when the antigen is expressed on the target cells at very low densities (Melief 1992). On the other hand, T_{reg} cells are also recruited in large numbers into the tumour microenvironment through chemokines such as CCL22 which is produced by tumour-infiltrating macrophages and some tumour cells themselves (Ishida et al., 2006; Curiel et al., 2004). Accumulating T_{reg} cells may become activated and expand in the tumour vicinity after recognizing tumour-associated antigens, a process which is further amplified by local tolerogenic dendritic cells (Gobert et al., 2009; Su et al, 2010; Ghiringhelli et al., 2005). Activated T_{reg} cells can then suppress the function of tumour-specific CTLs and thereby promote tumour growth (Chen et al., 2005). In fact, T_{reg} cell function is a major obstacle in the immunotherapeutic treatment of malignant melanoma (Gajewski, 2006). For this reason, murine melanoma models can not only be used as a tool to assess CTL and T_{reg} cell function *in vivo*, but also to investigate the balance between pro- and anti-inflammatory aspects of an immune response.

1.4 Aim of the thesis

The Hh signalling pathway is one of the most fundamental signal transduction pathways in embryonic development and also responsible for the homeostasis of many adult structures in both invertebrates and vertebrates. Many lines of evidence strongly suggest that this pathway is implicated in haematopoiesis and lymphopoiesis as well but its precise role in this context remains elusive due to conflicting data reported by different groups. The aim of this study was to gain further insights into the implication of Hh signalling in the development and function of T lymphocytes, a central component of the adaptive immune system. For this purpose, a mouse model was employed which is characterised by a T cell-specific inactivation of the Hh receptor Ptch. This was expected to constitutively activate the canonical signalling cascade and thus influence cell behaviour. In order to study potential effects of the Ptch ablation on the development and function of T cells, a comprehensive set

of experimental approaches was employed which focussed on various aspects of T cell development and function both *in vitro* and *in vivo*.

2 Material and Methods

2.1 Material

2.1.1 General Laboratory equipment

Instrument	Model	Manufacturer
Animal Balance	Type 1003	Sartorius, Göttingen, Germany
Animal Clipper	Moser Animalline ARCO Type 1856	Harotec, Berlin, Germany
Blood glucose meter	Ascensia CONTOUR	Bayer, Leverkusen, Germany
Calliper	Digital Calliper 0-150mm	Carl Roth, Karlsruhe, Germany
Cameras	Colorview	Olympus, Tokio, Japan
	Lumix DMC-TZ3	Panasonic, Osaka, Japan
Centrifuges	Centrifuge 5417R	Eppendorf, Hamburg, Germany
	Centrifuge 5804R	
	Labofuge 400R	Heraeus, Hanau, Germany
	Multifuge 4KR Type 2-5	Sigma Laborzentrifugen GmbH, Osterode am Harz, Germany
Electrophoresis chambers	Type 40-0708	Peqlab Biotechnology, Erlangen, Germany
	Type 40-1214	
	Type 40-1410	
Electrophoresis power supply	EPS 301	Amersham Biosciences, Freiburg, Germany
FACS	FACSCanto II	BD Biosciences, Heidelberg, Germany
Flattening table for clinical histopathology	HI1220	Leica Biosystems, Wetzlar, Germany

MATERIAL AND METHODS

Gel documentation system	UV Transilluminator and Camera system	Intas Science Imaging Instruments, Göttingen, Germany
Harvester	MicroBeta FilterMate-96	Perkin Elmer, Rodgau, Germany
Incubator	HERAcell 150 HERAcell 240	Heraeus, Hanau, Germany
Infrared Lamp	Balance 100W	Philips, Amsterdam, Netherlands
Laboratory Balance	TE313S	Sartorius, Göttingen, Germany
Laminar Airflow Workbench	HERAGuard HERAsafe Interactive Safechange Station	Heraeus, Hanau, Germany Tecniplast, Hohenpreißenberg, Germany
MACS	autoMACS	Miltenyi Biotech, Bergisch Gladbach, Germany
Microplate Spectrophotometer	PowerWave 340	BioTek Instruments, Bad Friedrichshall, Germany
Microscopes	Televal 31 Primostar Olympus BX51	Carl Zeiss, Oberkochen, Germany Olympus, Tokio, Japan
Microwave oven	R-212	Sharp, Osaka, Japan
Paraffin stretching bath	Type 25900	Medax, Kiel, Germany
PCR Cycler	Mastercycler EP Gradient	Eppendorf, Hamburg, Germany
pH-Meter	766 Calimatic	Knick, Berlin, Germany
Photometer	BioPhotometer	Eppendorf, Hamburg, Germany
Pipettes	Eppendorf research (variable) Eppendorf reference (variable) Transferpette S-12	Eppendorf, Hamburg, Germany Brand, Wertheim, Germany

MATERIAL AND METHODS

Pipetting aid	Accu-Jet pro	Brand, Wertheim, Germany
	Easypet	Eppendorf, Hamburg, Germany
Radiation System	RS255 X-Ray Research System	Gulmay Medical Systems, Surry, UK
Real Time PCR	7500 Real Time PCR System	Applied Biosystems, Foster City, CA, USA
Reciprocating Sample Shaker	GFL-3006	Gesellschaft für Labortechnik, Burgwedel, Germany
Rectal Probes for Rodent Thermometer	BIO-BRET-3	Bioseb, Vitrolles, France
Refrigerators	various	Liebherr, Bulle, Switzerland
Rodent Thermometer	TK9882	Bioseb, Vitrolles, France
Scintillation Counter	MicroBeta ² Plate Counter	Perkin Elmer, Rodgau, Germany
Sliding Microtome	SM2000R	Leica Biosystems, Wetzlar, Germany
Thermomixer	Thermomixer comfort	Eppendorf, Hamburg, Germany
Tissue Embedding Center	EG1160	Leica Biosystems, Wetzlar, Germany
Tissue Processor	TP1020	Leica Biosystems, Wetzlar, Germany
Vortexer	Vortex Genie2	Bender & Hobein, Zürich, Switzerland
Water bath	Type W12	Störk-Tronic, Stuttgart, Germany
Water purification system	Arium 611	Sartorius, Göttingen, Germany

2.1.2 Consumables

Item	Type	Manufacturer
Biopsy Pads	Q-Path black foam pad	Labonord, Templemars, France
Cell culture dishes	Tissue / Suspension Culture Dish 5 / 10 cm	Greiner Bio-One, Frickenhausen, Germany
Cell culture flasks	Cellstar 175 cm ²	Greiner Bio-One, Frickenhausen, Germany
Cell culture plates	Cellstar Suspension Culture Plates 6-, 12-, 24-, 48-well flat-bottom	Greiner Bio-One, Frickenhausen, Germany
	Cellstar Suspension Culture 96-well round-/flat-bottom	Greiner Bio-One, Frickenhausen, Germany
Cell strainer	Cell strainer 40µm	BD Biosciences, Heidelberg, Germany
	Celltrics 50 µm	Partec, Münster, Germany
Cover glasses	Cover glasses for haemocytometer	Menzel-Gläser, Braunschweig, Germany
	Cover Glasses 24 x 60 mm	Th. Geyer, Renningen, Germany
Cover sheets for qRT-PCR	MicroAmp Optical Adhesive Film	Applied Biosystems, Foster City, CA, USA
Cuvettes	UVette 200-1600 nm	Eppendorf, Hamburg, Germany
ELISA plates	Nunc Maxisorp flat-bottom 96 well plates	eBioscience, San Diego, CA, USA
FACS tubes	5 ml polystyrene round-bottom tubes	BD Biosciences, Heidelberg, Germany
Glass ware	various	Schott, Mainz, Germany
Glassfibre filters	Filtermat A	Perkin Elmer, Rodgau, Germany
Haemocytometer	Acc. to Neubauer	HBG Henneberg-Sander, Giessen-Lützelinden, Germany

MATERIAL AND METHODS

I.V. Catheter	Venflon Pro 22G x 25 mm	BD Biosciences, Heidelberg, Germany
MACS Columns	LS Separation Columns autoMACS Columns	Miltenyi Biotech, Bergisch Gladbach, Germany
Microscope slides	SuperFrost Plus	Menzel-Gläser, Braunschweig, Germany
Needles	BD Microlance 3 0,4x19 mm	BD Biosciences, Heidelberg, Germany
	BD Microlance 3 0,5x16 mm	
	Sterican 0,45x12 mm	B. Braun, Melsungen, Germany
	Sterican 0,55x25 mm	
PCR reaction tubes	Multiply- μ Strip Pro 8-strip	Sarstedt, Nümbrecht, Germany
Pipette tips	Ultratip 1000 μ l	Greiner Bio-One, Frickenhausen, Germany
	Ultratip 200 μ l	
	Pipette tip 10 μ l	Sarstedt, Nümbrecht, Germany
Reaction plates for qRT-PCR	96-well Optical reaction plate	Applied Biosystems, Foster City, CA, USA
Reaction tubes	Cellstar 50 ml PP	Greiner Bio-One, Frickenhausen, Germany
	Cellstar 15 ml PP	
	Reaction tube 2 / 1,5 / 0,5 ml	
Serological pipettes	Cellstar 5 / 10 / 25 ml	Greiner Bio-One, Frickenhausen, Germany
Solid Scintillator	MeltiLex	Perkin Elmer, Rodgau, Germany
Syringes	Discardit II 2 ml	BD Biosciences, Heidelberg, Germany
	Discardit II 5 ml	
	Soft-Ject 1 ml Tuberkulin	Henke-Sass Wolf, Tuttlingen, Germany
	Omnican 40 1 ml	B. Braun, Melsungen, Germany
Syringe filters	Filtropur S 0,2 μ l	Sarstedt, Nümbrecht, Germany
	Filtropur S 0,45 μ l	
Tissue cassettes	MacrOfFlow	Microm International, Walldorf, Germany

2.1.3 Chemicals and Reagents

Name	Manufacturer
2'-deoxythymidine triphosphate [³ H]	Hartmann Analytic, Braunschweig, Germany
2-Propanol Rotipuran p.a.	Carl Roth, Karlsruhe, Germany
7-Aminoactinomycin D	BD Biosciences, Heidelberg, Germany
Acetic acid glacial Rotipuran 100% p.a.	Carl Roth, Karlsruhe, Germany
Albumin from chicken egg white, Grade V	Sigma-Aldrich, Taufkirchen, Germany
Allhydrogel 2% VacciGrade	Sigma-Aldrich, Taufkirchen, Germany
Ammonium chloride p.a.	Merck, Darmstadt, Germany
Bovine Serum Albumin	PAA Laboratories, Pasching, Austria
Citric acid monohydrate p.a.	Merck, Darmstadt, Germany
Concanavalin A	Sigma-Aldrich, Taufkirchen, Germany
Dexamethasone, water soluble	Sigma-Aldrich, Taufkirchen, Germany
Dimethyl sulfoxide ≥99,8 % Rotipuran p.a.	Carl Roth, Karlsruhe, Germany
Di-sodium hydrogen phosphate Dodecahydrate ≥99% p.a.	Carl Roth, Karlsruhe, Germany
Entellan new	Merck, Darmstadt, Germany
Eosin (yellowish)	Merck, Darmstadt, Germany
Ethanol ≥99,8% p.a.	Carl Roth, Karlsruhe, Germany
Ethylenediaminetetraacetic acid tetrasodium salt hydrate ≥95% p.a.	Sigma-Aldrich, Taufkirchen, Germany
Ethidium bromide solution 1%	Carl Roth, Karlsruhe, Germany
Fetal Bovine Serum	Invitrogen, Carlsbad, CA, USA
Freunds Adjuvant Complete	Sigma-Aldrich, Taufkirchen, Germany
GeneRuler 1kb DNA ladder	Fermentas, St. Leon-Rot, Germany
Hem Alum solution acid acc. to Mayer	Carl Roth, Karlsruhe, Germany
Hydrogen peroxide 30% Rotipuran p.a.	Carl Roth, Karlsruhe, Germany
Ketamin 10%	MediStar, Ascheberg, Germany
Monopotassium phosphate p.a.	Merck, Darmstadt, Germany
Neomycin trisulfate salt hydrate p.a.	Sigma-Aldrich, Taufkirchen, Germany
Orange G	Sigma-Aldrich, Taufkirchen, Germany
Paraffin wax for histology	Sigma-Aldrich, Taufkirchen, Germany
PCR dNTP Mix	Genaxxon Bioscience, Ulm, Germany
Penicillin / Streptomycin	Invitrogen, Carlsbad, CA, USA
Potassium chloride p.a.	Merck, Darmstadt, Germany

Potassium dihydrogen phosphate p.a.	Merck, Darmstadt, Germany
Potassium hydrogen carbonate p.a.	Merck, Darmstadt, Germany
Protein G Plus Agarose	Santa Cruz Biotechnology, Heidelberg, Germany
Rompun 2%	Bayer, Leverkusen, Germany
Roti Histofix 4%	Carl Roth, Karlsruhe, Germany
Sevorane	Abbott, Wiesbaden, Germany
Sodium azide p.a.	Sigma-Aldrich, Taufkirchen, Germany
Sodium carbonate p.a.	Merck, Darmstadt, Germany
Sodium chloride ≥99,5% p.a.	Carl Roth, Karlsruhe, Germany
Sodium dodecyl sulphate ≥99% p.a.	Carl Roth, Karlsruhe, Germany
Sodium hydrogen carbonate p.a.	Merck, Darmstadt, Germany
Sulfuric acid 95-98% p.a.	Merck, Darmstadt, Germany
Tetramethylbenzidine 3,3',5,5'	Sigma-Aldrich, Taufkirchen, Germany
Tris Pufferan ≥99,9% p.a.	Carl Roth, Karlsruhe, Germany
Trypsin-EDTA 25%	Invitrogen, Carlsbad, CA, USA
Tween 20	Carl Roth, Karlsruhe, Germany
UltraPure Agarose	Invitrogen, Carlsbad, CA, USA
Xylol (isomers) >98% p.a.	Carl Roth, Karlsruhe, Germany

2.1.4 Media, Buffer and Solutions

2.1.4.1 Media

RPMI / FBS / PS

500 ml	RPMI Medium 1640 + GlutaMAX (Invitrogen, Carlsbad, CA, USA)
10%	FBS
100 U / ml	Penicillin
100 µg / ml	Streptomycin

DMEM / FBS / PS

500 ml	DMEM + GlutaMAX (Invitrogen, Carlsbad, CA, USA)
10%	FBS
100 U / ml	Penicillin
100 µg / ml	Streptomycin

L Cell Conditioned Medium (LCCM)

Supernatant of cultivated L292 cell line, see section 2.2.2.1.5.1.

2.1.4.2 Buffers and solutions

Cell dissociation buffer, enzyme-free

Invitrogen, Carlsbad, CA, USA

PBS

1000 ml	H ₂ O
80 g	NaCl
29 g	Na ₂ HPO ₄ x 12H ₂ O
2 g	KCl
2 g	KH ₂ PO ₄
pH	7,2 – 7,3

PBS / BSA

1000 ml	PBS
1 %	BSA

PBS / Tween

1000 ml	PBS
0,1 %	Tween 20

MACS Buffer

1000 ml	PBS
0,5 %	BSA
2 mM	EDTA

MACS Rinse Buffer

1000 ml	PBS
2 mM	EDTA

FACS Buffer

1000 ml	PBS
0,1 %	BSA
0,01 %	NaN ₃

Erythrocyte Lysis Buffer

1000 ml	di H ₂ O
168 mM	NH ₄ Cl
10 mM	KHCO ₃
0,1 mM	EDTA

TAC Buffer

1000 ml	di H ₂ O
155 mM	NH ₄ Cl
20 mM	Tris
pH	7,2

Tail Buffer

1000 ml	di H ₂ O
1 %	SDS
100 mM	NaCl
100 mM	EDTA
5 mM	Tris

TE Buffer

1000 ml	di H ₂ O
10 mM	Tris
1 mM	EDTA
pH	8,0

TAE Buffer

1000 ml	di H ₂ O
4,8 g	Tris
1,1 g	Acetic acid glacial
0,29 g	EDTA

Sodium Carbonate Coating Buffer

1000 ml	di H ₂ O
7,13 g	NaHCO ₃
1,59 g	Na ₂ CO ₃
pH	9,5

Substrate Solution (ELISA)

10 ml	Substrate Buffer
1 mg	TMB
100 µl	DMSO
20 µl	3,5% H ₂ O ₂

Substrate Buffer (ELISA)

1000 ml	di H ₂ O
21 g	citric acid
71,7 g	Na ₂ HPO ₄ x 12H ₂ O

2.1.5 Enzymes

Name	Manufacturer
Taq-Polymerase with Buffer S	Genaxxon Bioscience, Ulm, Germany
Proteinase K	Applichem, Darmstadt, Germany

2.1.6 Antibodies for flow cytometry, cell separation and stimulation

Specificity	Clone	Isotype	Conjugation	Application	Manufacturer
CD3	17A2	Rat IgG2b, κ	PerCP/Cy5.5	FACS	BioLegend
CD3ε	145-2C11	Hamster IgG1, κ	-	<i>In vitro</i> stimulation	BD Biosciences
CD3ε	145-2C11	Hamster IgG1, κ	-	<i>In vitro</i> stimulation	BioLegend
CD4	RM4-5	Rat IgG2a, κ	PerCP	FACS	BD Biosciences
CD4	RM4-5	Rat IgG2a, κ	APC	FACS	BD Biosciences
CD8α	53-6.7	Rat IgG2a, κ	PE	FACS	BD Biosciences
CD8α	53-6.7	Rat IgG2a, κ	PE-Cy7	FACS	eBioscience

MATERIAL AND METHODS

CD11b	M1/70	Rat IgG2b, κ	PE-Cy7	FACS	BD Biosciences
CD16/ CD32	2.4G2	Rat IgG2b, κ	-	FACS	BD Biosciences
CD25	PC61	Rat IgG1, λ	APC-Cy7	FACS	BD Biosciences
CD28	37.51	Hamster IgG2, λ1	-	<i>In vitro</i> stimulation	BD Biosciences
CD28	37.51	Hamster IgG2, λ1	-	<i>In vitro</i> stimulation	BioLegend
CD44	IM7	Rat IgG2b, κ	PE	FACS	BD Biosciences
CD45R/ B220	RA3-6B2	Rat IgG2a, κ	PE	FACS	BD Biosciences
CD69	H1.2F3	Hamster IgG1, λ3	Biotin	FACS	BD Biosciences
CD90.2	n/s	Rat IgG2b	Microbeads	Cell separation	Miltenyi Biotech
βTCR	H57-597	Hamster IgG2a, λ1	FITC	FACS	BD Biosciences
Biotin	-	(Streptavidin)	APC-Cy7	FACS	BD Biosciences
F4/80	CI:A3-1	Rat IgG2b	FITC	FACS	BioLegend
FoxP3	FJK-16S	Rat IgG2a, κ	APC	FACS	eBioscience
GITR	DTA-1	Rat IgG2b, λ	PE-Cy7	FACS	BD Biosciences
Ly-6G/-6C	RB6-8C5	Rat IgG2b, κ	APC-Cy7	FACS	BD Biosciences
Mouse IgE	polyclonal	Goat	HRP	Serum ELISA	Southern Biotech
Mouse IgG1	polyclonal	Goat	HRP	Serum ELISA	Southern Biotech
Mouse IgG2a	polyclonal	Goat	HRP	Serum ELISA	Southern Biotech

Siglec-F	E50-2440	Rat	PE	FACS	BD
		IgG2a, κ			Biosciences

Note: Antibodies which were part of commercially available assay are not included in this list.

<u>Manufacturer Information:</u>	BD Biosciences	Heidelberg, Germany
	BioLegend	San Diego, CA, USA
	eBioscience	San Diego, CA, USA
	Southern Biotech	Birmingham, AL, USA

2.1.7 Commercial Assays

Name	Manufacturer
CD4 ⁺ CD25 ⁺ Regulatory T Cell Isolation Kit, Mouse	Miltenyi Biotec, Bergisch Gladbach, Germany
Foxp3 / Transcription Factor Staining Buffer Set	eBioscience, San Diego, CA, USA
iScript cDNA Synthesis Kit	Bio-Rad Laboratories, München, Germany
Mouse IFN- γ ELISA MAX Standard	BioLegend, San Diego, CA, USA
Mouse IL-2 ELISA MAX Standard	BioLegend, San Diego, CA, USA
OptEIA Mouse IFN- γ ELISA Set	BD Biosciences, Heidelberg, Germany
OptEIA Mouse IL-2 ELISA Set	BD Biosciences, Heidelberg, Germany
Pan T Cell Isolation Kit II, Mouse	Miltenyi Biotec, Bergisch Gladbach, Germany
Power SYBR Green PCR Master Mix	Applied Biosystems, Foster City, CA, USA
Quick-RNA MiniPrep	Zymo Research, Irvine, CA, USA

2.1.8 Oligonucleotides

All oligonucleotides were purchased from Metabion, Martinsried, Germany or Qiagen, Hilden, Germany.

2.1.8.1 Oligonucleotides for genotyping

A - Transcript, B - Name, C - Sequence, D - Melting temperature, E - Amplicon size, F - Reference

A	B	C	D	E	F
Ptch wt	DelNx Fwd	TGGTAATTCTGGGCTCCCGT	61 °C	445 bp	Uhmann et al., 2007; Zibat et al., 2009
	wt Rev	TCAAGGAGCAGAGGCCCAA	61 °C		
Ptch del	DelNx Fwd	TGGTAATTCTGGGCTCCCGT	61 °C	150 bp	Uhmann et al., 2007; Zibat et al., 2009
	Nx Rev	CCGGTAGAATTAGCTTGAAGTTCCT	61 °C		
CD4Cre	GT1 Fwd	CCAGGCTAAGTGCCTTCTCTACA	62 °C	500 bp	Uhmann et al., 2011
	GT1	AATGCTTCTGTCCGTTTGCCGGT	66 °C		
	Rev				

2.1.8.2 Oligonucleotides for qRT-PCR

A - Transcript, B - Name, C - Sequence, D - Melting temperature, E - Amplicon size, F - Reference

A	B	C	D	E	F
Ptch wt	mPtch11	AAAGCCGAAGTTGGCCATGGGTAC	66 °C	263 bp	Uhmann et al., 2011
	mPtch-tq- Ex8R	TGCTTGGGAGTCATTAAGTGA	59 °C		
Ptch del	mPtch11	AAAGCCGAAGTTGGCCATGGGTAC	66 °C	237 bp	Uhmann et al., 2011
	mPtch-tq- Ex7/10R2	TAAACAGGCATAGGCAAGCTGAC	62 °C		
Ptch2	mPtch2-F	TCCAAGTATCACTCTATGGGAAATC	60 °C	116 bp	This work
	mPtch2-R	TTCTCAATCATCCGCTCGAT	61 °C		
Gli1	mGli1-tq-F	TACATGCTGGTGGTGCACATG	61 °C	115 bp	Nitzki et al., 2011
	mGli1-tq-R	ACCGAAGGTGCGTCTTGAGG	62 °C		
Gli2	Gli2-RT- PCR-F	GGTCATCTACGAGACCAACTGC	61 °C	272 bp	Uhmann et al., 2011
	Gli2-RT- PCR-R	GTGTCTTCAGGTTCTCCAGGC	61 °C		
HPRT1	HPRT1-F	GTCCTGTGGCCATCTGCCTA	62 °C	91 bp	Anna Karabinskaya (unpublished)
	HPRT1-R	GGGACGCAGCAACTGACATT	61 °C		

2.1.9 Cell lines

L292

L292 is a murine aneuploid fibrosarcoma cell line (Earle et al., 1943) which is frequently used as a source for macrophage colony-stimulating factor (M-CSF), a cytokine that promotes the differentiation of haematopoietic stem cells into macrophages (Ladner et al., 1988). The cell line was kindly provided by Prof. Dr. Jan Tuckermann from the Institute of General Zoology and Endocrinology at Ulm University, Ulm, Germany.

B16F10

B16F10 (Fidler, 1973) is a melanoma cell line of B6 mouse origin which developed spontaneously and has been used extensively as a highly aggressive model for murine tumour immunotherapy studies (Wang et al., 1998). Cells were a kind gift from Prof. Dr. Michael Schön, Department of Dermatology, University Medical Centre Göttingen, Germany.

2.1.10 Mice

C57BL/6N

An inbred strain with a characteristic black fur colour. Mice were obtained from Charles River Laboratories, Wilmington, USA.

BALB/c

An inbred strain with a characteristic white fur colour. Mice were obtained from Charles River Laboratories, Wilmington, USA.

$CD4Cre^{+/-} Ptch^{flox/flox}$

$CD4Cre^{+/-} Ptch^{flox/flox}$ mice were kindly provided by Prof. Dr. Heidi Hahn from the Institute of Human Genetics in Göttingen. They were generated by crossing $Ptch^{flox/flox}$ mice (Uhmann et al., 2007) with $CD4Cre$ transgenic mice that express the P1 bacteriophage-derived Cre recombinase under the control of the CD4 promoter (Wolfer et al., 2001). Expression of the Cre recombinase starts from DN3 stage of thymocyte development and catalyses the excision of exons 8 and 9 of $Ptch^{flox}$ alleles which additionally leads to a frame-shift in the following exons 10-23. This results in the generation of transcripts that cannot be translated into functional proteins. While mice with a mixed C57BL/6 and BALB/c genetic background were used for some *in vitro* investigations, most *in vitro* and all *in vivo* experiments were performed with mice that had been backcrossed to the C57BL/6 background for more than 10 generations.

2.1.11 Software

Name	Developer
4D v12	4D, Eching, Germany
Adobe Photoshop CS v8.01	Adobe Systems, San Jose, CA, USA
analySIS ^B	Olympus, Tokio, Japan
BD FACSDiva Software v6.1.2	BD Biosciences, Heidelberg, Germany
Gen5 v1.09.8	BioTek Instruments, Bad Friedrichshall, Germany
GraphPad Prism v5.04	GraphPad Software, La Jolla, CA, USA
Intas GDS	Intas, Göttingen, Germany
MicroBeta ² Windows Workstation v1.0	Perkin Elmer, Rodgau, Germany
MS Office 2003 SP3	Microsoft, Redmond, WA, USA
Sequence Detection Software v1.4	Applied Biosystems, Foster City, CA, USA

2.2 Methods

2.2.1 General animal work

2.2.1.1 Mouse husbandry

Mice were kept alone or in groups either in Makrolon cages type II and III (Tecniplast, Hohenpreißenberg, Germany) at the Institute of Human Genetics or under specific pathogen free (SPF) conditions in individually ventilated cages (IVC) at the European Neuroscience Institute (both part of the University Medical Center Göttingen, Göttingen, Germany). A 12 hour day/night cycle and constant temperature and humidity levels were maintained throughout breeding and experiments. Animals were provided with a standard laboratory rodent diet and drinking water *ad libitum*. All animal experiments were conducted in accordance with the ethical standards of humane animal care and approved by the appropriate authorities in Lower Saxony (LAVES).

2.2.1.2 Identification and genotyping of *CD4Cre*^{+/-} *Ptch*^{flox/flox} mice

Identification of individual animals was achieved using ear markings which were applied four weeks after birth. Tail biopsies were collected at the same time point and stored at -20 °C before they were used for genotyping. Therefore, genomic DNA was isolated from biopsies

and used for a polymerase chain reaction (PCR)-based characterisation with previously described primer combinations. (Uhmann et al., 2007; Zibat et al., 2009; Uhmann et al., 2011).

2.2.1.3 Tissue preparation and isolation of cells

2.2.1.3.1 Lymphocytes

Lymphocytes were either isolated from the spleen or from lymph nodes (nodi lymphoidei cervicales, nodi lymphoidei axillares, nodi lymphoidei inguinales, nodi lymphoidei mesenterici). Mice were sacrificed by cervical dislocation, the tissue was extracted and placed in a small petri dish with PBS / BSA. Tissue forceps were employed for mechanical breakup of the tissue and the emerging cell suspension was passed through a 40 µm cell strainer to remove cell clusters. The cells were then washed in PBS / BSA and centrifuged at 330 x g for 6 minutes.

2.2.1.3.2 Thymocytes

For isolation of thymocytes, mice were sacrificed in a carbon dioxide atmosphere and the thymi were extracted. Mechanical breakup and generation of a single cell suspension was achieved as described before.

2.2.1.3.3 Bone Marrow

Mice were sacrificed by cervical dislocation, hind limbs were dissected and femurs and tibiae cleaned from remaining tissue. Both ends were opened up with a scissor and the BM was flushed out with cold PBS / BSA using a syringe with a needle of the appropriate size. The BM was then resuspended several times to produce a homogenous cell suspension which was additionally passed through a 40 µl nylon strainer. Finally, the cells were washed in PBS / BSA and centrifuged at 330 x g for 6 minutes.

2.2.1.4 Anaesthesia

2.2.1.4.1 Short-term anaesthesia

For intranasal application of dissolved Ova, mice were lightly anaesthetised with sevoflurane (Sevorane). Induction and recovery from this inhalation anaesthesia proceeded quickly while mice remained unconscious for approximately 10 seconds.

2.2.1.4.2 Extended anaesthesia

An extended anaesthesia was used for fur removal prior to tumour induction and for the subcutaneous application of B16F10 melanoma cells itself. To this end, 10 µl of sterile PBS with 1% ketamin hydrochloride (Ketamin) and 0,4 ‰ xylazin hydrochloride (Rompun) were administered intraperitoneally per gram of body weight. Induction of anaesthesia occurred after 2-3 minutes and lasted for approximately 60 minutes. Mice were kept warm during anaesthesia to prevent hypothermia.

2.2.1.5 Irradiation

Mice were placed in an individually manufactured plastic box and irradiated with a RS 225 X-Ray Research System which was operated at 150 kV, 15 mA and with a 0,5 mm Cu filtration. A radiation dose of 1 Gy / min was given for a time of 8,5 minutes which resulted in a total radiation of 8,5 Gy.

2.2.2 *In vitro* methods

2.2.2.1 Cell culture

Manipulation of cells was always performed under sterile conditions using a laminar airflow workbench and sterile equipment. Unless stated otherwise, cells were centrifuged at 330 x g and 4°C for 6 minutes and incubated at 37°C under a humidified atmosphere of 5% CO₂.

2.2.2.1.1 Cell counting

Cell numbers were determined using a counting chamber according to Neubauer. With respect to the expected cell number, the cell suspension was diluted to a concentration of approximately 10^6 cells / ml and a minimum of 2 opposing quadrants were counted. Erythrocytes and apoptotic cells were morphologically identified and excluded. The total cell number was calculated according to the following formula: Average cells per quadrant x 10^4 x dilution x total volume.

2.2.2.1.2 Haemolysis

Removal of erythrocytes from isolated lymphocytes or thymocytes was achieved using erythrocyte lysis buffer or TAC buffer. If erythrocyte lysis buffer was used, cells were resuspended in 2 ml PBS, 5 ml buffer were added and the suspension was incubated for 5 minutes on ice. The reaction was stopped by adding 43 ml PBS / BSA and the cells were centrifuged. TAC buffer was exclusively employed to remove erythrocytes from total splenocytes which were used for *ex vivo* restimulation in allergic airway inflammation experiments. Here, cells were resuspended in 1 ml PBS and 6 ml TAC buffer were added before the cells were incubated for 12 min on ice. The reaction was also stopped by adding 43 ml PBS / BSA and the cells were centrifuged.

2.2.2.1.3 Thawing of cryopreserved cells

Cell aliquots which had been stored at -150°C were rapidly thawed at 37°C in a water bath and poured into a 50 ml reaction tube containing prewarmed medium and FBS at a ratio of 1:1. The cells were then centrifuged at $330 \times g$ and room temperature for 6 minutes before the supernatant was discarded. Cells were subsequently resuspended in prewarmed medium and placed in an incubator.

2.2.2.1.4 Detachment of adherent cells

In vitro differentiated macrophages were placed on ice for 15 minutes to induce retraction of cell protrusions. After that, the medium was removed and replaced with 1 ml cell dissociation buffer before the cells were incubated for another 5 minutes at 37°C in an incubator. Cells were then detached by rinsing with PBS, collected in a 50 ml reaction tube and washed with PBS / BSA. For detaching B16F10 melanoma and L929 cells, the medium was removed and the cells were washed twice with PBS. Depending on the size of the petri dish or culture flask, between 1 and 5 ml Trypsin-EDTA were added and the cells were incubated at 37°C

for 2-4 minutes. The dissociation process was frequently controlled under the microscope and stopped when the cells were almost completely detached by adding a large volume of PBS / BSA. Remaining adherent cells were rinsed off and the suspension was transferred to a 50 ml reaction tube and washed with PBS / BSA.

2.2.2.1.5 Generation of bone marrow-derived macrophages

2.2.2.1.5.1 Preparation of L cell conditioned medium

LCCM was used a source for M-CSF to promote the differentiation of HSCs into macrophages. L929 cells were thawed as described, resuspended in DMEM / FBS / PS and placed in a 10 cm petri dish which was incubated at 37°C and 5% CO₂ until the cell were grown to confluence. Cells were detached and washed, resuspended in fresh medium and split onto five 10 cm petri dishes. After the cells had grown to confluence again they were detached, washed and transferred with 40 ml of fresh medium into 175 cm² cell culture flasks. The conditioned medium was collected every other day, immediately frozen at -20°C and replaced with fresh medium. This procedure was repeated another three times before the cells were discarded. Prior to usage, the medium was thawed and diluted at a ratio of 1:4 with DMEM / FBS / PS.

2.2.2.1.5.2 *In vitro* differentiation of macrophages

A BM suspension was prepared from femurs and tibiae as described. Cells were washed in PBS / BSA, resuspended in 10 ml LCCM and transferred into a 175cm² cell culture flask in which they were incubated over night. On the following day, non-adherent cells were separated from adherent fibroblasts and stroma cells by soft rinsing. The medium containing the HSCs was split onto two 10 cm suspension culture petri dishes and 5 ml of fresh LCCM were added to each plate. After four days of incubation, an additional 5 ml LCCM were added and the cells were incubated for another 2-4 days. The differentiation process was controlled daily with a microscope and evaluated according to the cell's morphological changes. Finally, the cells were detached as described and tested by FACS with antibodies against F4/80 and CD11B in conjunction with a 7-Aminoactinomycin D (7-AAD) staining to identify apoptotic cells. On average, the cell viability was greater than 90% while more than 99% showed a high expression of both surface markers.

2.2.2.1.6 Cultivation of B16F10 melanoma cells

The mouse melanoma cell line B16F10 was cultured in RPMI / FCS / PS and taken into culture 3 days before usage. Cells of an identical passage number were used for all experiments.

2.2.2.2 Cell purification and depletion

Magnetic purification or depletion of cells was achieved using the autoMACS separator. The device was operated according to the manufacturer's instructions.

2.2.2.2.1 Isolation of conventional T cells

Conventional T cells were negatively isolated using the Miltenyi Pan T Cell Isolation Kit II. Spleens with or without lymph nodes were dissected, a homogenous single cell suspension was generated and the cells were counted as described. The cells were then washed and resuspended in 4 μ l MACS buffer plus 1 μ l biotin-antibody cocktail per 10^6 cells. After an incubation period of 10 minutes at 4°C, another 3 μ l buffer and 2 μ l anti-biotin microbeads were added per 10^6 cells. The suspension was mixed and incubated again at 4°C for 15 minutes. Finally the cells were washed in 30 ml MACS buffer, passed through a 50 μ l cell strainer and resuspended in a maximum volume of 2×10^9 cells per ml in MACS buffer before they were placed in the autoMACS separator and separated using the DEplete-Program. After separation, the cells were washed in PBS / BSA, counted and a sample was collected for FACS analysis. The average yield was 12-18% of nucleated cells with a purity of approximately 93% cells as defined by β -TCR expression.

2.2.2.2.2 Isolation of regulatory T cells

T_{reg} cells were isolated using the Miltenyi CD4⁺ CD25⁺ Regulatory T Cell Isolation Kit. Spleens were dissected, a single cell suspension was generated and the cells were washed and counted as described. For 10^6 cells, 4 μ l MACS buffer and 1 μ l biotin-antibody cocktail were added to the cells which were then incubated for 10 minutes at 4°C. Afterwards, 3 μ l MACS buffer were added together with 2 μ l anti-biotin microbeads and 1 μ l anti-CD25-PE per 10^6 cells. The suspension was mixed and incubated at 4°C for another 15 minutes. Cells were washed in 30 ml MACS buffer, passed through a 50 μ l cell strainer and resuspended in a maximum volume of 2×10^9 cells per ml in MACS buffer. Negative isolation of CD4⁺ T cells was achieved using the DEPL025 program of the autoMACS separator. Cells were washed after the separation, counted and resuspended in 9 μ l MACS buffer and 1 μ l anti-PE

microbeads per 10^6 cells. After a 15 minute incubation period at 4°C the cells were washed again with 30 ml MACS buffer and passed through a $50\ \mu\text{l}$ cell strainer. $\text{CD4}^+ \text{CD25}^+ \text{DP}$ and $\text{CD4}^+ \text{CD25}^- \text{SP}$ cells were finally separated using the POSSELD2 program of the autoMACS device. On average, the yield for $\text{CD4}^+ \text{CD25}^+$ cells was 2% of total cells with a purity of $>95\%$ as revealed by FACS analysis. Further discrimination between T_{reg} cells and activated conventional T_{h} cells within the $\text{CD4}^+ \text{CD25}^+$ population was achieved by an additional staining against FoxP3 and glucocorticoid induced tumour necrosis factor receptor family related gene (GITR). This revealed that on average $>85\%$ of isolated $\text{CD4}^+ \text{CD25}^+$ cells were *bona fide* T_{reg} cells.

2.2.2.2.3 Generation of T cell depleted bone marrow

T cells were removed from total BM using CD90.2 microbeads (Miltenyi) in aGvHD experiments. For this purpose, a single cell suspension was generated from BM as described. Cells were resuspended in $9\ \mu\text{l}$ MACS buffer plus $0,6\ \mu\text{l}$ anti-CD90.2 microbeads per 10^6 cells and incubated at 4°C for 20 minutes. After a washing step with 10 ml MACS buffer, the cells were passed through a $50\ \mu\text{l}$ cell strainer and resuspended in a maximum volume of 2×10^9 cells per ml in MACS buffer. Depletion of CD90.2 positive cells was accomplished with the DELPLETES program of the autoMACS separator. Successful depletion of T cells from the BM was verified by FACS with a staining against the TCR β -chain. Percentage of residual T cells among BM cells was routinely well below 1%.

2.2.2.3 Proliferation assays

2.2.2.3.1 Allogenic stimulation of T cells

Allogenic stimulation of Ptch-deficient and wild type T cells was performed in the setting of a mixed leukocyte reaction (MLR). T cells were isolated from $\text{CD4Cre}^{+/-} \text{Ptch}^{\text{flox/flox}}$ and $\text{Ptch}^{\text{flox/flox}}$ mice (C57/BL6 background) while macrophages were generated from the BM of BALB/c mice as described. 10^5 T cells were cocultured with an equal amount of BM derived macrophages (BMDM) in a total volume of $200\ \mu\text{l}$ RPMI / FBS / PS in 96-well round-bottom plates. T cells or macrophages alone served as negative controls while T cells activated with $2,5\ \mu\text{g} / \text{ml}$ Concanavalin A (ConA) were used as positive controls. All samples were analysed in triplicates to increase the informative value of the data. After a culture period of 72 hours, $50\ \mu\text{l}$ of supernatant was removed from each well and replaced with fresh medium containing tritiated thymidine with an activity of $740\ \text{kBq} / \text{ml}$. Supernatants were immediately

frozen at -20°C and used later for cytokine analysis. After another incubation of 16 hours, the cells were harvested and proliferation was determined by scintillation counting.

2.2.2.3.2 Polyclonal stimulation of T cells

T cells were isolated from *CD4Cre^{+/-} Ptch^{flox/flox}* and *Ptch^{flox/flox}* mice. 10^5 cells per well were seeded in 96-well flat-bottom plates in a total volume of 200 µl RPMI / FBS / PS. Stimulation was achieved by the addition of either ConA or soluble antibodies against CD3 ϵ and CD28 in optimal (2,5 µg / ml and 1,0 µg / ml each) or suboptimal (0,5 µg / ml and 0,01 µg / ml each) concentrations, respectively. T cells alone were used as negative controls and all samples were analysed in triplicates. After 24, 48 and 72 hours of culture, 50 µl of supernatant were removed from each well and replaced with fresh medium containing tritiated thymidine with an activity of 740 kBq / ml. The supernatants were immediately frozen at -20°C and used later for cytokine analysis while the cells were harvested and proliferation was determined by scintillation counting after an additional incubation of 16 hours.

2.2.2.3.3 Suppression assays

Suppression assays were performed for functional analysis of T_{reg} cells *in vitro*. Therefore, CD4⁺ CD25⁺ T_{reg} cells and CD4⁺ CD25⁻ T_h cells were isolated from *CD4Cre^{+/-} Ptch^{flox/flox}* and *Ptch^{flox/flox}* mice. 10^5 T_{reg} cells were seeded in 96-well round-bottom plates together with T_h cells at ratios of 1:1, 1:5, 1:10, 1:15 and 1:25 in a total volume of 200 µl RPMI / FBS / PS. Polyclonal stimulation was achieved by adding 1 µg / ml soluble anti-CD3 ϵ and 5 µg / ml anti-CD28 antibodies into the cultures. T_{reg} or T_h cells alone as well as stimulated T_{reg} cells served as negative controls while stimulated T_h cells were used as positive controls. Analysis was performed in triplicates for all samples. Supernatants were removed after 48 hours of culture, frozen at -20°C and used for later detection of cytokines.

2.2.2.3.4 Ex vivo restimulation of T cells with Ovalbumin

An *ex vivo* restimulation of T cells with Ova was performed in allergic airway inflammation experiments. For this purpose mice were sacrificed and single cell suspensions were generated from the spleens as described. 3×10^5 splenocytes were seeded in 96-well flat-bottom plates either alone or together with Ova in a concentration of 10 µg / ml in a total volume of 200 µl RPMI / FBS / PS. Cells were alternatively activated with 2,5 µg / ml ConA to obtain a positive control for cell responsiveness. All samples were analysed in triplicates. After an incubation period of 72 hours, 50 µl of supernatant was removed from each well and replaced with fresh medium containing tritiated thymidine with an activity of 740 kBq / ml.

Supernatants were immediately frozen at -20°C and used later for cytokine analysis. After another incubation of 16 hours, the cells were harvested and the proliferation was determined by scintillation counting.

2.2.2.3.5 Solid scintillation counting

Proliferation of T cells in *in vitro* assays was quantified by the metabolic incorporation of tritiated thymidine (³H-TdR) which was detected by solid scintillation counting. After incubation with ³H-TdR for 16 hours, the cells were harvested with a MicroBeta Filtermate-96 Harvester and the labelled DNA was collected onto Filtermat A glassfibre filters. The filters were allowed to dry at room temperature for at least 2 hours before the solid scintillator (MeltiLex) was melted onto them using a microwave oven. After the scintillator had solidified again at room temperature, the filters were placed in counting cassettes and the incorporated radioactivity was indirectly measured using a MicroBeta² β-scintillation counter.

2.2.2.4 Enzyme-linked Immunosorbent Assay

Enzyme-linked Immunosorbent Assays (ELISAs) were performed to detect cytokines in the supernatants of proliferation tests or Ova-specific immunoglobulins in the serum of animals during allergic airway inflammation experiments.

2.2.2.4.1 Detection of Cytokines

Secretion of the cytokines IL-2 and IFN-γ was quantified in the supernatant of proliferation- and suppression assays using commercially available assays from BD or Biolegend according to the manufacturer's instructions. In brief, the respective capture antibody was diluted in an assay-specific coating buffer and incubated over night at 4°C in Nunc MaxiSorp 96-well plates. On the following day, unbound capture antibody was removed and the wells were washed with PBS / Tween. The plates were then blocked with PBS with 10% FBS for one hour and washed again. Depending on the analysed cytokine, the samples were diluted between 1:2-fold and 1:5-fold before they were incubated together with a standard for two hours. In BioLegend assays, the samples were then incubated with a biotinylated detection antibody for one hour and with avidin-conjugated horseradish peroxidase (HRP) for another 30 minutes while both were incubated in parallel for one hour when assays from BD were used. Finally, the plates were washed and the substrate solution (see materials) was added before the plates were incubated for 5-20 minutes in the dark. The colour reaction was stopped with 50 µl 1M H₂SO₄ and the absorbance at 450 nm and 570 nm was examined with a microplate spectrophotometer.

2.2.2.4.2 Detection of Ovalbumin-specific Immunoglobulins

Detection of Ova-specific Immunoglobulins was performed in the serum of mice from allergic airway inflammation experiments. Therefore, Nunc MaxiSorp 96-well plates were coated with 50 µg / ml Ova dissolved in 100 µl sodium carbonate coating buffer per well and incubated at 4°C over night. On the following day, the plates were washed three times with PBS / Tween and subsequently blocked with 100 µl 10% FBS in PBS for one hour at room temperature. Serum samples were diluted 1000-fold and split for the detection of IgG and IgE isotypes. Samples for IgE detection were incubated with five volume percent Protein G coupled to agarose beads for one hour at room temperature on a sample shaker to remove antibodies of IgG isotypes. After this incubation, the solution was centrifuged at > 20.000 x g for five minutes and only the supernatant was used for IgE detection. The plate was then washed three times and, after 100 µl of each sample had been added, sealed and incubated at 4°C over night. On the next morning, the plates were washed and 100 µl of a 1:1000 dilution of anti-IgG1, anti-IgG2 and anti-IgE antibodies coupled to HRP were added to the samples and incubated for one hour at room temperature. After a final washing step, the substrate solution was added and plates were incubated for 1-5 minutes in the dark. As described before, the colour reaction was stopped with 50 µl 1M H₂SO₄ and the absorbance at 450 nm and 570 nm was examined with a microplate spectrophotometer.

2.2.2.5 Flow cytometry

2.2.2.5.1 Analysis of extracellular antigens

Approximately 10⁵ cells were transferred into FACS tubes, washed with 3 ml FACS buffer and centrifuged at 450 x g and 4°C for 5 minutes. The supernatant was discarded and the cells were resuspended in 200 µl FACS buffer. If necessary, the cells were incubated with anti-CD16/32 for 10 minutes to block F_C receptors and improve the subsequent staining. Afterwards, the respective fluorochrome- or biotin-conjugated antibodies were added to the cells. Optimal concentrations for individual antibodies were previously defined and ranged from dilutions of 200-fold to 2000-fold. The suspension was vortexed and incubated in the dark at 4°C for 15 minutes. When biotin-conjugated antibodies were used, the cells were washed and incubated again with fluorochrome-coupled streptavidin for another 15 minutes. Finally, the cells were washed with 3 ml FACS buffer, resuspended in 200 µl buffer and analysed.

2.2.2.5.2 Analysis of intracellular antigens

Intracellular detection of the transcription factor FoxP3 was performed using the FoxP3 / Transcription Factor Staining Buffer Set. Initially, staining of surface antigens was conducted for 10^6 cells as described above. The cells were then washed in 2 ml PBS at 450 x g and 4°C for 5 minutes and the supernatant was discarded. Fixation and permeabilisation of the cells for subsequent intracellular staining was achieved by adding 300 µl Fix / Perm under vortexing which was followed by a 30-minute incubation at room temperature. The cells were washed in 2 ml PBS and afterwards in 1 ml Perm buffer before a FoxP3-specific antibody was added. After another incubation period of 30 minutes, the cells were washed again with 1 ml Perm buffer and subsequently with 3 ml FACS buffer before they were analysed.

2.2.2.5.3 Apoptosis staining

Identification of apoptotic cells was achieved by using the fluorescent chemical compound 7-AAD which was applied in apoptosis assays as well as in most standard stainings. For this purpose, 1,5 µl of 7-AAD were added to the cells after the staining of extracellular antigens was completed. The suspension was vortexed and incubated at 4°C in the dark for 5 minutes. Thereafter, the cells were directly analysed

2.2.2.6 Histology

2.2.2.6.1 Tissue fixation

Histological analyses of lung tissue was performed in allergic airway inflammation experiments. Mice were sacrificed by cervical dislocation, the lungs were dissected, filled with a 4% paraformaldehyde solution (Roti Histofix) and incubated in the same solution at room temperature for two days. After this fixation step, the lungs were put into PBS for at least 2 hours, cut into small slices of approximately 2-4 mm diameter, embedded in biopsy pads and placed in tissue cassettes. These cassettes were again placed in PBS for at least one hour before the tissue was sequentially dehydrated through a series of graded ethanol baths and infiltrated with paraffin wax utilising a benchtop tissue processor according to the following protocol:

Step	Duration	Solution
Dehydration	60 min	50% EtOH
	60 min	70% EtOH
	2 x 60 min	80% EtOH
	2 x 90 min	96% EtOH
	2 x 90 min	99% EtOH
	2 x 60 min	Xylol
Paraffinisation	2 x 120 min	Paraffin

2.2.2.6.2 Preparation and sectioning of paraffin blocks

After the dehydration process, the tissue biopsies were placed in moulds which were filled with molten paraffin and attached to tissue cassettes using a tissue embedding station. The wax blocks were separated from the moulds when the paraffin had solidified and sectioned using a sliding microtome. For this purpose, the blocks were fixed on the microtome and aligned in the vertical plane. Slices were cut with a thickness of 5 μ m, stretched in a water bath at 40°C and floated onto the surface of microscope slides where they were dried at 37°C.

2.2.2.6.3 Hematoxylin and eosin stain

Once the microscope slides had dried, a hematoxylin and eosin (HE) stain was performed according to the following protocol:

Step	Duration	Solution
Deparaffinisation	2 x 15 min	Xylol
	2 x 3 min	99% EtOH
	2 x 3 min	96% EtOH
	2 x 3 min	70% EtOH
	2 x 3 min	de-ionized water
Staining of nuclei	10 min	Hem alum solution
	3 min	Running tap water
	10 min	de-ionized water
Staining of tissue	5 min	0,1% Eosin Y
	3 min	de-ionized water
Dehydration	2 x 3 min	70% EtOH
	2 x 3 min	96% EtOH
	2 x 3 min	99% EtOH
	2 x 15 min	Xylol

In brief, residual paraffin was removed from the tissue with decreasing alcohol concentrations. After the samples had been rehydrated, an acidic hemalum solution according to Mayer was used to obtain a blue staining of nuclei while yellowish eosin was used to colour eosinophilic structures in various shades of pink. Finally, the tissue slices were again dehydrated with increasing alcohol concentrations, embedded with Entellan and analysed microscopically.

2.2.3 Molecular biological methods

2.2.3.1 Isolation of genomic DNA from biopsies

Mouse tail biopsies were collected four weeks after birth. They were digested in 750 µl tail buffer supplemented with 200 µg Proteinase K at 54°C over night in a thermomixer. On the next day, 280 µl of saturated NaCl solution were added to precipitate proteins. The mixture was kept at room temperature for 5 minutes before it was centrifuged at > 20.000 x g for 10 minutes. 850 µl supernatant were transferred into another reaction tube containing 600 µl 2-propanol to precipitate the genomic DNA. The solution was vortexed and allowed to sit for 3 minutes at room temperature before it was centrifuged at > 20.000 x g for 10 minutes. After the supernatant was discarded, the DNA-containing pellet was washed with 500 µl 70%

EtOH and centrifuged again at $> 20.000 \times g$ for 5 minutes. Finally, the supernatant was completely removed and the DNA dried at 50°C for at least one hour before the pellet was resuspended in $100 \mu\text{l}$ TE buffer.

2.2.3.2 Isolation of total RNA from cells

Total RNA was prepared from cells with the help of the Quick-RNA MiniPrep kit. Up to 5×10^6 cells were placed in a $1,5 \text{ ml}$ reaction tube and centrifuged at $400 \times g$ and 4°C for 5 minutes. The supernatant was removed, the pellet resuspended in $600 \mu\text{l}$ ZR buffer and placed on a RNA-binding column. The lysate was centrifuged at $> 20.000 \times g$ and 4°C for one minute before the flow-through was discarded. After that, the column was washed sequentially with $400 \mu\text{l}$ pre-wash buffer for one minute, then with $700 \mu\text{l}$ and $400 \mu\text{l}$ wash buffer for 30 seconds each. After a penultimate centrifugation at $> 20.000 \times g$ for 2 minutes to remove residual wash buffer, the RNA was eluted by adding $50 \mu\text{l}$ of RNase-free water into a $1,5 \text{ ml}$ reaction tube at $> 20.000 \times g$ for 30 seconds. The concentration of the RNA was measured and the sample was immediately frozen at -150°C .

2.2.3.3 Measurement of nucleic acid concentration

Nucleic acid concentrations were determined photometrically. For this purpose, DNA or RNA samples were diluted 50-fold in $\text{di H}_2\text{O}$ and placed in photometric cuvettes which were analysed with a BioPhotometer.

2.2.3.4 Reverse Transcription

RNA samples were reverse transcribed employing the iScript cDNA Synthesis Kit for use in quantitative reverse transcription polymerase chain reactions (qRT-PCR). To this end, $1 \mu\text{g}$ of RNA was incubated with $0,25 \mu\text{l}$ Reverse Transcriptase and $4 \mu\text{l}$ $5\times$ iScript reaction mix in a total volume of $20 \mu\text{l}$. After a 5-minute incubation at 25°C , the transcription process was allowed to proceed at 42°C for another 30 minutes before the reaction was stopped at 85°C for 5 minutes. Complementary DNA (cDNA) was stored at -20°C until usage.

2.2.3.5 Polymerase Chain Reaction

PCR was used for genotyping of $CD4\text{Cre}^{+/-} Ptch^{\text{flox/flox}}$ mice. For this purpose, 1% of the genomic DNA which was extracted from tail biopsies was used. The respective forward and reverse oligonucleotides were added in a concentration of 400 nM each together with 5 mM PCR dNTP mix, 10% Buffer S and 2 U *Thermus aquaticus* (Taq) DNA polymerase I.

Nuclease-free water was added to a final volume of 25 µl and the PCR was performed according to the following three-step protocol using a Mastercycler EP Gradient before the products were analysed by agarose gel electrophoresis.

Step	Temperature	Time	
Initial denaturation	94°C	3 minutes	
Denaturation	94°C	15 seconds	30 cycles
Annealing	64°C	20 seconds	
Elongation	72°C	60 seconds	
Terminal extension	72°C	5 minutes	

2.2.3.6 Real Time Quantitative Reverse Transcription PCR

Quantitative Real Time PCR was used to study the expression of genes that are associated with the Hh signalling cascade. Complementary DNA was reverse transcribed from RNA that was extracted from purified T cells as described. Approximately 10 ng of cDNA were mixed with the appropriate forward and reverse oligonucleotides in a concentration of 300-400 nM each together with 12,5 µl Power SYBR Green PCR Master Mix in a total volume of 25 µl. The reaction mix was prepared in 96-well Optical Reaction Plates on ice which were sealed with MicroAmp Optical Adhesive Film before the reaction was started. PCR was performed according to the following two-step protocol on a 7500 Real Time PCR System:

Step	Temperature	Time	
Preheating	50°C	2 minutes	
Polymerase activation & initial denaturation	95°C	10 minutes	
Denaturation	95°C	15 seconds	40 cycles
Annealing & elongation	60°C	60 seconds	
	95°C	15 seconds	
Dissociation stage	60°C	60 seconds	
	95°C	15 seconds	

Analysis was performed using the delta delta cycle threshold ($\Delta\Delta C_T$) approximation method. In brief, the cycle number at which the transcript of an endogenous control gene reached a certain threshold was subtracted from the cycle number at which a specific target gene reached the same threshold. From this ΔC_T value, the C_T value of a calibrator sample was subtracted to obtain the $\Delta\Delta C_T$ value. The relative quantitative difference between two transcripts was calculated with the formula $2^{-\Delta\Delta C_T}$.

2.2.3.7 Agarose Gel Electrophoresis

PCR products were analysed by agarose gel electrophoresis. Gels containing 2% agarose were generated by dissolving the appropriate amount of agarose in TAE buffer in a microwave oven. After the agarose had cooled to approximately 60°C, ethidium bromide was added to a final concentration of 1 µg / ml. The agarose was poured into a gel tray with a comb and allowed to solidify before it was placed in a gel chamber filled with TAE buffer. Samples from PCR were mixed with one fourth of the volume Orange G loading buffer and loaded onto the gel. Depending on the size of the chamber, the gels were run at 130-150 V until the desired separation was achieved. DNA fragments were visualized by placing the gel onto an UV screen (wavelength 302 nm) and photographed.

2.2.4 Disease models

2.2.4.1 Allergic airway inflammation

For allergic airway inflammation experiments, only female mice between the age of 6 and 12 weeks were used in experimental groups while control groups were made up of male and female mice of the same age. Group sized were at least 5 for experimental groups and 3 for control groups.

2.2.4.1.1 Induction

Mice were initially sensitised against Ova by an intraperitoneal (i.p.) injection of 10 µg Ova together with 1,5 mg aluminium hydroxide (Allhydrogel 2%, abbreviated as Alum) as an adjuvant and PBS in a total volume of 150 µl. Control animals received Alum and PBS without Ova. The emulsions were vortexed for at least 10 minutes and frequently mixed prior to injection to assure an evenly distribution of its components. To further enhance the immune response, booster injections with the same composition that was used before were administered on days 9 and 18 after sensitisation. Finally, antigen challenge was performed

four weeks after initial sensitisation and ten days after the final booster injection for both immunised and control mice. For this purpose, mice were lightly anaesthetised and received an intranasal (i.n.) application of 150 µg Ova dissolved in PBS. This procedure was repeated on three consecutive days and followed by a one day resting phase.

2.2.4.1.2 Analysis

Mice were sacrificed by CO₂ inhalation and a midline neck incision was made to cannulate the trachea. Lungs were rinsed once with 500 µl cold PBS and the recovered bronchoalveolar lavage fluid (BALF) was transferred to a 1,5 ml reaction tube with 200 µl FBS. The cells were kept on ice until they were counted and used for FACS analysis while the lungs were dissected, fixed and used for histological analysis as described. Cells from the BALF were stained with antibodies against CD3, CD4, CD11b, Ly-6G/-6C, F4/80 and Siglec F to identify different populations of infiltrating cells. CD4⁺ T cells were identified as CD3⁺ CD4⁺ cells with low forward- and side scatter (FSC / SSC) intensity values. Macrophages displayed a larger and more granular phenotype and were highly positive for the markers F4/80 and CD11b. Eosinophil granulocytes were identified as large and granular cells with a high expression of Siglec-F while neutrophils showed intermediate expression of this marker in conjunction with a high CD11b and Ly-6G/C expression. Blood was collected from mice for serum analysis of Ova-specific immunoglobulins. For this purpose, the *vena renalis* was punctured and the collected blood was centrifuged at > 20.000 x g for 30 minutes. The serum was removed and stored at -20°C before it was analysed by ELISA as described above. Finally, splenocytes were isolated and an *ex vivo* restimulation assay was performed.

2.2.4.2 Acute Graft-versus-Host disease

For aGvHD experiments, 8-12 week old male BALB/c recipient mice with a minimal weight of 20 g were used. Groups consisted of at least 6 animals in experimental groups and three animals in control groups.

2.2.4.2.1 Induction

Initially, mice received a total body irradiation of 8,5 Gy. On the following day, T cells were isolated from spleens and lymph nodes of *CD4Cre^{+/-} Ptch^{flox/flox}* and *Ptch^{flox/flox}* mice and T cell depleted BM was generated from C57BL/6 mice as described. 10⁷ T cell depleted BM cells were mixed with 2 x 10⁶ T cells and injected in a total volume of 200 µl PBS into the tail vein. Control mice received BM without T cells. Starting from one day prior to cell transfer, mice

were kept on drinking water supplemented with neomycin at a concentration of 25 µg / ml for four weeks.

2.2.4.2.2 Monitoring of disease progression

Mice were monitored daily during the first ten days after cell transfer and then every other day until the experiment ended. They were weighted and their health status was assessed according to five clinical parameters which are commonly employed to evaluate GvHD severity (Cooke et al., 1996). The relevant parameters are described in the following table:

Parameter	Grade 0	Grade 1	Grade 2
Posture	normal	Slightly hunched when resting	Severely hunched
Activity	normal	Slightly reduced	Motionless unless stimulated
Fur ruffling	normal	Slight ruffling	Absent grooming and ruffled fur
Diarrhoea	normal	Mild	severe
Weight loss	< 10%	10-25%	> 25%

Each parameter received a score from 0 (without symptoms) to 2 (severe symptoms), resulting in a total score between 0 and 10. Due to ethical reasons, mice were sacrificed when the total clinical score exceeded a value of 7 for more than one day. Additionally, blood glucose and body temperature were measured for the first ten days of the experiment. For this purpose, the tail vein was punctured and a drop of blood was analysed with a blood glucose meter. Body temperature was measured rectally with a rodent thermometer.

2.2.4.3 B16 Melanoma model

Experiments were performed with 2 to 8 month old mice of both genders that were evenly distributed among groups. Individual experiments had group sizes of 5 to 8 animals.

2.2.4.3.1 Induction of subcutaneous tumour development

B16F10 cells were prepared as described, washed twice in PBS to remove residual medium and counted. Mice were anaesthetised and the fur on the right flank was removed using an animal clipper before 10^4 B16F10 cells were subcutaneously injected.

2.2.4.3.2 Anti-tumour immunisation

For some experiments, an anti-tumour immunisation was performed prior to the application of melanoma cells. To this end, B16F10 cells were irradiated with 125 Gy and mixed at a ratio of two volumes of cell suspension to one volume of Complete Freund's adjuvant (CFA). Cells were injected in a total volume of 150 μ l into the left flank of anaesthetised mice. Animals were challenged with live B16F10 cells ten days after immunisation.

2.2.4.3.3 Monitoring of disease progression

Starting from day 7 after challenge, mice were regularly monitored for palpable tumours. Tumour size was recorded from two calliper measurements of the longest (a) and shortest (b) diameter and the tumour volume was calculated according to the following formula: volume = $axb^2 \times 0,4$ (Hwang et al., 2001). The experiment was terminated for individual mice when the tumour volume exceeded 800 mm³ or when ulceration or bleeding occurred.

2.2.5 Statistical analysis

Statistical analysis was performed by unpaired t-test with the GraphPad Prism software. Data is always depicted as mean \pm standard error of the mean (SEM). Statistical significance is indicated by asterisks according to the following scheme:

p-value > 0,05 \rightarrow ns; p-value \leq 0,05 \rightarrow *; p-value \leq 0,01 \rightarrow **; p-value \leq 0,001 \rightarrow ***

3 Results

3.1 Investigation of thymocyte development

The evolutionary highly conserved Hh signalling pathway plays an important role in cell differentiation and cell patterning in a wide variety of tissues including the immune system. However, its specific role in the development and function of T cells remains controversial, although different studies suggested that it might play a role in this cell population as well. To address the role of Hh signalling specifically in T cells, the group of Prof. Dr. Heidi Hahn developed the *CD4Cre^{+/-} Ptch^{flox/flox}* mouse which forms the basis of the study at hand. In this model, the Cre recombinase is expressed under the control of a CD4 promoter which leads to the excision of exons 8 and 9 from *Ptch^{flox}* alleles. This prevents translation of functional Ptch proteins which was expected to cause activation of canonical Hh signalling. The mouse model was initially characterised and described by Uhmman and colleagues in 2011. The authors showed an almost complete recombination of the *Ptch* locus in thymocytes which was accompanied by a large reduction in the expression of wild type Ptch transcripts in favour of an increased expression of non-functional (*Ptch^{del}*) transcripts. Despite the successful inactivation of Ptch in T cells, no effect on different developmental stages of thymocytes could be observed. This, however, was in contrast to several reports in the literature which found that active Hh signalling affected the transition of DN to DP and DP to SP cells (Rowbotham et al., 2007; Drakopoulou et al. 2010; Furmanski et al., 2012). Since the experiments of Uhmman and colleagues had been performed with mice on a mixed C57BL/6 and 129/Sv genetic background, I decided to repeat these experiments on a larger experimental base and on a pure C57BL/6 background to verify the previously obtained results.

Initially, I investigated the morphology and cellularity of thymi from *CD4Cre^{+/-} Ptch^{flox/flox}* mutant and *Ptch^{flox/flox}* control mice. For this purpose I sacrificed mice from both genotypes and dissected the thymus. As shown in Figure 3A, size and morphology were similar for thymi from both genotypes. I then prepared single cell suspensions from these organs and counted the nucleated cells. With a cell count of around 10^8 , cellularity was within normal limits and also comparable between both genotypes (Figure 3B).

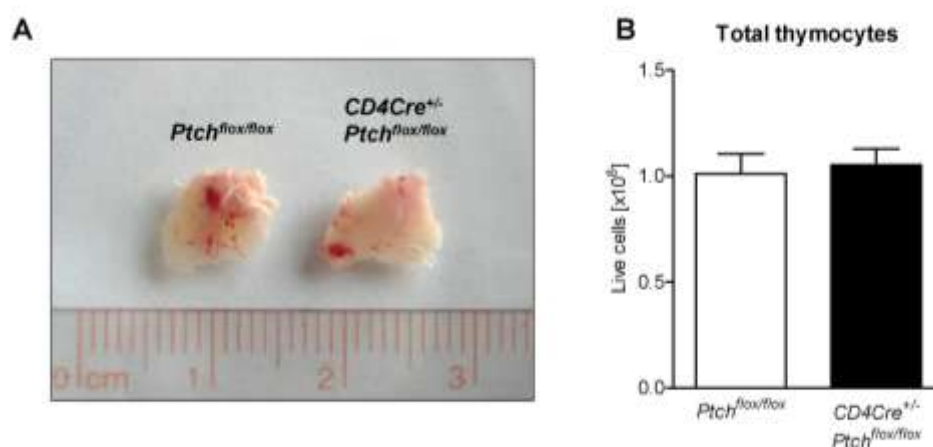


Figure 3. Comparison of thymic morphology and cellularity between *Ptch^{flox/flox}* and *CD4Cre^{+/-} Ptch^{flox/flox}* mice.

Twenty week old mice from both genotypes were sacrificed in a carbon dioxide atmosphere and the thymi were carefully dissected. (A) One representative thymus from a mouse of each genotype is shown. (B) Single cell suspensions were generated from thymi of four mice per genotype and live nucleated cells were counted. The diagram shows the mean cell number \pm SEM for both genotypes.

Thymocyte development starts with the immigration of precursor cells from the BM into the thymus. A number of distinct maturation stages can be classified based on the expression of cell surface markers. The earliest stage is the DN stage in which cells lack surface expression of both CD4 and CD8. This stage can be further subdivided into the DN1 (CD25⁻CD44⁺), DN2 (CD25⁺CD44⁺), DN3 (CD25⁺CD44⁺) and (CD25⁻CD44⁻) DN4 stages (Haks et al., 1999). Following the expression of a functional $\alpha\beta$ TCR, the cells start expressing both CD4 and CD8 in the DP stage before they finally become CD4 or CD8 SP cells. Thus I analysed T cell development by staining isolating thymocytes from mice of both genotypes with antibodies against CD4, CD8 and CD44 to identify the different developmental stages (Figure 4). A direct comparison of early DN cells (DN1 and DN2 stages) before T cell lineage commitment and late DN cells (DN3 and DN4 stages) after commitment to the T cell lineage is depicted in Figure 4B. As expected from the late activation of the CD4 promoter at the DN3 stage, no difference could be seen between the numbers of early DN cells in both genotypes. The same was true for late DN cells as well as for the total number of DN cells (Figure 4C). Surprisingly and in contrast to previous data obtained from this mouse model, I found a small but significant increase in the percentage of DP cells in *CD4Cre^{+/-} Ptch^{flox/flox}* mice compared to mice that lacked expression of the Cre recombinase. This increase in DP cells led to a corresponding reduction in the percentage of SP cells which was especially pronounced in the CD4 SP population. The observed impact of the *Ptch* inactivation on the

development of T cells encouraged me to investigate whether peripheral T cells were also affected by this mutation.

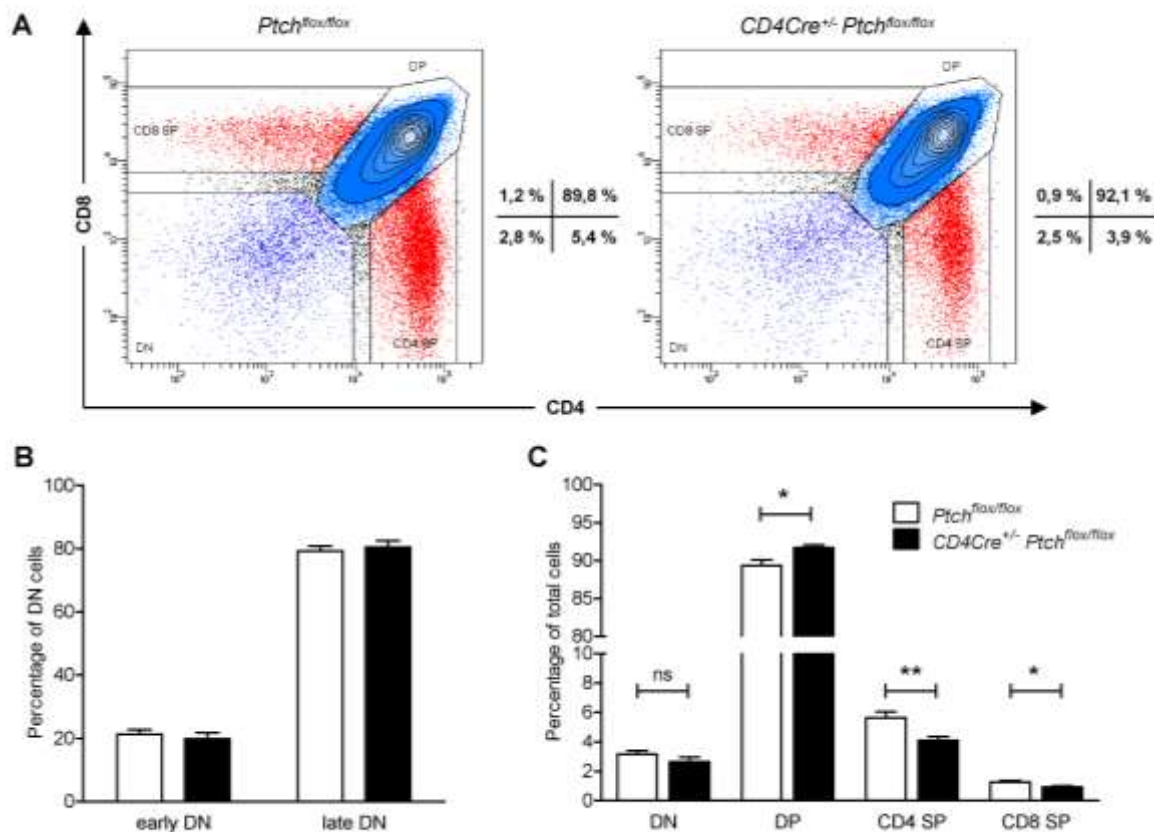


Figure 4. Flow cytometric analysis of thymocyte development

Thymocytes were isolated from twenty week old *CD4Cre^{+/-} Ptch^{flox/flox}* or *Ptch^{flox/flox}* mice and stained for the surface markers CD4, CD8 and CD44 to discriminate between different developmental stages. (A) A representative staining of live thymocytes with antibodies against CD4 and CD8 is shown for both genotypes. (B) CD4 and CD8 DN thymocytes were further subclassified into early DN cells (encompassing DN1 and DN2 stages) and late DN cells (encompassing DN3 and DN4 stages) according to the expression of CD44. (C) The percentage of total DN cells, CD4 and CD8 DP cells and CD4 or CD8 SP cells are shown. Panels B and C show the mean \pm SEM for six *CD4Cre^{+/-} Ptch^{flox/flox}* and four *Ptch^{flox/flox}* mice.

3.2 Characterisation of peripheral T cells

3.2.1 Efficiency and molecular effects of Ptch inactivation

It was previously reported by Uhmman and colleagues that the recombination of the *Ptch* locus along with the expression of the non-functional *Ptch* allele was already very pronounced among thymocytes in mutant mice (Uhmman et al., 2011). *Ptch* is a negative regulator of Smo and represses Smo-mediated activation of the Gli transcription factors in the context of the canonical Hh signalling cascade. According to the general understanding of this pathway, the inactivation of *Ptch* should result in derepression of Smo and thus lead to the activation of canonical Hh signalling. Contrary to expectations, Uhmman et al. found that elevated expression of the Gli transcription factors which are indicative of canonical signalling could not be detected in thymocytes. To investigate whether the *Ptch* deletion led to the expected upregulation of Hh target genes in peripheral T cells, I isolated splenocytes from mice of both genotypes and performed qRT-PCR to study the expression of relevant transcripts (Figure 5). Here I found a strong reduction in the expression of the wt *Ptch* transcript in T cells from *CD4Cre^{+/-} Ptch^{flox/flox}* mice compared to cells from control mice (Figure 5A). In parallel, a corresponding increase in the expression of the non-functional *Ptch^{del}* transcript could be observed in Cre-transgenic T cells while the transcript was not detectable in T cells lacking the Cre recombinase (Figure 5B). *Ptch2*, a homolog of *Ptch* which shows a highly similar sequence and has been reported to have partially overlapping functions with *Ptch* was also analysed. Expression of *Ptch2* however could not be detected in *Ptch*-deficient or control T cells while it was clearly detectable in cDNA generated from a wt mouse embryo at E10.5 that served as a positive control. Expression of the Gli transcription factors Gli1 and Gli2 which are upregulated upon Hh signalling was similar in *Ptch*-deficient and control T cells. Thus, the obtained data from peripheral T cells were again contrary to the expectations but comparable to the results which were previously reported for thymocytes. The data suggest that canonical Hh signalling is not active in peripheral T cells either despite the functional inactivation of *Ptch*.

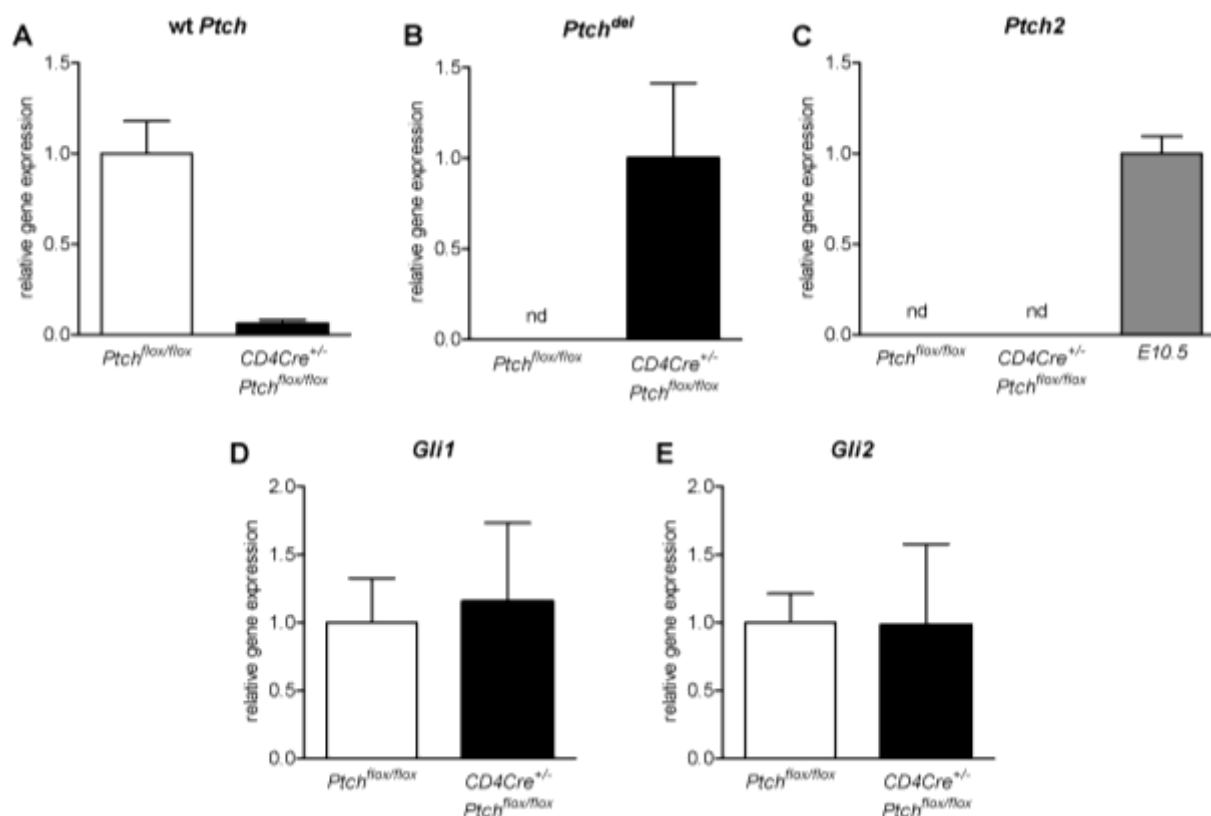


Figure 5. Gene expression analysis of peripheral T cells

Splenic T cells were isolated from five *Ptch*^{flox/flox} and three *CD4Cre*^{+/-} *Ptch*^{flox/flox} mice and used to generate cDNA for qRT-PCR analysis. Relative expression of the wild type *Ptch* allele (wt *Ptch*; A), its truncated form after Cre-mediated excision of exons 8 and 9 (*Ptch*^{del}; B), the *Ptch* homolog *Ptch2* (C) as well expression of the transcription factors *Gli1* (D) and *Gli2* (E) are shown. All samples were measured in duplicates and normalized to the expression of HPRT1. (nd = not detected)

3.2.2 T cell populations and their activation state in the periphery

In order to unravel potential effects of *Ptch* ablation on T cells which do not require the activation of canonical Hh signalling, I began to study peripheral T cells. Initially, I focused on the spleen which, as the major secondary lymphoid organ, is an important site of T cell homeostasis and activation. For this purpose I dissected spleens from *CD4Cre*^{+/-} *Ptch*^{flox/flox} mutant and *Ptch*^{flox/flox} control mice, evaluated their overall appearance and determined the total number of nucleated cells. Morphology of spleens from *CD4Cre*-transgenic mice were inconspicuous and did not show any difference to organs which originated from control mice (Figure 6A). I then enumerated total cells in the spleens of mice from both genotypes. As shown in Figure 6B, the average amounts of nucleated cells in the spleens were

approximately $1,3 \times 10^8$ for $CD4Cre^{+/-} Ptch^{flox/flox}$ mutant mice as well as for control mice showing that the *Ptch* inactivation does not affect the total number of splenocytes.

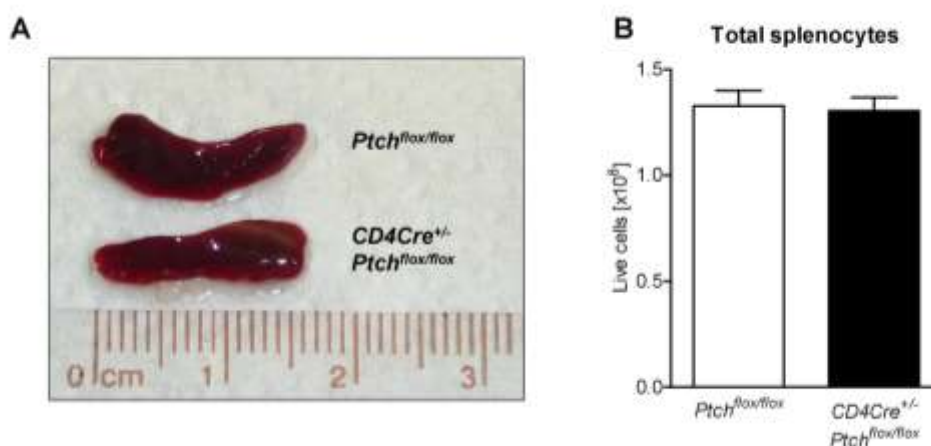


Figure 6. Comparison of splenic morphology and cellularity

Spleens were isolated from *Ptch^{flox/flox}* control and $CD4Cre^{+/-} Ptch^{flox/flox}$ mutant mice. (A) A representative organ from each genotype is depicted. (B) Single cell suspensions were generated and live splenocytes counted. The diagram shows the mean cell number \pm SEM for ten *Ptch^{flox/flox}* and eight $CD4Cre^{+/-} Ptch^{flox/flox}$ mice.

Since I was not able to find any differences in the absolute number of cells, I continued to investigate the composition of peripheral T cells more closely by flow cytometry. For this purpose, I determined the percentage of βTCR^+ T cells on total lymphocytes and enumerated the amount of $CD4^+$ and $CD8^+$ cells among total T cells. This was done for blood, mesenteric lymph node as a vital part of the gut-associated lymphoid tissue and the spleen which is important as the largest secondary lymphoid organ (Figure 7A-C).

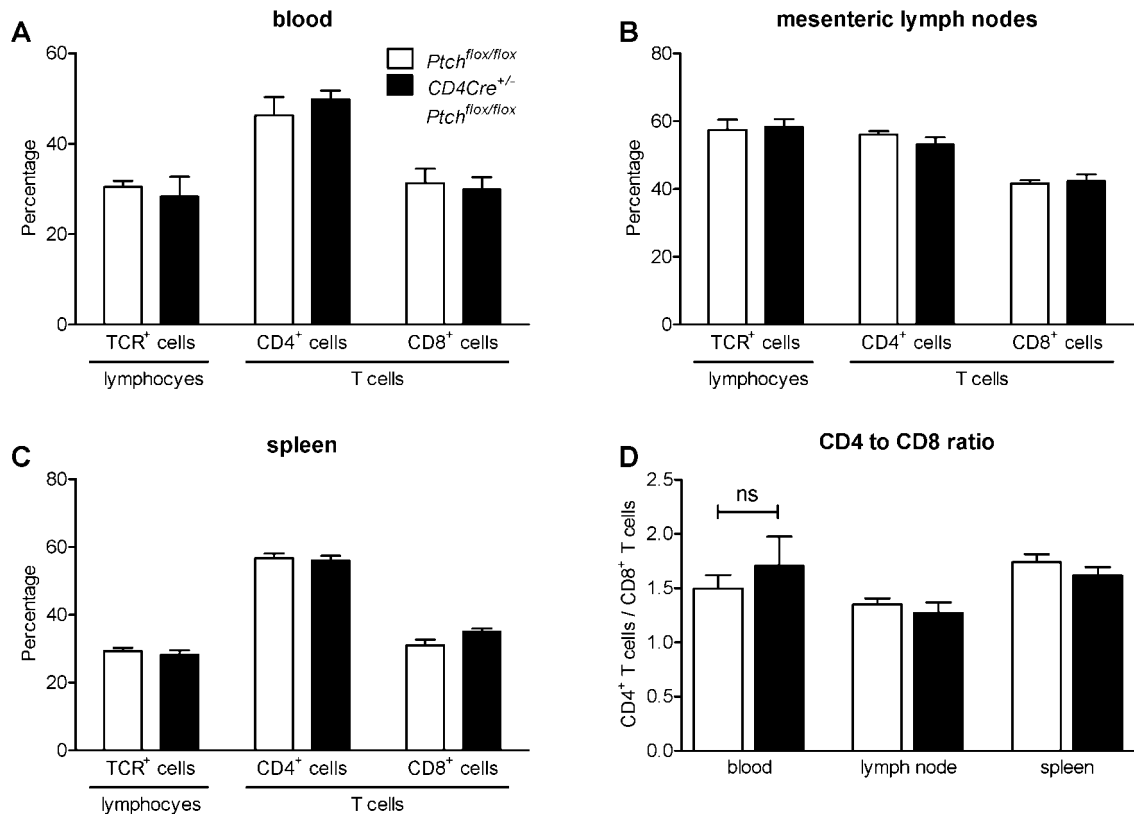


Figure 7. Flow cytometric analysis of peripheral T cell populations

Leukocytes were isolated from blood, mesenteric lymph nodes and spleens of *Ptch*^{flox/flox} control and *CD4Cre*^{+/-} *Ptch*^{flox/flox} mutant mice. Cells were stained with antibodies against the TCR beta chain (β TCR), CD4 and CD8 before they were analysed by flow cytometry to identify T cells and their major subpopulations. The percentage of β TCR expressing cells is given among the lymphocyte fraction together with cells expressing CD4 and CD8 among β TCR⁺ T cells for blood (A), mesenteric lymph nodes (B) and spleens (C). The ratio between CD4⁺ and CD8⁺ T cells was calculated and is shown in panel D. All diagrams show the mean percentage or ratio \pm SEM for at least four *Ptch*^{flox/flox} and at least five *CD4Cre*^{+/-} *Ptch*^{flox/flox} mice.

Percentages of total T cells among leukocytes ranged from 30% in blood to 60% in mesenteric lymph nodes but were not significantly different between *CD4Cre*^{+/-} *Ptch*^{flox/flox} and control mice in all analysed tissues. CD4⁺ T cells, which were the dominant T cell subpopulation, accounted for 55% to 60% of T cells in the blood as well as in mesenteric lymph nodes and spleens. This observation could be made for mutant and also for control mice. With around 30% to 40% of total T cells, CD8⁺ cells formed a smaller T cell subpopulation and their percentage was also comparable between both analysed genotypes. The peripheral CD4 to CD8 T cell ratio is tightly regulated and generally maintained above 1

in healthy mice although it decreases with age (Kappes & He, 2005). A number of T cell intrinsic factors can lead to a shift of this ratio, including an alteration in the TCR signalling strength (Hayes & Love, 2006). Thus, the peripheral CD4 to CD8 ratio can be employed as a tool to gain insight into the functionality of T cells. I therefore determined the percentages of CD4⁺ and CD8⁺ T cells and calculated the ratio between them for blood, mesenteric lymph nodes and spleens. I found that it was well above a value of one and ranged from 1,4 in mesenteric lymph nodes up to 1,7 in spleens. For every organ analysed, the ratio was highly similar between *CD4Cre^{+/-} Ptch^{flox/flox}* and control mice. Taken together, these data demonstrate that the T cell population as a whole and its two major subpopulations were not numerically affected by Ptch ablation.

To investigate whether the Ptch-deficiency had more subtle effects on T cells, I focussed on both major T cell subpopulations and determined the percentage of cells that were positive for CD69 or showed a high expression of CD44 by flow cytometry (Figure 8). CD69 is a C-type lectin which is one of the earliest inducible cell surface proteins during lymphocyte activation and can thus be used to identify recently activated T cells (Cambiaggi et al., 1992). CD44 on the other side is a surface protein that is involved in cell migration and cell-cell interactions due to its ability to interact with carbohydrates. Expression of CD44 is upregulated following TCR stimulation and is sustained on effector as well as memory cells (DeGrendele et al., 1997) which allows its usage as a marker for effector memory T cells *in vivo*.

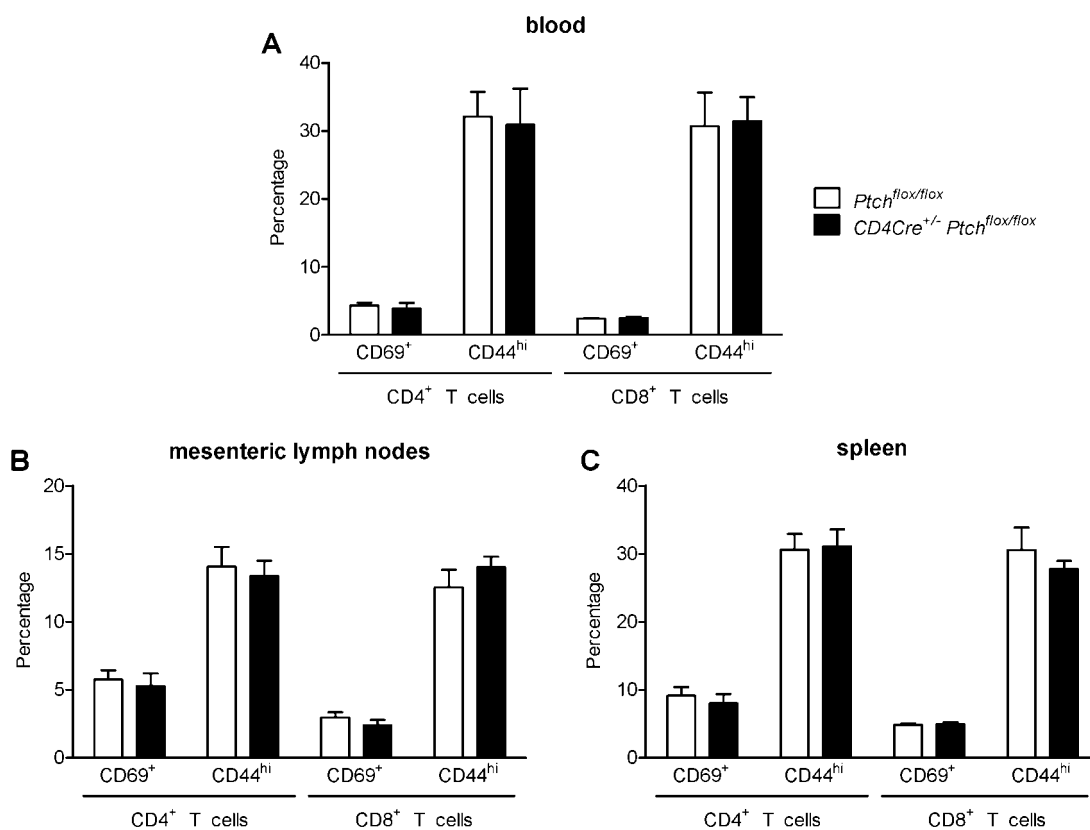


Figure 8. Activation state of peripheral T cells

Leukocytes were isolated from blood, mesenteric lymph nodes and spleens of *Ptch^{flox/flox}* and *CD4Cre^{+/-} Ptch^{flox/flox}* mice. Cells were stained with antibodies against the β TCR, CD4, CD8, CD69 and CD44 to identify T cell subpopulations and reveal their activation state. Cells showing a recently activated (CD69⁺) or effector memory (CD44^{hi}) phenotype are shown among the CD4⁺ and CD8⁺ T cell populations for blood (A), mesenteric lymph nodes (B) and spleens (C). All diagrams show the mean percentage \pm SEM for at least four *Ptch^{flox/flox}* and six *CD4Cre^{+/-} Ptch^{flox/flox}* mice.

I found that between 3% and 6% of CD4⁺ and CD8⁺ T cells stained positively for CD69 in blood and lymph nodes while up to 10% of CD4⁺ T cells expressed this marker in the spleen. A direct comparison of *CD4Cre^{+/-} Ptch^{flox/flox}* and control mice however did not reveal any difference in the amount of recently activated T cells between both genotypes. With around 15% in lymph nodes and up to 30% in spleens and blood, effector memory T cells as identified by their high expression of CD44 represented a much larger fraction of CD4⁺ and CD8⁺ T cells than recently activated cells. Percentages in this compartment were also highly similar between both genotypes, suggesting that *Ptch* ablation does not considerably impact on the activation state of T cells in the periphery either.

3.3 Functional analysis of conventional T cells *in vitro*

Since I could not find any differences in the numbers or activation state of peripheral T cells in $CD4Cre^{+/-} Ptch^{flox/flox}$ mice, I switched to *in vitro* assays in order to study whether *Ptch* ablation had any impact on functional characteristics of T cells. Under physiologic conditions, naïve T cells become activated when they encounter their specific antigen in the periphery. Antigen is presented on MHC molecules in the form of a peptide that is between 9 and 25 amino acids in length. Presentation of antigen is usually performed by professional APCs such as dendritic cells and macrophages. The MHC:peptide complex is recognized by the TCR and initiates the activation process of the T cells which eventually leads to the secretion of cytokines such as the autocrine growth factor IL-2 and the effector cytokine IFN- γ . This process can be mimicked *in vitro* in the form of a MLR. T cells cultured together with APCs of a different MHC haplotype become activated due to the MHC mismatch between both cells. This alloreactivity is mainly based on MHC-dominant cross-reactivity of the TCR which occurs irrespective of antigen (Whitelegg & Barber 2004). The results of this allogeneic T cell stimulation are shown in Figure 9.

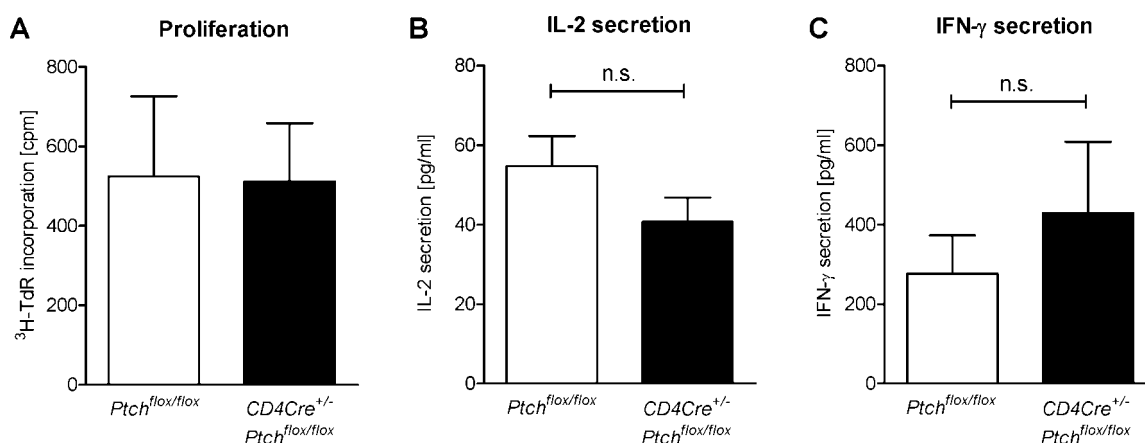


Figure 9. Allogeneic stimulation of T cells

10^5 splenic T cells were isolated from $Ptch^{flox/flox}$ and $CD4Cre^{+/-} Ptch^{flox/flox}$ mice on a C57BL/6 background and cocultured with an equal amount of BALB/c-derived BMDM in 96-well round-bottom plates for 72 hours. Thereafter, 50 μ l of medium were removed for cytokine analysis and replaced with the same amount of fresh medium containing 3H -TdR with an activity of 37 kBq before the cells were incubated for another 16 hours. (A) Incorporation of 3H -TdR was assessed by scintillation counting and is depicted as counts per minute (cpm). IL-2 (B) and IFN- γ (C) levels in the supernatant were quantified by ELISA. All samples were measured in triplicates. Each diagram shows the mean \pm SEM from at least six independent experiments.

Proliferation of T cells was assessed after a stimulation period of 72 hours by $^3\text{H-TdR}$ incorporation for another 16 hours (Figure 9A). With an average of 500 cpm, the proliferation was rather weak as expected due to the low percentage of alloreactive cells. T cells isolated from $CD4\text{Cre}^{+/-} Ptch^{\text{lox/lox}}$ mice responded with a proliferation which was comparable to that of control mice. In addition, secretion of the growth factor IL-2 and the effector cytokine IFN- γ were measured by ELISA. Consistent with the low incorporation of $^3\text{H-TdR}$, IL-2 levels were relatively low with a maximal concentration of less than 60 pg / ml in the supernatant (Figure 9B). On average, *Ptch*-deficient T cells produced less of this cytokine but the differences remained insignificant. Secretion of IFN- γ was much higher for cells of both genotypes and ranged from 300 pg / ml up to 500 pg / ml (Figure 9C). Here, T cells that lacked functional *Ptch* produced on average higher amounts of IFN- γ but the difference to the amounts produced by control cells were not significant either.

Since the allogeneic stimulation affected only few cross-reactive T cells, I wondered whether a more general stimulation of all T cells could unravel a potential effect of *Ptch* ablation on the T cell population as a whole. For this purpose, I stimulated T cells polyclonally either with the lectin ConA or with stimulating monoclonal antibodies (mAb) directed against the ϵ -chain of CD3 and against the co-stimulatory molecule CD28. Both stimuli were used at suboptimal and optimal concentrations to investigate the T cell response under different conditions. Proliferation of T cells was assessed by $^3\text{H-TdR}$ incorporation (Figure 10). Under suboptimal stimulation conditions, T cells activated with ConA or antibodies against CD3 and CD28 showed a weak proliferative response that was comparable to the response observed following allogeneic stimulation. In contrast, optimal stimulation led to a much stronger response of up to 4000 cpm when cells were stimulated with ConA. Under optimal conditions, *Ptch*-deficient T cells showed a slightly stronger proliferation at all time points which nonetheless did not reach significance. When suboptimal stimulation was employed, proliferation was highly comparable between both genotypes. Data obtained from the measurement of IL-2 secretion is shown in Figure 11A. Here, suboptimal stimulation with ConA led to an accumulation of the cytokine in the supernatant over time with no significant difference being detectable between both genotypes. When anti-CD3 and anti-CD28 antibodies were used for suboptimal stimulation, an appropriate accumulation of the cytokine could not be observed. Application of higher antibody concentrations that led to an optimal stimulation in the described system caused an increase in IL-2 secretion with ConA being again more potent than anti-CD3 and anti-CD28 antibodies.

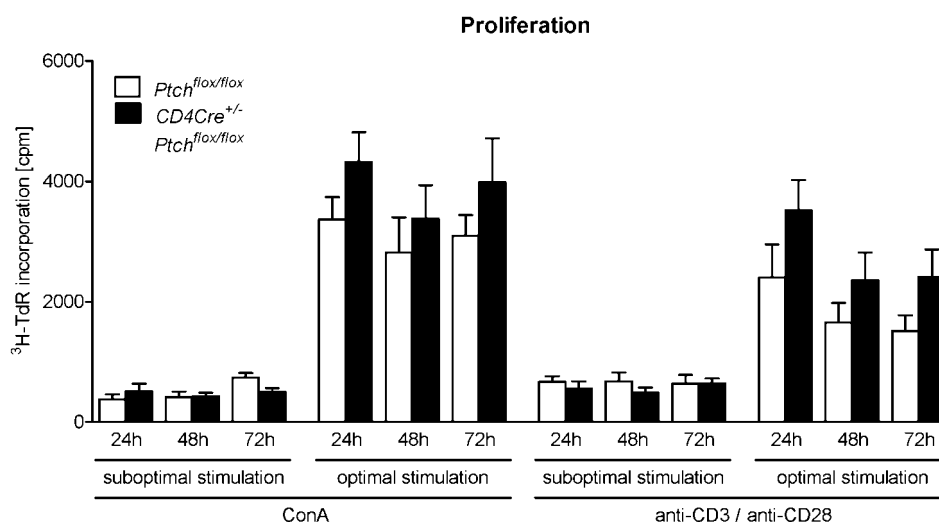


Figure 10. Proliferation of polyclonally stimulated T cells

Splenic T cells were isolated from *Ptch*^{flox/flox} and *CD4Cre*^{+/-} *Ptch*^{flox/flox} mice. 10⁵ cells per well were stimulated in 96-well plates with different concentrations of ConA or mAb against CD3 and CD28. For suboptimal stimulation, ConA was used at a concentration of 0,5 µg / ml while anti-CD3 and anti-CD28 mAb were used at concentrations of 0,01 µg / ml each. Optimal stimulation was achieved by adding 2,5 µg / ml ConA or 1 µg / ml anti-CD3 and anti-CD28 mAb each. After 24, 48 or 72 hours, 37 kBq ³H-TdR were added per well prior to another incubation period of 16 hours. Incorporation of ³H-TdR was measured by scintillation counting and is depicted as cpm. The diagram shows the mean ± SEM from two to ten independent experiments. Differences are not statistically significant unless otherwise indicated.

In contrast to the data obtained by measuring ³H-TdR incorporation, IL-2 production was by trend higher in T cells derived from control mice than in *Ptch*-deficient cells. This was especially true for cells stimulated with ConA, but even here no significant difference between both genotypes could be observed. Finally, secretion of the effector cytokine IFN-γ was assessed and the results are shown in Figure 11B. Irrespective of the employed stimulus, IFN-γ secretion was barely detectable when a suboptimal stimulation was performed. In contrast, optimal stimulation of the cells led to a pronounced secretion of the cytokine which accumulated in the supernatants over time. Cells from mice of either genotype showed a highly comparable IFN-γ production in response to stimulation. In summary, the data argue against a significant impact of *Ptch* ablation on both the proliferative response and the secretion of effector cytokines of polyclonally activated T cells *in vitro*.

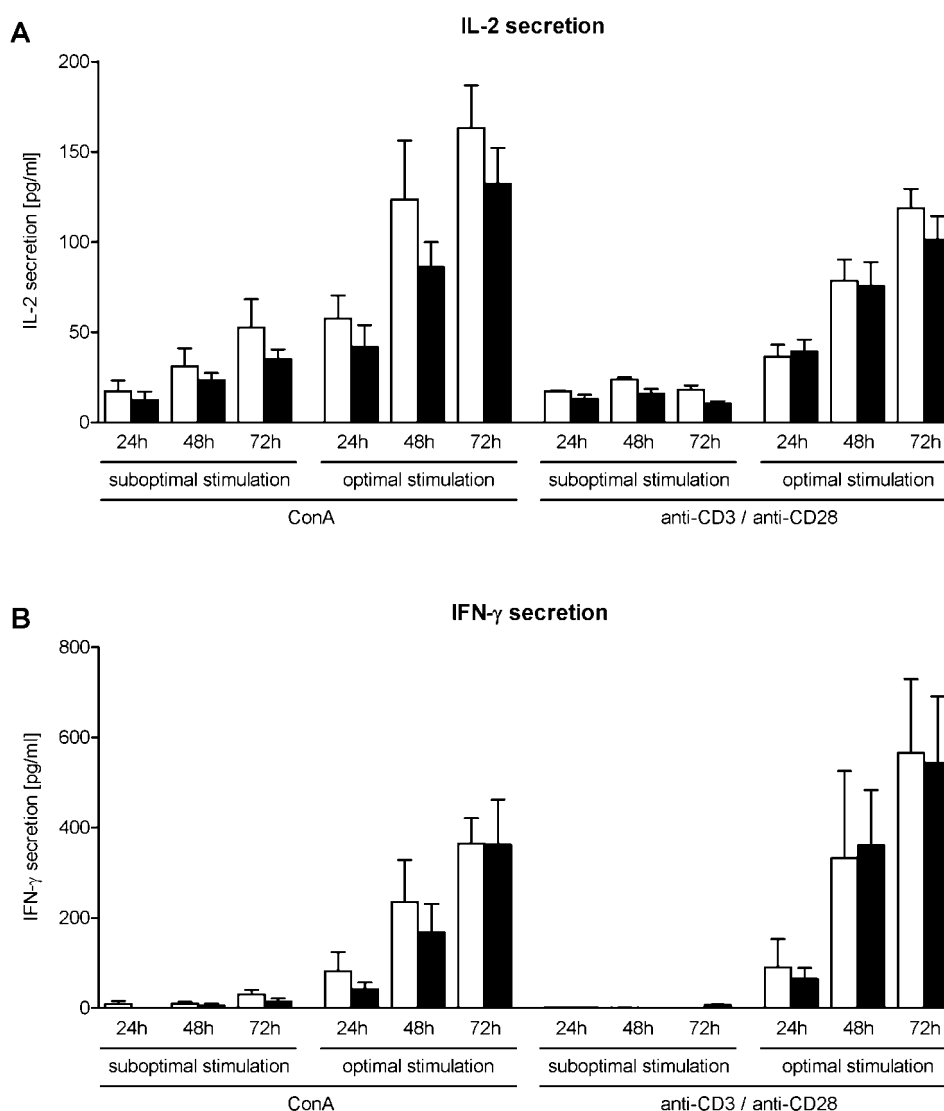


Figure 11. Cytokine secretion of polyclonally stimulated T cells

T cells were isolated from spleens of $CD4Cre^{+/-} Ptch^{flox/flox}$ mutant and $Ptch^{flox/flox}$ control mice. 10^5 cells per well were stimulated in 96-well plates with different concentrations of ConA or antibodies against CD3 and CD28. Suboptimal stimulation was achieved by adding ConA at a concentration of $0,5 \mu\text{g} / \text{ml}$ or by adding anti-CD3 and anti-CD28 mAb at concentrations of $0,01 \mu\text{g} / \text{ml}$ each. For optimal stimulation, ConA was added at a concentration of $2,5 \mu\text{g} / \text{ml}$ while anti-CD3 and anti-CD28 mAb were used at $1 \mu\text{g} / \text{ml}$ each. After 24, 48 or 72 hours, $50 \mu\text{l}$ of supernatant were collected for cytokine analysis. Quantification of IL-2 (A) and IFN- γ (B) was performed by ELISA and all samples were measured in triplicates. Each diagram shows the mean \pm SEM from two to ten independent experiments. Differences are not statistically significant unless otherwise indicated.

3.4 Analysis of naturally occurring regulatory T cells

T_{reg} cells are a subpopulation of T cells which are capable of negatively modulating immune responses. Their primary function was initially defined to be the prevention of autoimmune diseases by maintaining self-tolerance but continuous research has revealed several other functions. Those include the induction of tolerance against non-harmful environmental antigens and a negative feedback control of effector T cell responses. T_{reg} cells come in many forms with the naturally occurring T_{reg} cells being the best defined. This subpopulation can be identified by expression of several markers including the IL-2 receptor α -chain, the surface molecule GITR and the transcription factor FoxP3. In mice, FoxP3 is not only a marker for T_{reg} cells but also a key regulator in the development and function of this population (Zhang & Zhao, 2007). Given the importance that T_{reg} cells play in immune responses, I decided to investigate whether Ptch ablation had any effect on this population. For this purpose, I enumerated β TCR⁺CD4⁺CD25⁺GITR⁺FoxP3⁺ T_{reg} cells in the spleens of *CD4Cre^{+/-} Ptch^{flox/flox}* mutant and *Ptch^{flox/flox}* control mice by flow cytometry (Figure 12A). With a percentage of around 9% among CD4⁺ T cells and approximately 5% among total T cells, T_{reg} cells were normally distributed with no significant difference being detectable between both genotypes. Expression levels of the transcription factor FoxP3 were quantified by determining the mean fluorescent intensity (MFI) of intracellular stainings using FoxP3-specific antibodies (Figure 12B). FoxP3 expression was evenly distributed among cells and was found to be similar between T_{reg} cells that originated from mice of either genotype. A key characteristic of T_{reg} cells is their capability to suppress the proliferation and IL-2 secretion of activated conventional T cells which can be easily assessed *in vitro*. For this purpose, I isolated T_{reg} cells from mice of both genotypes, cocultured them with conventional CD4⁺ T cells that were stimulated with anti-CD3 and anti-CD28 antibodies and determined the concentration of secreted IL-2 in the supernatants (Figure 12C).

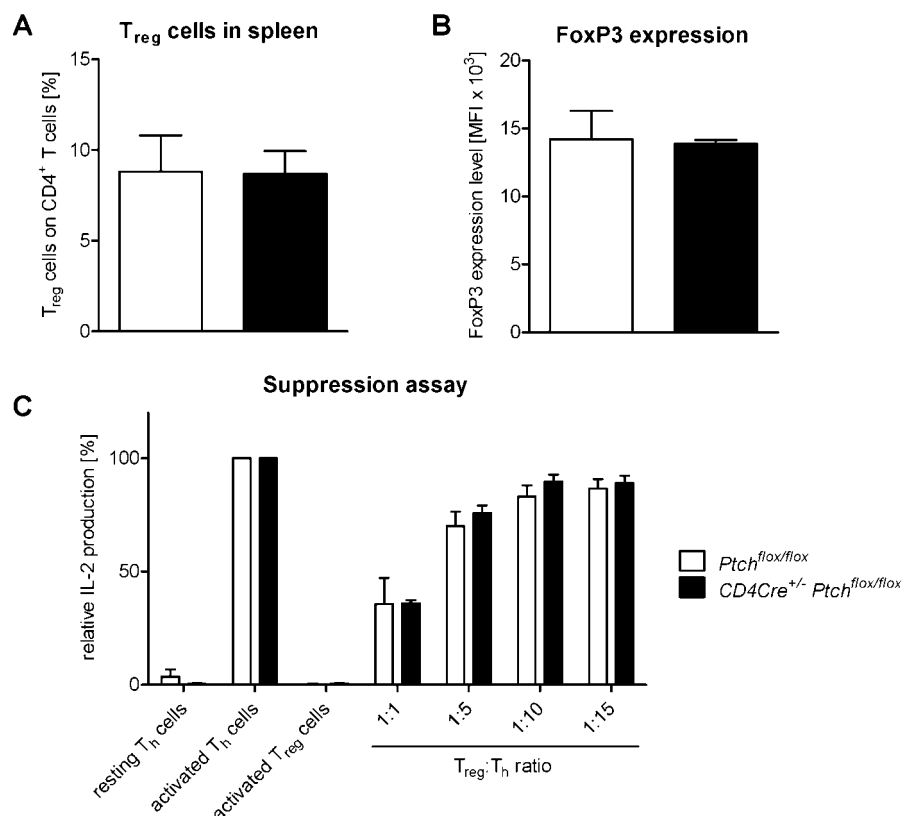


Figure 12. Analysis of naturally occurring T_{reg} cells

Spleens were isolated from *Ptch^{flox/flox}* and *CD4Cre^{+/-} Ptch^{flox/flox}* mice, stained for β TCR, CD4, CD25, GITR and FoxP3 and analysed by flow cytometry to identify T_{reg} cells. (A) The percentage of T_{reg} cells among CD4⁺ T cells is given. (B) Levels of intracellular FoxP3 expression in T_{reg} cells are shown as MFI. (C) 10⁵ freshly isolated T_{reg} cells were cocultured with CD4⁺ T_h cells at the indicated ratios. Polyclonal stimulation was achieved by adding anti-CD3 mAb and anti-CD28 mAb in concentrations of 1 and 5 μ g / ml respectively. Unstimulated or stimulated T_h cells as well as stimulated T_{reg} cells alone served as controls. After 48 hours, the supernatants were removed and used to determine IL-2 levels which were normalised to samples derived from activated T_h cells. Diagrams show the mean \pm SEM from three (*Ptch^{flox/flox}*) and four (*CD4Cre^{+/-} Ptch^{flox/flox}*) independent experiments.

While CD4⁺ T_h cells responded to the stimulation with a high secretion of IL-2, T_{reg} cells did not secrete detectable amounts of this cytokine as expected. A coculture of T_{reg} cells and T_h cells at different ratios revealed a ratio-dependent suppression of cytokine production by T_{reg} cells. Both the response of T_{reg} cells to activation and their suppressive capacity were however not influenced by ablation of functional Ptch. The obtained data therefore are not in favour of a role of Ptch in the development, distribution or function of naturally occurring T_{reg} cells.

3.5 Susceptibility of T cells to apoptosis

Programmed cell death or apoptosis is a key process for proper tissue development and homeostasis in metazoans. It is also vital for the correct function of the immune system due to its implication in virtually every stage of lymphocyte development and activity. Shaping of the T cell repertoire in the thymus is highly dependent on apoptosis during the processes of positive and negative selection while it is also crucial for the termination of immune responses upon pathogen clearance and in the prevention of autoimmunity. Due to the central importance of programmed cell death in T cell development and activity, I decided to investigate whether it is affected by the *Ptch* deficiency. Therefore, I isolated T cells from *CD4Cre^{+/-} Ptch^{flox/flox}* and control mice and investigated their susceptibility to apoptosis in response to three different stimuli. I treated cells either with the synthetic glucocorticoid dexamethasone (Dex), exposed them to γ -radiation or incubated them in medium that was devoid of survival factors such as IL-2. The percentage of live cells was determined daily by flow cytometry using 7-AAD as a marker for apoptotic cells that had lost their membrane integrity. The results of this experiment are depicted in Figure 13.

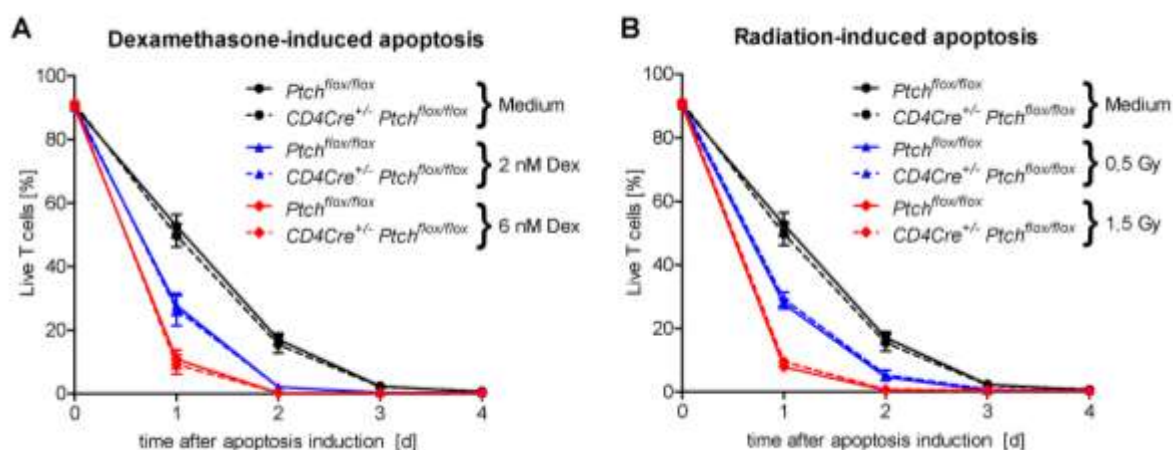


Figure 13. Sensitivity of resting T cells to apoptosis

2×10^5 resting T cells from spleens of *Ptch^{flox/flox}* or *CD4Cre^{+/-} Ptch^{flox/flox}* mice were treated with Dex, exposed to γ -radiation or left unmanipulated. Viability was assessed daily by FACS analysis using 7-AAD as a marker for apoptotic cells. (A) Cells were treated with 2 or 6 nM water-soluble Dex to induce apoptosis or left untouched. The diagram shows the combined data from three independent experiments per genotype. (B) Cells were exposed to γ -radiation at doses of 0,5 or 1,5 Gy or not irradiated at all. The combined data from three independent experiments per genotype is shown. All data points depict the mean percentage of live cells \pm SEM.

In the absence of exogenous survival factors, T cell viability rapidly declined and reached a value of less than 60% after 24 hours which further decreased to less than 30% after 48 hours (Figure 13A, upper curve). 96 hours after the start of the experiment, only very few live cells could still be detected in the culture. Addition of 2 nM Dex into the medium accelerated this process and T cell viability reached a value of less than 30% after 24 hours and dropped down to less than 3% within the following 24 hours (Figure 13A, middle curve). When Dex was added at a higher concentration of 6 nM, cell viability reached a value of approximately 10% already after 24 hours and no viable cells were detectable 48 hours after the start of the experiment (Figure 13A, lower curve). Under all conditions, Ptch-deficient T cells showed a highly similar response compared to control T cells. In parallel, cells were subjected to different doses of γ -radiation (Figure 13B). An exposure of T cells to a dose of 0,5 Gy led to a considerable drop in viability after 24 hours whereas a dose of 1,5 Gy had an even more severe effect on cell survival and led to a reduction of cell viability to approximately 5% after 24 hours of culture. A difference between Ptch-deficient and control T cells could not be observed in this setting either, suggesting that Ptch ablation did not affect the susceptibility of resting T cells to apoptosis.

Upon activation, T cells are known to acquire an increased resistance to apoptosis due to the upregulated expression of several Bcl-2 family proteins which regulate the apoptotic pathways. During an ongoing immune response, this is highly beneficial for the organism since it accelerates removal of the pathogen. Because I was not able to observe an effect of Ptch on the susceptibility of resting T cells to apoptosis, I wondered whether Ptch ablation might specifically affect this regulatory network in activated T cells. In order to explore if this was the case, I isolated T cells from mice of both genotypes and prestimulated them either with anti-CD3 and anti-CD28 mAb or with ConA for 24 hours (Figure 14). Subsequently, I added the synthetic glucocorticoid Dex to amplify apoptosis induction. Due to the higher tolerance threshold of activated T cells against glucocorticoids, I increased the concentration of Dex by more than two magnitudes to a final value of 1 μ M.

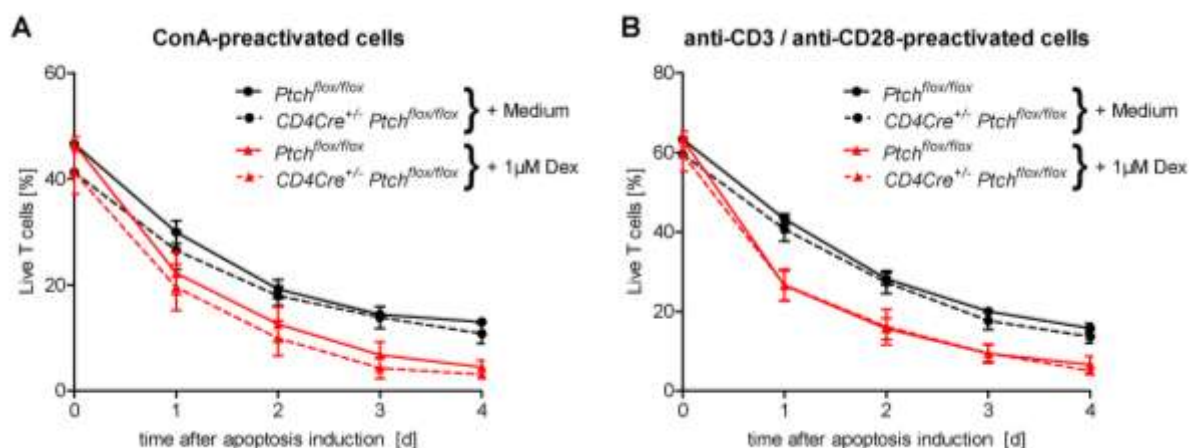


Figure 14. Sensitivity of activated T cells to apoptosis

2×10^5 splenic T cells were isolated from *Ptch*^{flox/flox} or *CD4Cre*^{+/-} *Ptch*^{flox/flox} mice and prestimulated either with 2,5 µg / ml ConA (A) or with 1,5 µg / ml anti-CD3 mAb and anti-CD28 mAb (B) for 24 hours. Afterwards, 1 µM water-soluble Dex was added to induce apoptosis or cells were left untreated. Viability was assessed daily by FACS analysis using 7-AAD. Diagrams show the mean ± SEM from four *Ptch*^{flox/flox} control and three *CD4Cre*^{+/-} *Ptch*^{flox/flox} mutant mice.

I observed that in the absence of Dex, T cell viability initially declined but stabilized at approximately 15% from day four after the start of the experiment (Figure 14A). This differed from the response of resting T cells and underlined the reduced susceptibility of activated T cells towards apoptosis. There was however no difference in the response of *Ptch*-deficient versus control T cells. Addition of Dex further reduced the viability of T cells which reached its minimum level of approximately 5% on day four after apoptosis induction. Again cells from *CD4Cre*^{+/-} *Ptch*^{flox/flox} and control mice behaved in a similar fashion. When T cells were preactivated with stimulating mAb against CD3 and CD28 instead of ConA, survival during the preactivation phase was much better (Figure 14B). Nevertheless, viability of T cells declined to a value of less than 20% on day four. Addition of Dex again had a pronounced negative effect on T cell survival with less than 10% of T cells being alive after four days. A different behaviour between *Ptch*-deficient and control T cells, could not be observed either. In summary, the obtained data argues against a role of *Ptch* in the susceptibility of both resting and activated T cells to apoptosis.

3.6 *In vivo* analysis of Ptch-deficient T cells

3.6.1 Allergic airway inflammation

Since I had not observed any significant difference in the distribution of T cells *in vivo* or their function *in vitro*, I wondered whether a potential impact of Ptch ablation might become evident only under physiological conditions during immune responses *in vivo*. For this purpose I initially studied T cells in allergic airway inflammation experiments which represent an experimental model of human asthma, a chronic inflammatory disorder of the airways that is characterised by reversible airflow obstruction, airway inflammation and airway remodelling. A murine model for allergic airway inflammation can not only provide insights into the mechanisms underlying the development of human asthma, but can also be used as a valuable tool to investigate the function of different T cell populations during an immune response *in vivo*. Thus I decided to investigate whether the Ptch deficiency in T cells affects a T_H2 biased immune response in this model. To this end, I sensitised $CD4Cre^{+/-} Ptch^{flox/flox}$ and $Ptch^{flox/flox}$ mice against Ova in the presence of the T_H2-promoting adjuvant Alum and evaluated the elicited immune response according to different parameters after intranasal antigen challenge.

Initially I focussed on the lungs where I enumerated infiltrating inflammatory cells and characterised them by flow cytometry (Figure 15). In control mice which were challenged with but not previously sensitized against Ova, I found on average less than 4×10^4 cells in the BALF (Figure 15A). In contrast, mice that were previously sensitized against the antigen showed a more than 8-fold increase in total cell numbers. Differences between $CD4Cre^{+/-} Ptch^{flox/flox}$ and $Ptch^{flox/flox}$ mice were marginally, however, and did not reach statistical significance. In-depth characterisation of airway-infiltrating cells is shown in Figure 15B/C. Upon antigen challenge, cellular inflammation was largely dominated by eosinophils which on average accounted for 70% of total cells. A clear increase could also be seen in the numbers of CD4⁺ T cells whereas neutrophil granulocyte numbers were only slightly elevated in sensitised mice. In contrast, fewer macrophages could be detected as compared to control mice. Among all analysed cell populations, numerical differences between sensitised mice of both genotypes remained insignificant. Thus, both the absolute number of lung-infiltrating cells as well as their cellular composition showed no indication for an impact of Ptch deficiency on this aspect of the immune response.

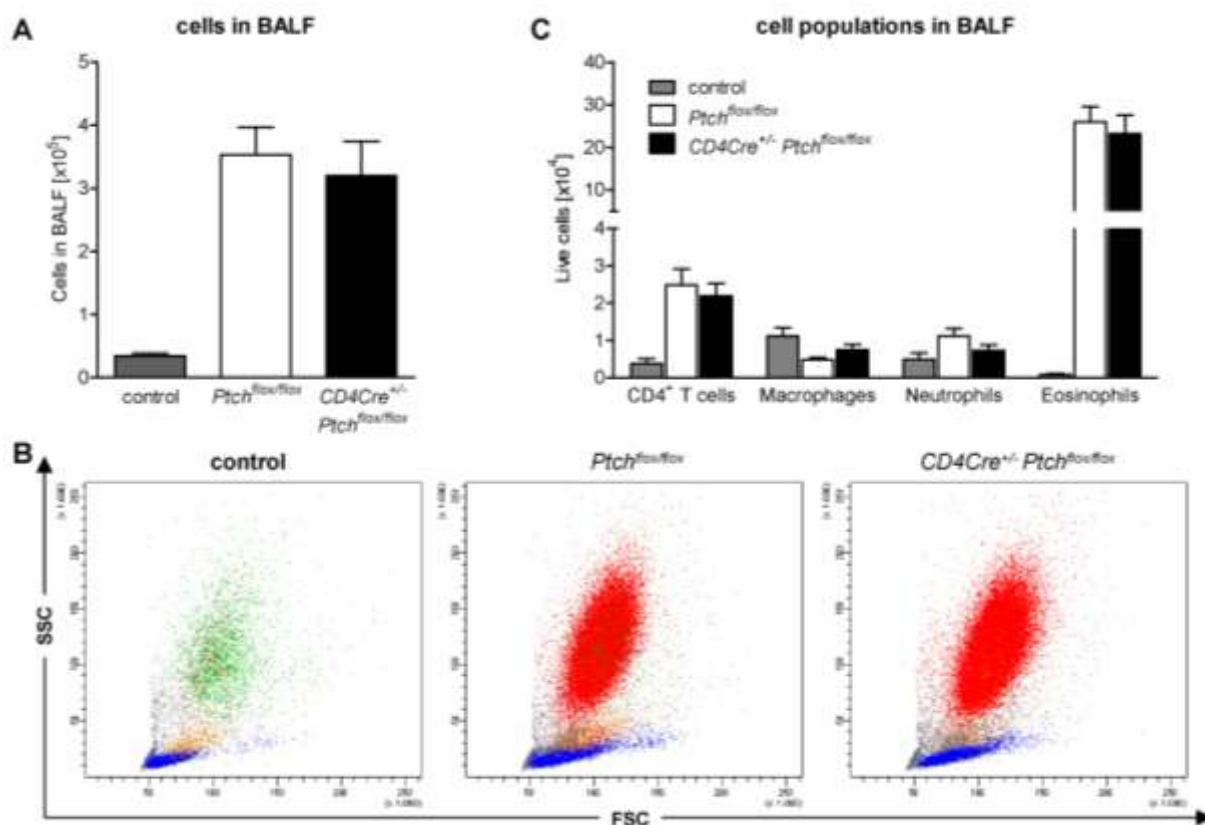


Figure 15. Lung infiltration in allergic airway inflammation experiments

Allergic airway inflammation was induced by repeated intraperitoneal sensitisations of *Ptch*^{lox/lox} and *CD4Cre*^{+/-} *Ptch*^{lox/lox} mice with 10 μ g Ova together with 1,5 mg Alum. Control mice (*Ptch*^{lox/lox}) were treated with Alum alone. All mice were challenged ten days after final sensitisation by intranasal application of 150 μ g Ova dissolved in PBS on three consecutive days. Analysis was performed after a one day resting phase. (A) Mice were sacrificed and the lungs were rinsed with PBS to obtain the BALF in which total nucleated cells were counted by light microscopy. (B) FACS analysis was performed with BALF cells to identify different populations according to the expression of CD3, CD4, CD11b, F4/80, Siglec-F and Ly-6G/C. A representative FSC versus SSC plot is shown for each group. T cells appear in blue, neutrophil granulocytes in orange, macrophages in green and eosinophil granulocytes in red. Cell debris was identified by low FSC values and has been excluded. (C) Mean numbers of different infiltrating cell population from the FACS analysis of BALF cells are depicted. Diagrams show the mean \pm SEM for nine control mice, thirteen *Ptch*^{lox/lox} and fourteen *CD4Cre*^{+/-} *Ptch*^{lox/lox} mice from three independent experiments.

I next performed histopathological studies of lungs to investigate structural changes present in the airways and lung parenchyma upon antigen challenge (Figure 16). In control mice, the lung tissue appeared normal with few nucleated cells being distributed among alveoli (small hollow structures) and around bronchioles (larger hollow structures; Figure 16A). In *Ptch*^{flox/flox} mice that were sensitised and challenged with Ova, I could observe severe differences compared to control mice (Figure 16B). Tissue-infiltrating nucleated cells were massively increased in numbers and accumulated around the airways. In addition, thickening of the airway walls could be observed along with increased mucus secretion that narrowed the lumen of bronchioles. Tissue samples from *CD4Cre*^{+/-} *Ptch*^{flox/flox} mice also showed a massive cellular infiltration that closely resembled the situation seen in *Ptch*^{flox/flox} mice with no obvious difference being recognizable (Figure 16C).

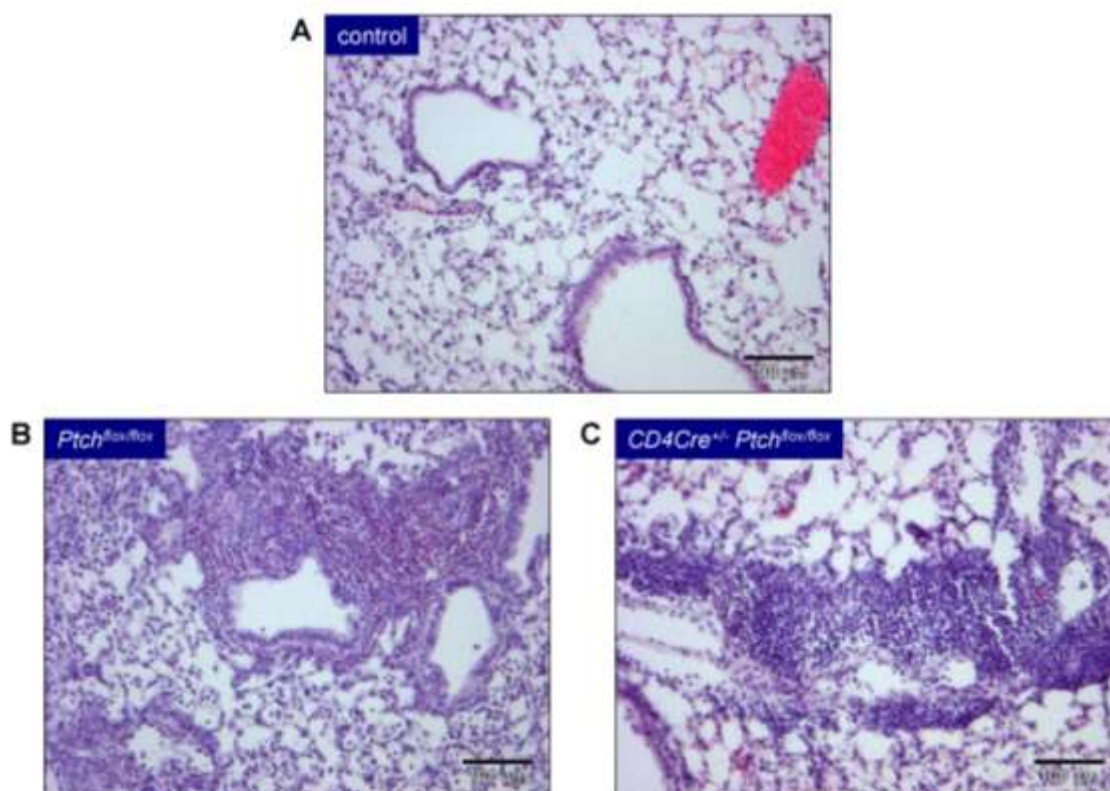


Figure 16. Histologic analysis of lung tissues in allergic airway inflammation experiments

Mice from allergic airway inflammation experiments were sacrificed 48 hours after the final antigen challenge. Lungs were dissected, fixed in 4% paraformaldehyde and embedded in paraffin from which 5 μ m slices were prepared. A HE stain was performed on the slices before they were analysed microscopically. Representative images are shown from control mice which were not sensitised to the antigen (A) as well as from sensitised *Ptch*^{flox/flox} (B) and *CD4Cre*^{+/-} *Ptch*^{flox/flox} (C) mice. Scale bars in the lower right corner of all images equal 100 μ m.

In order to investigate whether the elicited immune response was T_H2 -biased as intended and to evaluate its strength, I determined the amount of Ova-specific immunoglobulins in the serum of mice (Figure 17A). While Ova-specific antibodies were virtually absent in control mice, those that had been immunised and challenged with antigen showed high titers of specific antibodies in the serum. These were predominantly of the IgG1 isotype which is indicative of a pronounced T_H2 response. Antibodies of IgG2a and IgE isotypes were also increased to a certain extent in immunised mice. However, serum titers of all three isotypes were comparable between CD4Cre transgenic and non-transgenic mice. Finally, I isolated splenocytes from mice of all groups and restimulated them *ex vivo* with Ova (Figure 17B). While the proliferative response was increased as compared to cells isolated from control mice, it was also similar between cells obtained from $CD4Cre^{+/-} Ptch^{flx/flx}$ and $Ptch^{flx/flx}$ mice. In summary, despite the different readouts that were used to evaluate the immune response in this model of allergic airway inflammation, no impact of the *Ptch*-deficiency on T cell function could be observed.

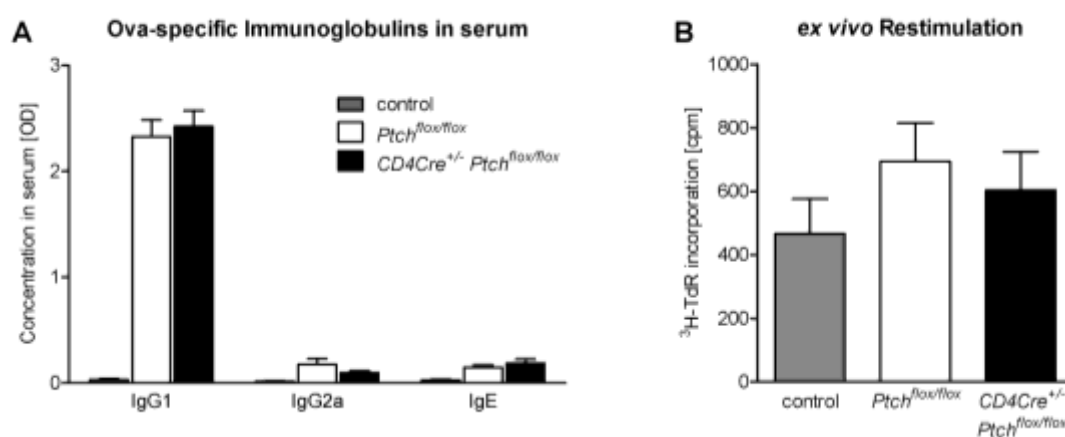


Figure 17. Antibody response and T cell function after induction of allergic airway inflammation.

(A) Serum was prepared from blood 48 hours after the last antigen challenge. Ova-specific immunoglobulins of IgG1, IgG2a and IgE isotypes were quantified by ELISA and are shown in the form of optical densities (OD). Results represent data from nine control mice and fifteen mice from both experimental groups. (B) Splenocytes were isolated and restimulated *ex vivo* with 10 μ g / ml Ova for 72 hours. Proliferation was quantified using 3H -TdR incorporation and is given as cpm. Measurements were performed in triplicates. The diagram shows combined data from six control mice and ten mice from each experimental group.

3.6.2 Acute Graft-versus-Host disease

GvHD is a common complication following the transplantation of immunocompetent allogeneic tissue. Its main cause are mature CD4⁺ and CD8⁺ $\alpha\beta$ T cells which become activated by a broad range of host antigens and subsequently engage host tissues. This occurs through the production of large amounts of inflammatory cytokines and through cell-mediated cytotoxicity. Due to its dependency on the function of both T_h cells and CTLs and its well understood pathophysiology, murine models for the acute form of GvHD can also be used to investigate the functionality of these T cell subpopulations in a physiologic setting. Therefore I decided to employ a model of allogeneic aGvHD to investigate a potential effect of Ptch ablation on T cells *in vivo*. For this purpose I sublethally irradiated BALB/c mice and reconstituted them with allogeneic BM that contained a defined number of mature allogeneic T cells. Control mice received T cell depleted BM only after irradiation. Progression of the disease was regularly evaluated based on several clinical symptoms which were combined into a mean clinical score (Figure 18A).

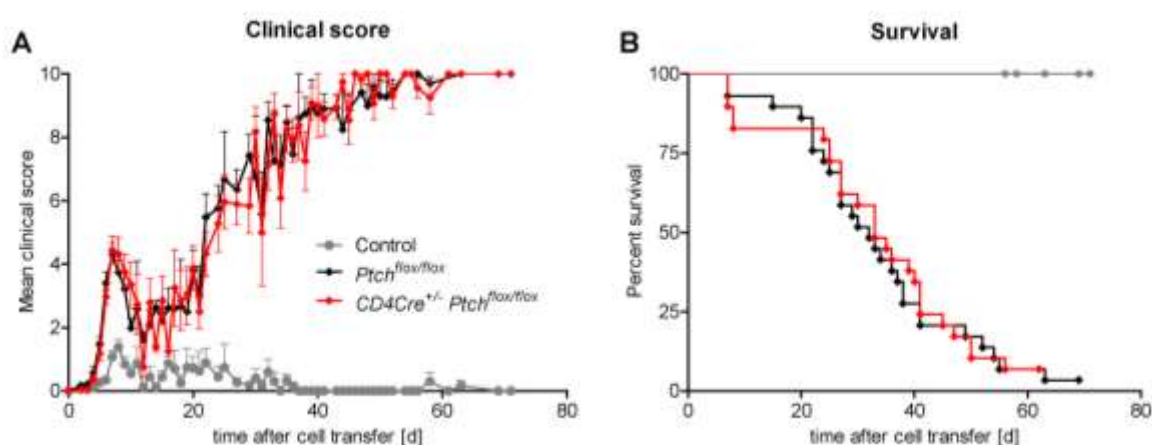


Figure 18. Disease course of aGvHD

Induction of aGvHD was initiated by total body irradiation of male BALB/c mice with a dose of 8,5 Gy. On the following day, mice received 10^7 T cell depleted allogeneic BM cells with (experimental groups) or without (control groups) 2×10^6 T cells from either *Ptch*^{flox/flox} or *CD4Cre*^{+/-} *Ptch*^{flox/flox} mice. (A) Animals were monitored regularly for different clinical symptoms that were combined into a mean clinical score with a maximum of 10. (B) Survival was monitored regularly for experimental and control groups. Both figures show combined data from six independent experiments with twenty-nine mice per experimental group and thirteen mice for the control group. Clinical score is given as the mean \pm SEM.

Starting from approximately day 5 after cell transfer, mice began to show a declining health status which was mainly characterized by weight loss, absent grooming and reduced activity.

The mean clinical score reached a preliminary peak 6 to 8 days after the cells had been transferred and began to decline again. Control mice which had not received T cells did also show clinical symptoms which peaked at the same time point but were less pronounced. Mice from all groups partially recovered in the following days and showed only mild but persistent symptoms for a time period of roughly 10 days. Approximately three weeks after cell transfer, the health status of mice began to decline again and clinical symptoms, which now frequently included diarrhoea, quickly exceeded the values of the initial peak and eventually led to the death of individual mice. In contrast, control mice which had only received T cell depleted BM became virtually free of symptoms 5 weeks after the experiment had been started. Notably, disease progression as assessed by observable symptoms was almost congruent between groups that received Ptch-deficient or control T cells. In parallel, survival of animals was also assessed and is depicted in Figure 18B. When T cells were administered, 10% of mice died on average during the initial disease phase which occurred before day 10 after cell transfer. Only few mice deceased during the recovery phase until the survival rate began to constantly drop starting after day 20. Although survival during the initial phase was slightly better in groups which received wt T cells, the overall survival curves were again highly similar between groups that received Ptch-deficient or control T cells and revealed no significant difference in disease progression.

In addition to evaluating the severity of aGvHD using clinical parameters that were assessed visually, I also determined body temperature and blood glucose levels during the first 10 days of the experiments (Figure 19). These factors are not directly related to an aGvHD reaction but can be used to indirectly evaluate the health status of the mice. Body temperature of animals that had received BM in combination with T cells constantly declined starting from day 4 after cell transfer while temperature from control mice remained relatively constant (Figure 19A). At all time points, values for mice that had received Ptch-deficient or control T cells were highly comparable. Assessment of blood glucose levels also gave similar results and showed that levels declined by trend in groups that received T cells while control animals were less affected (Figure 19B). As before, no significant difference between both experimental groups could be observed. Thus the obtained results from aGvHD experiments argue against an impact of Ptch on the function of T_H and CTLs *in vivo*.

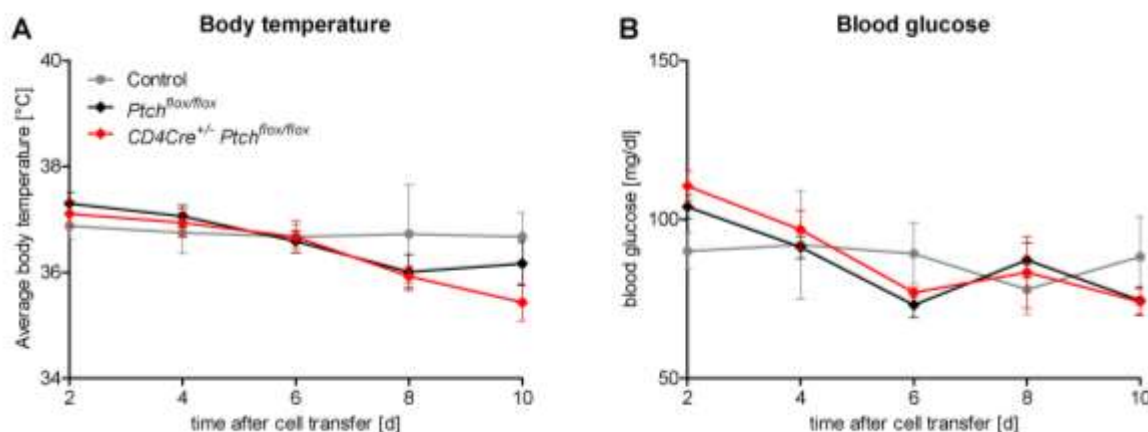


Figure 19. Body temperature and blood glucose levels in aGvHD

Acute GvHD was induced as described before. From day two until day ten after cell transfer, body temperature was determined rectally using a rodent thermometer (A) and glucose levels were measured in blood that was collected from the tail vein (B) every other day. Figures show the mean value \pm SEM from thirteen mice of the experimental groups and from four control mice.

3.6.3 B16 Melanoma model

Although I had previously investigated the peripheral distribution of naturally occurring T_{reg} cells and CTLs *in vivo* and the functionality of T_{reg} cells *in vitro*, I wondered whether ablation of Ptch might exert a subliminal effect on these cell types that could only become evident *in vivo*. Both cell types are known to play critical roles during anti-tumour immune responses which persuaded me to employ an *in vivo* tumour model in order to analyse the functionality of these cells in a physiologic setting. Tumour-specific CTLs are highly effective in the elimination of neoplastic cells while T_{reg} cells, which are also recruited in large numbers into the tumour microenvironment, can suppress the function of anti-tumour effector cells and thereby promote tumour growth. In order to investigate the function of both cell types *in vivo* in the context of an anti-tumour immune response, I inoculated *CD4Cre*^{+/-} *Ptch*^{flox/flox} and control mice subcutaneously with 10⁴ B16F10 melanoma cells and evaluated the development of primary tumours (Figure 20). Subcutaneous tumours initially became visible on control mice ten days after the cells had been transferred and affected all mice by day 22 of the experiment (Figure 20A). Tumour onset and progression were comparable between control and *CD4Cre*^{+/-} *Ptch*^{flox/flox} mice. Individual tumour growth was also measured and is shown in Figure 20B. Starting approximately from day 14 after cell inoculation, the tumours entered an exponential growth phase and quickly reached volumes of more than 300 mm³

after another seven days. Individual tumour development however was again highly similar between both genotypes.

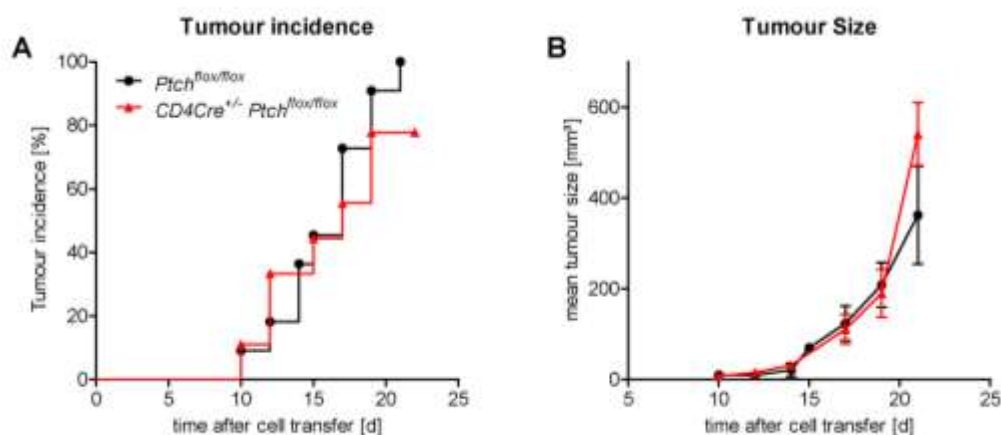


Figure 20. Development of subcutaneous tumours after inoculation of B16F10 melanoma cells

Ptch^{flox/flox} and *CD4Cre*^{+/-} *Ptch*^{flox/flox} mice were inoculated with 10⁴ B16F10 melanoma cells into the right flank. Mice were monitored frequently for palpable tumour and their incidence (A) and size (B) were recorded over a period of three weeks. Both graphs show the mean ± SEM from the combined data of eleven *Ptch*^{flox/flox} and nine *CD4Cre*^{+/-} *Ptch*^{flox/flox} mice.

Although as little as 10⁴ B16F10 cells were inoculated, primary tumours grew fast and became visually detectable already on day ten after cell transfer. Being part of the adaptive immune system, T cells which were in the focus of this experiment require a certain amount of time to recognize their specific antigen, expand and differentiate from naïve T cells to armed effector cells. Thus it was highly conceivable that a potential impact of *Ptch* ablation on T cell function did not become visible due to the high growth rate of the melanoma cells. Furthermore, B16F10 cells are known to be poorly immunogenic which might have further exacerbated the induction of an adaptive immune response (Wang et al., 1998). To overcome this problem, I vaccinated the mice with a mixture of inactivated B16F10 cells and adjuvant in order to elicit a protective anti-tumour immune response. Subsequently, I challenged the mice with 10⁴ live B16F10 cells and observed the development of primary tumours (Figure 21).

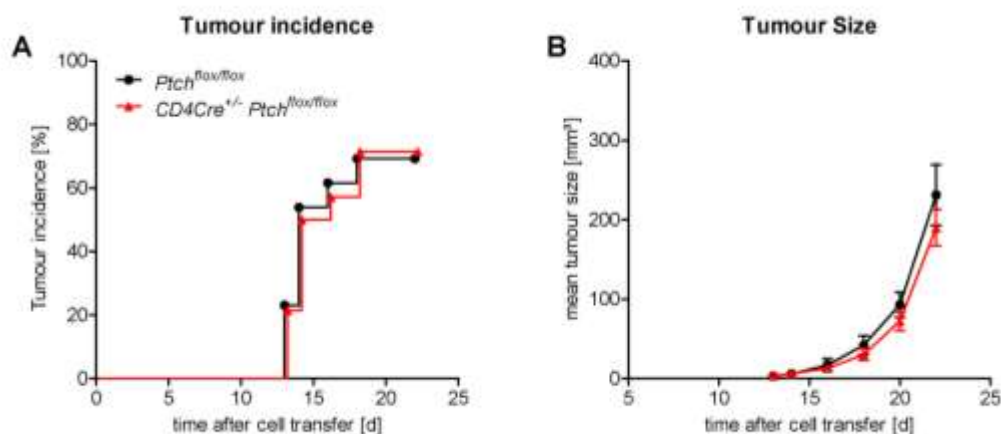


Figure 21. Development of subcutaneous tumours after inoculation of B16F10 melanoma cells in immunised mice

Protective immunity against B16F10 melanoma cells was generated in *Ptch*^{flox/flox} and *CD4Cre*^{+/-} *Ptch*^{flox/flox} mice by immunising them with 10⁶ lethally irradiated cells mixed with CFA into the left flank. After ten days, mice were challenged with 10⁴ live B16F10 cells into the right flank and incidence (A) and size (B) of developing tumours were recorded over time. Tumour incidence rate and mean size ± SEM are shown for fourteen *Ptch*^{flox/flox} and *CD4Cre*^{+/-} *Ptch*^{flox/flox} mice each.

The anti-tumour vaccination delayed tumour onset which did not occur prior to day 13 after cell inoculation (Figure 21A). Interestingly, the tumour incidence rate could also be reduced to approximately 70% whereas the growth rate of individual tumours that managed to outgrow the immune response was not affected (Figure 21B). Despite the protective effect of the anti-tumour vaccination which clearly demonstrated partially successful engagement of the adaptive immune system, no difference in tumour onset, incidence rate or growth could be observed between *CD4Cre*^{+/-} *Ptch*^{flox/flox} and control mice. Thus, my data suggests that the *Ptch*-deficiency does not impact on the function of T_{reg} cells or CTLs during an immune response against inoculated tumours.

4 Discussion

The Hh signalling pathway specifies cell fate and patterning during embryonic development and is involved in homeostasis and renewal of several adult tissues including skin, lung, intestine and thymus. Furthermore, there is evidence that genes which are involved in cell fate decisions during development may also play a role in the continuous decisions made by cells of the adaptive immune system during responses against pathogens (Benson et al., 2004). The role of Hh signalling in the development and function of T cells however remains unclear due to the few groups that have investigated this topic, their different experimental approaches and their largely contradictory results. To gain further insights into the role of this signalling pathway in T cells which are central constituent of the adaptive immune system, the group of Prof. Dr. Heidi Hahn has developed a mouse model in which the Hh receptor Ptch is specifically inactivated in T cells. This $CD4Cre^{+/-} Ptch^{flox/flox}$ mouse formed the basis of this study. In this model, inactivation of Ptch occurs at the DN3 stage of thymocyte development due to the activity of a CD4 promoter-controlled Cre recombinase which catalyses excision of two exons from $Ptch^{flox}$ alleles. According to the general view of Hh signalling, it was expected that the lack of functional Ptch would lead to the activation of canonical Hh signalling that in turn might effect development and/or function of T cells. In this context, different *in vitro* and *in vivo* approaches were performed to unravel potential effects of the Ptch ablation on this cell population.

4.1 Thymocyte development is marginally affected by the Ptch ablation while numbers, distribution and activation states of peripheral T cells remain unaltered

In previous analysis that were performed with $CD4Cre^{+/-} Ptch^{flox/flox}$ mice on a mixed C57BL/6 and 129/Sv genetic background, it was found that thymocyte development was normal and indistinguishable from $Ptch^{flox/flox}$ control mice (Uhmann et al., 2011). Since this was in contrast to several other reports which found that Hh signalling affected the development of thymocytes (Rowbotham et al., 2007; Drakopoulou et al. 2010; Furmanski et al., 2012), I initially focussed my analysis on T cell development in $CD4Cre^{+/-} Ptch^{flox/flox}$ mice which had been backcrossed to the C57BL/6 genetic background. My first observations were that neither the size of the thymi nor the total numbers of thymocytes were altered as compared to control mice, thus indicating that T cell development was not grossly affected by Ptch ablation. Flow cytometric analysis of different developmental stages revealed that neither the percentage of early DN cells which were not yet committed to the T cell lineage, nor of late DN cells after T lineage commitment were altered between both genotypes. This observation

was expected and can be explained by the “late” activation of the CD4 promoter which does not occur before the DN3 stage of thymocyte development (Wolfer et al., 2001). Considering the time that is needed for the expression of the Cre recombinase following promoter activation, the Cre mediated recombination of the *Ptch*^{flox} alleles and the decrease of functional Ptch due to normal protein turnover, one would assume that a potential effect of the Ptch inactivation might not become evident before the DP stage. Indeed, when I investigated thymocyte development beyond the DN stage, I found that the percentage of DP cells was increased in *CD4Cre* transgenic mice with a corresponding reduction in the CD4 SP and CD8 SP cell compartments. These differences were qualitatively in line with some previous reports that studied the effect of Hh signalling on developing thymocytes. Despite being statistically significant however, the differences were only of a small magnitude and barely affected the overall composition of thymocytes. For this reason, the results need to be treated with caution since they might indicate an effect of the Ptch inactivation on T cell development but could also be the result of a side effect following the expression of the Cre recombinase. Although no such observations have been specifically reported in *CD4Cre* transgenic mice, it is known that expression of the Cre recombinase itself can already induce a stress response leading to decreased cell growth, chromosomal aberrations and several metabolic alterations in different cell types (Silver and Livingston, 2001; Xiao et al., 2012).

In order to investigate whether the observed differences in thymocyte development had any implications for peripheral T cells, I continued by studying the frequency, composition and activation state of this population. I started by evaluating the spleen as the largest secondary lymphoid organ but was unable to find differences in either the size of the organ or the total amount of harboured cells indicating that T cell homeostasis was not generally disturbed. Further analysis of both the percentage of T cells among immune cells in different peripheral sites as well as the percentage of both major T cell subsets among total T cells also failed to reveal any difference between *CD4Cre*^{+/-} *Ptch*^{flox/flox} and control mice. Accordingly, the ratio of CD4⁺ to CD8⁺ T cells which can be indicative of altered TCR signalling was unchanged as well. Together these data demonstrated that the observed marginal difference in the development of thymocytes neither led to an impaired homeostatic regulation of T cell numbers in the periphery nor to an imbalance within the T cell compartment. Since the maintenance of the homeostatic equilibrium involves cellular interactions, the competition for survival factors such as IL-7 along with the regulation of proliferation and cell death (Marrack et al., 2000; Tan et al., 2002), these data suggested that not only T cell numbers were unaltered by the Ptch inactivation but also that different critical features of T cells were not affected either.

Since until then I had only investigated T cells without an immunological context, I continued to focus on T cells that had already been in contact with their specific antigen *in vivo*. Using flow cytometry, I identified recently activated T cells and effector memory T cells in different immunologically relevant sites. I found that up to 30% of CD4⁺ and CD8⁺ T cells were highly positive for CD44 and thus had already become activated in response to foreign antigen. In addition, 5-10% of both populations had encountered antigen recently as indicated by CD69 expression. Hence, despite the fact that the mice were kept under SPF conditions, they were regularly exposed to pathogens that challenged the adaptive immune system. Notably, I was not able to see differences in the percentage of T cells that showed either a recently activated or effector memory phenotype between both genotypes. This was a first loose indication that T cell responses can be elicited *in vivo* and lead to the differentiation of naïve T cells into effector cells irrespective of the presence of functional Ptch.

4.2 Ptch does not impact on functional characteristics of T cells *in vitro*

During the flow cytometric phenotype analysis of T cells, I had already found some indications that the Ptch inactivation was not only largely dispensable for the development and homeostasis of T cells, but might also be expendable for at least some of their functional characteristics. Yet it might have been possible that functional impairment existed which did not affect the cells in a way that became apparent in these analysis. For this reason I performed several *in vitro* experiments which specifically aimed at the investigation of functional characteristics of T cells. Initially I performed a MLR which is based on the alloreactivity of T cells against MHC-mismatched APCs and represents a useful experimental tool to investigate T cell responses *in vitro*. According to the expectations, T cell proliferation was rather weak in this setup. This is a common feature of MLRs and is caused by the low frequency of alloreactive T cells which become activated (Sherman and Chattopadhyay 1993). The proliferative response however was highly comparable between Ptch-deficient and control T cells. Secretion of the autocrine survival factor IL-2 and the effector cytokine IFN- γ were also not significantly different between both groups. Although Ptch-deficient T cells showed on average a tendency towards slightly lower IL-2 and higher IFN- γ production, the differences were not only contrary but also highly inconsistent between individual experiments thus arguing against a biologic relevance. By employing this experimental approach, I was therefore not able to observe any meaningful difference between Ptch-deficient and control T cells.

Since the number of responding T cells following an allogeneic stimulation ranges from only 1-10% (Kovalik et al., 2000), I considered it possible that this circumstance might have

masked a potential effect of Ptch on T cell activation in MLR experiments. In addition, the limited availability of costimulation in this setup might have also contributed to these observations by favouring the activation of T cells that received very strong signals through the TCR while those with an average affinity for the MHC:peptide complex might have been unable to overcome the activation threshold. I therefore continued with the analysis of T cell responses following polyclonal activation which theoretically affected all T cells equally. In addition to employing ConA which is a commonly used polyclonal mitogen, I also stimulated cells with activating antibodies against the TCR-associated signalling molecule CD3 and the costimulatory molecule CD28. In this way, I could employ a less artificial form of stimulation compared to ConA-mediated activation on the one hand and ensure that the T cells would receive both primary and costimulatory signals on the other hand. All stimulations were additionally conducted at suboptimal and optimal concentrations to allow the detection of beneficial and attenuating effects, respectively. As a readout, both the proliferation rate and the secretion of the cytokines IL-2 and IFN- γ were assessed at different time points. Despite this extensive setup, I was unable to observe any significant difference between Ptch-deficient and control T cells. Under optimal stimulation conditions, the proliferative response was by trend only slightly stronger in cells that lacked expression of functional Ptch while it was similar under suboptimal conditions as observed during MLR experiments. This slight and insignificant increase in proliferation however did not correlate with the secretion of IL-2 which was even slightly lowered in Ptch-deficient T cells when ConA was used as a stimulus or equal when the cells were stimulated with antibodies. Secretion of IFN- γ was highly comparable under all conditions and at all time points. Taken together, the data again argued against a role of Ptch in T cells during the activation and expansion phases. Neither the capability of T cells to transduce signals via the TCR:CD3 complex nor the reception of costimulatory signals through CD28 seemed to be reinforced or disturbed. Following the two-signal activation, the cells were fully capable of secreting as well as responding to IL-2 and subsequently undergo mitosis during the clonal expansion phase. Production of the effector cytokine IFN- γ which requires proper priming of naïve T cells also appeared to be unaffected. Thus, several key characteristics of conventional T cells were not altered following Ptch ablation.

Although I found no evidence that the function of conventional T cell was affected by ablation of Ptch in my model, I wondered whether the same was also true for T_{reg} cells. This specialised T cell subpopulation fulfils specific tasks in the immune system by maintaining tolerance to self-antigens and dampening both physiological and pathological immune responses. Similar to conventional T cells, naturally occurring T_{reg} cells arise from DP precursors in the thymus, albeit at lower numbers. The observed increase in the percentage

of DP cells in thymi from *CD4Cre^{+/-} Ptch^{flx/flx}* mice thus may have indicated a potential effect on this population. I found however, that the number of peripheral T_{reg} cells was highly comparable between mice that lacked expression of functional Ptch and control mice. This excluded that the development of naturally occurring T_{reg} cells in the thymus was numerically affected as well as their maintenance in the periphery. Next I determined the expression level of the transcription factor FoxP3 in T_{reg} cells but found it not to be altered either. Since FoxP3 is not only required for proper function of T_{reg} cells but its expression also correlates with the functional status of T_{reg} cells (Chauhan et al., 2009), these data already indicated that not only the frequency of T_{reg} cells might be unaltered but also their suppressive capacity. Indeed when I performed a suppression assay where I cocultured T_{reg} cells with activated conventional T cells, I could not observe any differences between cells that were deficient for Ptch versus control cells. T_{reg} cells from mice of both genotypes did not respond to stimulation and were equally potent in the ratio-dependent suppression of conventional T cell proliferation. Hence the obtained data argue against a role of Ptch in the development and function of naturally occurring T_{reg} cells. Due to the focus of my studies on this specific subpopulation, however, I cannot exclude effects of Ptch ablation on induced T_{reg} cells which develop in the periphery and also play important roles during inflammatory responses.

Apoptosis is a process of controlled cell death that occurs as part of normal tissue development but is also implicated at virtually every stage of lymphocyte development and function. Not only does it mediate the removal of non-functional or potentially autoreactive cells in the thymus but it is also crucial for shutting down immune response after pathogen clearance and for the deletion of autoreactive cells that escaped into the periphery. Considering its relevance, I decided to explore whether Ptch might influence this process in T cells. Initially, I studied apoptosis of resting cells which was induced by survival factor deprivation in cell culture, by Dex treatment or by γ -radiation. All three stimuli lead to the induction of apoptosis by activating the intrinsic or mitochondria-mediated apoptotic pathway which is characterised by the permeabilisation of the mitochondrial membrane and subsequent release of cytochrome c into the cytoplasm. This leads to the formation of a multi-protein complex which initiates activation of the caspase cascade through caspase 9 eventually leading to the degradation of cellular constituents. In my experiments, I found that apoptosis occurred similarly in Ptch-deficient and control T cells irrespective of the stimulus indicating that the Ptch ablation did not affect the intrinsic apoptotic pathway in resting T cells. However, one critical feature of activated T cells is their reduced susceptibility to apoptosis which improves their effectiveness during an immune response. This is due to the increased expression of several Bcl-2 family members such as the anti-apoptotic proteins Bcl-2 and Bcl-X_L. In addition, activated T cells also upregulate the expression of numerous

pro-apoptotic proteins including members of the Bcl-2 homology 3 (BH3)-only subgroup BIM and PUMA (Broome et al., 1995; Erlacher et al., 2006). Together, these proteins tightly regulate the mitochondrial apoptotic pathway through activation or inhibition of the Bcl-2 family members Bax and Bak (Sentman et al., 1991; Strasser et al., 1991; Puthalakath and Strasser, 2002). Speculating about a possible involvement of Ptch in the anti-apoptotic regulation process in activated T cells, I continued to investigate apoptosis susceptibility in activated T cells. Indeed I found that resistance to apoptosis in general was strongly increased upon cell activation but an influence of Ptch could not be revealed in this context either. Taken together, no evidence could be found that Ptch is involved in the process of programmed cell death in both resting and activated T cells. It is noteworthy however that all employed stimuli focussed on the activation of the intrinsic apoptotic pathway. The extrinsic pathway on the other hand is activated upon ligand binding to death receptors of the TNFR family including TNFR-1 and Fas which are expressed on the cell surface. Although both pathways converge in the caspase cascade which eventually leads to apoptosis, it cannot be excluded from the obtained data that Ptch might interfere with the extrinsic pathway before caspase activation and thus modulate apoptosis.

4.3 Expression of Ptch in T cells is dispensable for adaptive immunity

Although I found that Ptch ablation only slightly affected thymocyte development and did not impact on the peripheral distribution of T cells or their functionality *in vitro* either, I still considered it possible that it might exert a subliminal effect which might only become evident in functional *in vivo* studies. For this reason I employed three different disease models which focussed on the function of different T cell subpopulations.

In my first approach I performed allergic airway inflammation experiments as a model for human asthma. In this model, mice were sensitised against Ova to elicit a T_H2-biased immune response which was evaluated upon intranasal challenge with the antigen. This led to an extensive influx of inflammatory cells into the airways which was dominated by eosinophils but also comprised CD4⁺ T cells, macrophages and neutrophil granulocytes. By using histological analysis, a strong cellular infiltration could also be observed in the lung tissue where cells accumulated around bronchioles. Furthermore, the induction of a humoral immune response could be detected where IgG1 was the predominant isotype which identified the response to be T_H2-biased. While all observed features were characteristic for a murine model of allergic airway inflammation (Ohkawara et al., 1997), no difference could be found between sensitised mice regardless of functional Ptch expression in T cells. Thus, the antigen-driven differentiation of naïve T_H0 cells into T_H2 effector cells which plays a central

role in this model appeared not to be affected. Indirect evidence further suggested that production of the T_h2-specific cytokines IL4, IL-5 and IL-13 was also not altered. Influx of inflammatory cells into the lungs depends on IL-4 and IL-13 which induce expression of vascular cell adhesion molecule-1 (VCAM-1) on the vascular endothelium thus directing cellular infiltration (Moser et al., 1992; Bochner et al., 1995). In addition, IL-4 synergizes with IL-5 in promoting eosinophil survival, activation and chemotaxis through the increased expression of eotaxins (Mochizuki et al., 1998; Collins et al., 1995) and in directing B cell class switching to IgG1-secreting cells. Although these cytokines are not exclusively produced by T cells, the obtained results strongly suggested that the capability of T_h2 cells to secrete specific cytokines was not affected in this model either.

Next I studied a potential effect of Ptch on T cell function during a T_h1-biased immune response in a murine model for aGvHD. This model is based on the alloreactivity of CD4⁺ and CD8⁺ donor T cells which are transferred into an immunodeficient and H-2 incompatible recipient. Upon activation by donor and host APCs, T cells expand and cause severe cytotoxicity in various tissues which leads to a systemic syndrome of weight loss, diarrhoea, skin changes and high mortality. Indeed I could observe that the health status of mice began to decline quickly and reached a preliminary minimum around day seven after cell transfer. This rapidly occurring effect is frequently seen in murine models of GvHD (Duran-Struuck et al., 2001; Albring et al.; 2010) and caused both by the activation of naïve T cells and the conditioning regimen which precedes cell transfer. For this reason, a similar but less pronounced effect could also be observed in control mice which received T cell depleted BM only. Following a short recovery phase, disease severity began to rise vigorously due to the activity of fully differentiated effector T cells which caused extensive tissue damage eventually leading to death of the animals. Importantly, this phase was completely absent in control mice demonstrating that it was solely caused by T cell activity. A difference between mice that received T cells from *CD4Cre*-transgenic or control mice could neither be observed during the early nor during the late phase of the disease course. In conclusion, results from aGvHD experiments suggest that Ptch does not affect the activation, differentiation or effector function of CTL or T_h cells during a T_h1-biased immune response *in vivo*.

In another approach to study a potential effect of Ptch on T cells *in vivo*, I employed a transplantable murine melanoma model based on the B16F10 cell line. Subcutaneous inoculation of melanoma cells led to the development of primary tumours which allowed the evaluation of the CTL-mediated anti-tumour immune response on the one hand and tumour-enhancing effects of T_{reg} cells on the other hand. I found that without previous protective immunisation, tumours grew rapidly and could not be controlled by the immune system.

Following an anti-tumour immunisation, tumour control was much improved and approximately 30% of mice remained free of observable tumours during the experiments. Ablation of *Ptch* did not influence the ability to control tumour development under both conditions. Thus, that data obtained from tumour transplantation experiments was in line with the observations made during aGvHD experiments and showed that functional *Ptch* was also dispensable for the function of CTLs and T_{reg} cells during an anti-tumour immune response *in vivo*.

In summary, three different *in vivo* models have been employed to investigate general T cell features and proper functioning of several T cell subpopulations in a physiologic environment. Under all conditions, T cells from $CD4Cre^{+/-} Ptch^{flox/flox}$ mice were highly comparable to cells derived from $Ptch^{flox/flox}$ control mice. Supported by the observations from *in vitro* experiments, the data convincingly demonstrates that T cell intrinsic expression of the Hh receptor *Ptch* is dispensable for proper T cell function in adaptive immune responses.

4.4 Absence of *Ptch* in T cells does not lead to the activation of canonical Hh signalling

In previous studies that focussed on the characterization of $CD4Cre^{+/-} Ptch^{flox/flox}$ mice, it was reported that Cre-mediated recombination at the $Ptch^{flox}$ locus was almost complete in thymocytes which led to the predominant expression of the incomplete $Ptch^{del}$ allele (Uhmann et al., 2011). However, this did not lead to the activation of canonical Hh signalling which was demonstrated by unaltered expression of the indicative transcription factors *Gli1* and *Gli2*. During expression analysis of peripheral T cells I was able to make similar observations. Although the reduction in wt *Ptch* expression was even more pronounced as compared to thymocytes and accompanied by expression of the $Ptch^{del}$ allele, *Gli* transcription factor levels remained unaltered in $CD4Cre^{+/-} Ptch^{flox/flox}$ mice. This demonstrated that the inability to activate canonical Hh signalling by *Ptch* ablation in T cells was not restricted to the thymus but also holds true for cells in the periphery. Although these observations were in line with the findings of Uhmann et al., they were still contrary to the consensus view that inactivation of *Ptch* should lead to active Hh signalling due to the discontinuation of its inhibitory effect on *Smo*. One possible explanation for this discrepancy could be the activity of a compensatory mechanism that takes effect after functional *Ptch* is lost. A possible candidate in this context might have been the *Ptch* homolog *Ptch2*. It has been shown that *Ptch2* can bind Hh proteins with similar affinity to *Ptch1*, although it fails to compensate for the lack of *Ptch1* in distinct cell types (Carpenter et al., 1998; Zaphiropoulos et al., 1999; Stone et al., 1996). Considering it possible that it may fulfil a compensatory role

in T cells, I analysed the expression of Ptch2 but was unable to detect transcripts in T cells at all whereas it was clearly detectable in mouse embryo samples. Considering the sensitivity of a PCR-based approach, the presence of Ptch2 in T cells and therefore a potential effect can be excluded. Yet it is conceivable that other compensatory mechanisms may exist which prevent pathway activation in T cells despite the lack of functional Ptch. A synergistic function of other signalling pathways may also contribute to the masking of a phenotype in our model. Indeed, it has been shown that developmental signalling pathways such as Notch and Wnt are capable of interacting with Hh signalling (Yang and Niswander, 1995; Hallahan et al., 2004). It is possible that they play overlapping roles in thymopoiesis and may thus partially or totally compensate for any deficiencies in Hh signalling.

A likely explanation for the lack of canonical Hh signalling in T cells despite Ptch ablation comes from the morphological characteristics of this cell type. Regarding the importance of the primary cilium for Hh signalling not only as a site of action but also as an integral component (Cheung et al., 2009; Endoh-Yamagami et al., 2009; Liem et al., 2009), the lack of pathway activation in this model could be explained by the absence of this organelle in cells of the haematopoietic lineage including T cells (Pazour and Witman 2003). It is conceivable that due to the lack of this compartment, proper interaction between Ptch and Smo or Smo and the Gli transcription factors cannot take place anymore which renders the cells incapable of responding to Hh ligands. In this scenario, gain- or loss-of-function mutations in upstream signalling components would not lead to the activation of Gli transcription factors and thus not affect cell function. This hypothesis is supported by findings of different groups in addition to our own. Gao and colleagues reported that the conditional inactivation of Smo did not influence development or function of HSCs or lymphocytes (Gao et al., 2009). Furthermore, the authors reported that they were unable to detect active Hh signalling in wild type HSCs or myeloid progenitor cells in the presence of Hh ligands despite the fact that the receptor Ptch and Smo were expressed. Alternative approaches which employed mouse models carrying a Gli1 deficiency or a gain-of-function mutation in Smo also failed to show any effect on the development of HSCs or lymphocytes. A different group which used the same conditional Smo knockout model confirmed these findings and additionally showed that continuous *in vivo* application of a Hh antagonist did not affect peripheral blood composition (Hofmann et al., 2009). Other studies conducted by Siggins et al. also supported this notion by demonstrating that intrinsic Ptch expression is not required for the development of different haematopoietic cells and does not lead to activation of Hh signalling either (Siggins et al., 2009). Further support for this hypothesis comes from observations which were made in our cooperating laboratories. It was found that specific inactivation of Ptch in myeloid cells (Pelczar et al., 2012) or B cells (unpublished

observations by Kai Dittmann, Department of Cellular and Molecular Immunology, University Medical Centre Göttingen, Germany) did neither cause activation of canonical Hh signalling nor affect normal development or function of cells either. Importantly, all these observations were made exclusively for cells of the haematopoietic lineage including HSCs while Hh signalling is clearly implicated in the homeostasis and differentiation of neural stem cells (Lai et al., 2003; Cai et al., 2008), intestinal stem cells (Ramalho-Santos et al., 2000), mammary stem cells (Liu et al., 2006) as well as embryonic stem cells (Kiprilov et al., 2008). Taken together, these data suggest that independency of intrinsic Hh signalling is a characteristic feature of the haematopoietic lineage starting from HSCs. Since this coincides with the absence of primary cilia which are appreciated as cellular signalling centres, it is thus conceivable that the inability to transduce Hh signals is caused by the lack of this cellular compartment.

4.5 Investigations on the role of Hh signalling in the development and function of T cells

Different studies have been conducted to elucidate the role of Hh signalling in lymphocyte function and development. Initial investigations were performed using FTOC to analyse fetal thymocyte development under physiologic conditions. It was reported that the application of rShh led to a block of thymocyte development at the DN stage while Hh antagonists prevented the transition from DP to SP stage (Outram et al., 2000). Later research found that the transcription factors Gli1 and Gli2 were required for the proper development of thymocytes (Drakopoulou et al., 2010). Although I suggest that T cells themselves are not capable of responding to Hh ligands, these observations may be explained by an indirect effect mediated through accessory cells present in the thymus. Moreover, it is important to note that fetal haematopoiesis is considerably different from adult haematopoiesis (Mold et al., 2010). It is thus conceivable that fetal and adult thymopoiesis may also have unique and distinct Hh signalling requirements.

Further *in vitro* approaches focussed on the effect of recombinant Hh ligands or Hh antagonists on isolated peripheral T cells from wild type mice or humans. It was found that treatment with recombinant Hh ligands led to hyperactivation of T cells which was characterised by increased proliferation, cytokine production and the upregulation of activation markers (Stewart et al., 2002; Lowrey et al., 2002, Chan et al., 2006). Application of Hh antagonists had opposing effects and negatively affected T cell activation. Since these findings were based on the unspecific treatment of partially purified T cell populations, they can also be explained by an indirect effect through another cell type present in the culture. In

fact, this is supported by the finding that treatment of T cells with rShh, despite affecting cell proliferation, did not lead to activation of canonical Hh signalling in these cells (Chan et al., 2006). However it is also conceivable that Hh ligands executed a stimulatory effect on T cells through non-canonical mechanisms. Nevertheless, due to the artificial nature of *in vitro* experiments these results may not necessarily reflect the physiological function of Hh signalling in T cells.

More sophisticated analyses on the role of Hh signalling in T cells were performed using transgenic mouse models that overexpressed either the transcriptional activator or repressor form of Gli2 to study the effect of constitutive activation or repression of Hh signalling, respectively (Rowbotham et al. 2007, Rowbotham et al., 2008 Rowbotham et al. 2009, Furmanski et al., 2012). It was reported that overexpression of the transcriptional activator led to the activation of canonical Hh signalling which caused an attenuation in TCR signalling strength. This had negative implications for thymocyte development, homeostasis of peripheral T cells and mature T cell function. The opposite effects could be observed when the transcriptional repressor was overexpressed instead. Despite the fact that these models gave consisting results, the biologic relevance of the findings needs to be carefully evaluated. Due to the model design, activation or repression of Hh signalling occurs independent of upstream signalling components. If, according to my hypothesis, the signal initiation under normal conditions was blocked at the level of the surface receptors, then data from these models would not reflect the physiologic function of Hh signalling in T cells. However, it is important to note that transcriptional repression of Hh signalling should not effect T cell development or function in this scenario. The fact that repression of Hh signalling nevertheless affected T cell function is not consistent with my hypothesis so far. Yet another constituent of the experimental design may offer an explanation for this discrepancy. To ensure lymphocyte specificity expression, the modified transcription factors were placed under the control of an Lck promoter which is active in early thymocytes of both fetal and adult thymi (Aono et al., 2000). Especially during fetal thymopoiesis, other developmental pathways such as Notch or Wnt are active which might interact with Hh signalling at the level of transcriptional regulators. Suppression of this interaction by overexpression of a transcriptional repressor may therefore explain the discrepancy between these observations and my proposed model.

Other groups focussed their investigations on the transmembrane protein Smo which is an upstream component of the Hh signalling machinery and an interaction partner of Ptch. El Andaloussi and colleagues showed that a shutdown of Smo after pre-TCR expression did not affect T cell development or function at all (El Andaloussi et al., 2006). On the other hand,

they reported that early ablation of Smo in an Mx1-based inducible system negatively impacted T cell development causing thymic atrophy and a significant loss in peripheral T cell numbers. They thus speculated that Hh signalling was only implicated in early thymocyte development. Using the same experimental approach however, two different studies obtained contrary results and showed that inducible shutdown of Smo did not affect haematopoiesis at all (Gao et al., 2009, Hofmann et al., 2009). These observations are in line with my own findings as they argue against a role of physiologic Hh signalling in the development of T cells. Furthermore, they support the notion that primary cilia are required for Hh signal transduction since they provide additional evidence that inactivation of upstream signalling component does not lead to the activation of canonical Hh signalling in T cells.

Further insights into the role of Hh signalling in T cell development came from studies that focussed on the Hh receptor Ptch itself. Uhmman and colleagues reported that inducible Ptch ablation prevented lymphocyte development already at the level of CLP in the BM (Uhmman et al., 2007). Furthermore, they demonstrated that lymphocyte-intrinsic Ptch expression was dispensable for their development and suggested that its expression was required in the stromal cell compartment instead. In a subsequent study, they further excluded that Ptch expression in the thymic stroma was required and suggested that its expression might be relevant in prethymic stromal cells (Uhmman et al., 2011). This hypothesis was supported by the work of another group which reported that specific inactivation of Ptch in the haematopoietic system failed to affect T cell development or function (Siggins et al., 2009). Instead, they proposed a model in which Ptch expression was required in epithelial cells for proper lymphocyte development. These findings are of central importance for the understanding of Hh signalling in T cells as they help to reconcile much of the previously contradictory data. Several groups which performed studies in this field employed models in which the manipulation of Hh signalling components was not restricted to haematopoietic cells although they were in the focus of the study. Since it is difficult if not impossible to differentiate between cell-intrinsic and -extrinsic effects of Hh signalling in these models, it can be misleading to draw conclusions out of these experiments. Indeed, the majority of observations which are inconsistent with the model proposed in this study could be explained by indirect effects on T cells which were mediated by non-haematopoietic cells.

Taken together, various studies have been performed to investigate the role of Hh signalling in haematopoiesis. The choice of different experimental approaches, the spatially and temporally complex regulation of this developmental pathway and functional redundancy of its components have yielded different and partially contrary results. Based on the study of the

CD4Cre^{+/-} Ptch^{flox/flox} mouse model, my data is not in favour of a role for Hh signalling in adult T cell development after the DP stage of thymopoiesis. In addition, my study demonstrates that inactivation of Ptch does not affect the function of mature T cell both *in vitro* and *in vivo*. Ablation of Ptch in this model also did not lead to the activation of canonical Hh signalling which is supposedly caused by the lack of primary cilia on haematopoietic cells. There is also no indication for non-canonical signalling activity which might affect cellular behaviour by circumventing the Smo-Gli axis. Thus I propose a model in which Ptch-mediated intrinsic Hh signalling is dispensable for intermediate and late T cell development as well as for the function of mature T cells. This model is supported by several reports from different groups and can be reconciled with the majority of other observations. In conclusion, my data provides new insights into the role of Hh signalling in T cells and might help to gain a better understanding of this signalling pathway.

5 Summary

The hedgehog signalling pathway is a highly conserved key regulator of animal development and required for homeostasis of adult tissues both in invertebrates and vertebrates. In addition, a large number of studies have suggested that this pathway is also implicated in different aspects of vertebrate haematopoiesis and lymphopoiesis. Its precise role in this context however appears to be complex and conflicting data reported from different groups have prevented a comprehensive understanding of its implication. The aim of the study at hand was to further improve the understanding of Hh signalling and its involvement in the development and function of T cells which are a central component of the adaptive immune system. For this purpose, a mouse model was employed in which expression of the Hh receptor Ptch was ablated specifically in T cells. Since Ptch is known to be a negative regulator of Hh signalling, its inactivation was expected to activate the canonical Hh signalling pathway and thus affect T cell behaviour. However, it was found that Ptch ablation only marginally affected the development of thymocytes at the transition from the DP to the SP stage. This minor effect did not have any implications for the total number of peripheral T cells or for the composition of the T cell pool. Furthermore, the activation state of peripheral T cells was found to be unaltered upon Ptch ablation indicating that functional characteristics were not affected either. Indeed, different experimental approaches *in vitro* which focused on several key characteristics of mature T cell populations failed to reveal any impact of the Ptch inactivation. Similar results were obtained from analyses of Ptch-deficient T cells in several disease models *in vivo* thus confirming that T cell-intrinsic Ptch expression is dispensable for proper T cell function even under physiological conditions. Interestingly and contrary to the consensus view, it was found that Ptch ablation did not result in the activation of the canonical Hh signalling cascade. Although this discrepancy can be explained in several ways, it is most likely accounted for by the lack of primary cilia on T cells which have emerged as important initiation sites of different signalling pathways. This hypothesis is supported by several independent reports which demonstrated that ablation of another upstream pathway component in cells of the haematopoietic lineage did not cause pathway activation or affect development or function of these cells either. Taken together, this thesis presents comprehensive evidence that intrinsic expression of the Hh receptor Ptch is dispensable for intermediate and late T cell development as well as for T cell function both *in vitro* and *in vivo*. In addition, it suggests that intrinsic canonical Hh signalling in T cells is not required under physiological conditions either.

6 References

Albring JC, Sandau MM, Rapaport AS, Edelson BT, Satpathy A, Mashayekhi M, Lathrop SK, Hsieh CS, Stelljes M, Colonna M, Murphy TL, Murphy KM. Targeting of B and T lymphocyte associated (BTLA) prevents graft-versus-host disease without global immunosuppression. *J Exp Med.* 2010 Nov 22;207(12):2551-9.

Alcedo J, Ayzenzon M, Von Ohlen T, Noll M, Hooper JE. The *Drosophila* smoothed gene encodes a seven-pass membrane protein, a putative receptor for the hedgehog signal. *Cell.* 1996 Jul 26;86(2):221-32.

Alexandre C, Jacinto A, Ingham PW. Transcriptional activation of hedgehog target genes in *Drosophila* is mediated directly by the cubitus interruptus protein, a member of the GLI family of zinc finger DNA-binding proteins. *Genes Dev.* 1996 Aug 15;10(16):2003-13.

Allen BL, Tenzen T, McMahon AP. The Hedgehog-binding proteins Gas1 and Cdo cooperate to positively regulate Shh signaling during mouse development. *Genes Dev.* 2007 May 15;21(10):1244-57.

Allen BL, Song JY, Izzi L, Althaus IW, Kang JS, Charron F, Krauss RS, McMahon AP. Overlapping roles and collective requirement for the coreceptors GAS1, CDO, and BOC in SHH pathway function. *Dev Cell.* 2011 Jun 14;20(6):775-87.

Aono A, Enomoto H, Yoshida N, Yoshizaki K, Kishimoto T, Komori T. Forced expression of terminal deoxynucleotidyl transferase in fetal thymus resulted in a decrease in gammadelta T cells and random dissemination of Vgamma3Vdelta1 T cells in skin of newborn but not adult mice. *Immunology.* 2000 Apr;99(4):489-97.

Apionishev S, Katanayeva NM, Marks SA, Kalderon D, Tomlinson A. *Drosophila* Smoothed phosphorylation sites essential for Hedgehog signal transduction. *Nat Cell Biol.* 2005 Jan;7(1):86-92.

Avaron F, Hoffman L, Guay D, Akimenko MA. Characterization of two new zebrafish members of the hedgehog family: atypical expression of a zebrafish indian hedgehog gene in skeletal elements of both endochondral and dermal origins. *Dev Dyn.* 2006 Feb;235(2):478-89.

Aza-Blanc P, Kornberg TB. Ci: a complex transducer of the hedgehog signal. *Trends Genet.* 1999 Nov;15(11):458-62.

Bai CB, Stephen D, Joyner AL. All mouse ventral spinal cord patterning by hedgehog is Gli dependent and involves an activator function of Gli3. *Dev Cell.* 2004 Jan;6(1):103-15.

Baker MB, Altman NH, Podack ER, Levy RB. The role of cell-mediated cytotoxicity in acute GVHD after MHC-matched allogeneic bone marrow transplantation in mice. *J Exp Med.* 1996 Jun 1;183(6):2645-56.

Barnes EA, Kong M, Ollendorff V, Donoghue DJ. Patched1 interacts with cyclin B1 to regulate cell cycle progression. *EMBO J.* 2001 May 1;20(9):2214-23.

Beachy PA, Karhadkar SS, Berman DM. Tissue repair and stem cell renewal in carcinogenesis. *Nature.* 2004 Nov 18;432(7015):324-31.

Beachy PA, Hymowitz SG, Lazarus RA, Leahy DJ, Siebold C. Interactions between Hedgehog proteins and their binding partners come into view. *Genes Dev.* 2010 Sep 15;24(18):2001-12.

Beilhack A, Schulz S, Baker J, Beilhack GF, Wieland CB, Herman EI, Baker EM, Cao YA, Contag CH, Negrin RS. In vivo analyses of early events in acute graft-versus-host disease reveal sequential infiltration of T-cell subsets. *Blood.* 2005 Aug 1;106(3):1113-22

Belgacem YH, Borodinsky LN. Sonic hedgehog signaling is decoded by calcium spike activity in the developing spinal cord. *Proc Natl Acad Sci U S A.* 2011 Mar 15;108(11):4482-7.

Benson RA, Lowrey JA, Lamb JR, Howie SE. The Notch and Sonic hedgehog signalling pathways in immunity. *Mol Immunol.* 2004 Jul;41(6-7):715-25.

Bettencourt-Dias M, Hildebrandt F, Pellman D, Woods G, Godinho SA. Centrosomes and cilia in human disease. *Trends Genet.* 2011 Aug;27(8):307-15.

Bhardwaj G, Murdoch B, Wu D, Baker DP, Williams KP, Chadwick K, Ling LE, Karanu FN, Bhatia M. Sonic hedgehog induces the proliferation of primitive human hematopoietic cells via BMP regulation. *Nat Immunol.* 2001 Feb;2(2):172-80.

Bijlsma MF, Spek CA, Zivkovic D, van de Water S, Rezaee F, Peppelenbosch MP. Repression of smoothened by patched-dependent (pro-)vitamin D3 secretion. *PLoS Biol.* 2006 Jul;4(8):e232.

Bijlsma MF, Borensztajn KS, Roelink H, Peppelenbosch MP, Spek CA. Sonic hedgehog induces transcription-independent cytoskeletal rearrangement and migration regulated by arachidonate metabolites. *Cell Signal.* 2007 Dec;19(12):2596-604.

Bochner BS, Klunk DA, Sterbinsky SA, Coffman RL, Schleimer RP. IL-13 selectively induces vascular cell adhesion molecule-1 expression in human endothelial cells. *J Immunol.* 1995 Jan 15;154(2):799-803.

Bonati A, Zanelli P, Ferrari S, Plebani A, Starcich B, Savi M, Neri TM. T-cell receptor beta-chain gene rearrangement and expression during human thymic ontogenesis. *Blood.* 1992 Mar 15;79(6):1472-83.

Bousquet J, Jeffery PK, Busse WW, Johnson M, Vignola AM. Asthma. From bronchoconstriction to airways inflammation and remodeling. *Am J Respir Crit Care Med.* 2000 May;161(5):1720-45.

Braun MY, Lowin B, French L, Acha-Orbea H, Tschopp J. Cytotoxic T cells deficient in both functional fas ligand and perforin show residual cytolytic activity yet lose their capacity to induce lethal acute graft-versus-host disease. *J Exp Med.* 1996 Feb 1;183(2):657-61.

Bredesen DE, Mehlen P, Rabizadeh S. Apoptosis and dependence receptors: a molecular basis for cellular addiction. *Physiol Rev.* 2004 Apr;84(2):411-30.

Brennan D, Chen X, Cheng L, Mahoney M, Riobo NA. Noncanonical Hedgehog signaling. *Vitam Horm.* 2012;88:55-72.

Bretscher P, Cohn M. A theory of self-nonsel self discrimination. *Science.* 1970 Sep 11;169(3950):1042-9.

Broome HE, Dargan CM, Krajewski S, Reed JC. Expression of Bcl-2, Bcl-x, and Bax after T cell activation and IL-2 withdrawal. *J Immunol.* 1995 Sep 1;155(5):2311-7.

Bullens DM, Truyen E, Coteur L, Dilissen E, Hellings PW, Dupont LJ, Ceuppens JL. IL-17 mRNA in sputum of asthmatic patients: linking T cell driven inflammation and granulocytic influx? *Respir Res.* 2006 Nov 3;7:135.

Burke R, Nellen D, Bellotto M, Hafen E, Senti KA, Dickson BJ, Basler K. Dispatched, a novel sterol-sensing domain protein dedicated to the release of cholesterol-modified hedgehog from signaling cells. *Cell.* 1999 Dec 23;99(7):803-15.

Cai C, Thorne J, Grabel L. Hedgehog serves as a mitogen and survival factor during embryonic stem cell neurogenesis. *Stem Cells.* 2008 May;26(5):1097-108.

Cambiaggi C, Scupoli MT, Cestari T, Gerosa F, Carra G, Tridente G, Accolla RS. Constitutive expression of CD69 in interspecies T-cell hybrids and locus assignment to human chromosome 12. *Immunogenetics.* 1992;36(2):117-20.

Cantor H, Weissman I. Development and function of subpopulations of thymocytes and T lymphocytes. *Prog Allergy.* 1976;20:1-64.

Carlyle JR, Zúñiga-Pflücker JC. Requirement for the thymus in alphabeta T lymphocyte lineage commitment. *Immunity.* 1998 Aug;9(2):187-97.

Carpenter D, Stone DM, Brush J, Ryan A, Armanini M, Frantz G, Rosenthal A, de Sauvage FJ. Characterization of two patched receptors for the vertebrate hedgehog protein family. *Proc Natl Acad Sci U S A.* 1998 Nov 10;95(23):13630-4.

Caruso A, Licenziati S, Corulli M, Canaris AD, De Francesco MA, Fiorentini S, Peroni L, Fallacara F, Dima F, Balsari A, Turano A. Flow cytometric analysis of activation markers on stimulated T cells and their correlation with cell proliferation. *Cytometry.* 1997 Jan 1;27(1):71-6.

Chamoun Z, Mann RK, Nellen D, von Kessler DP, Bellotto M, Beachy PA, Basler K. Skinny hedgehog, an acyltransferase required for palmitoylation and activity of the hedgehog signal. *Science.* 2001 Sep 14;293(5537):2080-4.

Chan VS, Chau SY, Tian L, Chen Y, Kwong SK, Quackenbush J, Dallman M, Lamb J, Tam PK. Sonic hedgehog promotes CD4+ T lymphocyte proliferation and modulates the expression of a subset of CD28-targeted genes. *Int Immunol.* 2006 Dec;18(12):1627-36.

Chang H, Li Q, Moraes RC, Lewis MT, Hamel PA. Activation of Erk by sonic hedgehog independent of canonical hedgehog signalling. *Int J Biochem Cell Biol.* 2010 Sep;42(9):1462-71.

Chauhan SK, Saban DR, Lee HK, Dana R. Levels of Foxp3 in regulatory T cells reflect their functional status in transplantation. *J Immunol.* 2009 Jan 1;182(1):148-53.

Chen ML, Pittet MJ, Gorelik L, Flavell RA, Weissleder R, von Boehmer H, Khazaie K. Regulatory T cells suppress tumor-specific CD8 T cell cytotoxicity through TGF-beta signals in vivo. *Proc Natl Acad Sci U S A.* 2005 Jan 11;102(2):419-24.

Chen Y, Sasai N, Ma G, Yue T, Jia J, Briscoe J, Jiang J. Sonic Hedgehog dependent phosphorylation by CK1 α and GRK2 is required for ciliary accumulation and activation of smoothened. *PLoS Biol.* 2011 Jun;9(6):e1001083.

Chen JK, Taipale J, Cooper MK, Beachy PA. Inhibition of Hedgehog signaling by direct binding of cyclopamine to Smoothened. *Genes Dev.* 2002 Nov 1;16(21):2743-8.

Chen W, Ren XR, Nelson CD, Barak LS, Chen JK, Beachy PA, de Sauvage F, Lefkowitz RJ. Activity-dependent internalization of smoothened mediated by beta-arrestin 2 and GRK2. *Science.* 2004 Dec 24;306(5705):2257-60.

Cheung HO, Zhang X, Ribeiro A, Mo R, Makino S, Puvindran V, Law KK, Briscoe J, Hui CC. The kinesin protein Kif7 is a critical regulator of Gli transcription factors in mammalian hedgehog signaling. *Sci Signal.* 2009 Jun 23;2(76):ra29.

Chiang C, Litingtung Y, Lee E, Young KE, Corden JL, Westphal H, Beachy PA. Cyclopia and defective axial patterning in mice lacking Sonic hedgehog gene function. *Nature.* 1996 Oct 3;383(6599):407-13.

Chinchilla P, Xiao L, Kazanietz MG, Riobo NA. Hedgehog proteins activate pro-angiogenic responses in endothelial cells through non-canonical signaling pathways. *Cell Cycle.* 2010 Feb 1;9(3):570-79.

Chuang PT, McMahon AP. Vertebrate Hedgehog signalling modulated by induction of a Hedgehog-binding protein. *Nature.* 1999 Feb 18;397(6720):617-21.

Collins PD, Marleau S, Griffiths-Johnson DA, Jose PJ, Williams TJ. Cooperation between interleukin-5 and the chemokine eotaxin to induce eosinophil accumulation in vivo. *J Exp Med*. 1995 Oct 1;182(4):1169-74.

Constant SL, Bottomly K. Induction of Th1 and Th2 CD4+ T cell responses: the alternative approaches. *Annu Rev Immunol*. 1997;15:297-322.

Cooke KR, Kobzik L, Martin TR, Brewer J, Delmonte J Jr, Crawford JM, Ferrara JL. An experimental model of idiopathic pneumonia syndrome after bone marrow transplantation: I. The roles of minor H antigens and endotoxin. *Blood*. 1996 Oct 15;88(8):3230-9.

Corbit KC, Aanstad P, Singla V, Norman AR, Stainier DY, Reiter JF. Vertebrate Smoothed functions at the primary cilium. *Nature*. 2005 Oct 13;437(7061):1018-21.

Corcoran RB, Scott MP. Oxysterols stimulate Sonic hedgehog signal transduction and proliferation of medulloblastoma cells. *Proc Natl Acad Sci U S A*. 2006 May 30;103(22):8408-13.

Corry DB, Grünig G, Hadeiba H, Kurup VP, Warnock ML, Sheppard D, Rennick DM, Locksley RM. Requirements for allergen-induced airway hyperreactivity in T and B cell-deficient mice. *Mol Med*. 1998 May;4(5):344-55.

Cridland SO, Keys JR, Papathanasiou P, Perkins AC. Indian hedgehog supports definitive erythropoiesis. *Blood Cells Mol Dis*. 2009 Sep-Oct;43(2):149-55.

Croft M, Duncan DD, Swain SL. Response of naive antigen-specific CD4+ T cells in vitro: characteristics and antigen-presenting cell requirements. *J Exp Med*. 1992 Nov 1;176(5):1431-7.

Curiel TJ, Coukos G, Zou L, Alvarez X, Cheng P, Mottram P, Evdemon-Hogan M, Conejo-Garcia JR, Zhang L, Burow M, Zhu Y, Wei S, Kryczek I, Daniel B, Gordon A, Myers L, Lackner A, Disis ML, Knutson KL, Chen L, Zou W. Specific recruitment of regulatory T cells in ovarian carcinoma fosters immune privilege and predicts reduced survival. *Nat Med*. 2004 Sep;10(9):942-9.

Darrah PA, Patel DT, De Luca PM, Lindsay RW, Davey DF, Flynn BJ, Hoff ST, Andersen P, Reed SG, Morris SL, Roederer M, Seder RA. Multifunctional TH1 cells define a correlate of vaccine-mediated protection against *Leishmania major*. *Nat Med*. 2007 Jul;13(7):843-50.

de la Hera A, Marston W, Aranda C, Toribio ML, Martinez C. Thymic stroma is required for the development of human T cell lineages in vitro. *Int Immunol*. 1989;1(5):471-8.

DeGrendele HC, Kosfisz M, Estess P, Siegelman MH. CD44 activation and associated primary adhesion is inducible via T cell receptor stimulation. *J Immunol*. 1997 Sep 15;159(6):2549-53.

Del Sal G, Ruaro ME, Philipson L, Schneider C. The growth arrest-specific gene, *gas1*, is involved in growth suppression. *Cell*. 1992 Aug 21;70(4):595-607.

Detmer K, Thompson AJ, Garner RE, Walker AN, Gaffield W, Dannawi H. Hedgehog signaling and cell cycle control in differentiating erythroid progenitors. *Blood Cells Mol Dis*. 2005 Jan-Feb;34(1):60-70.

Dierks C, Beigi R, Guo GR, Zirlik K, Stegert MR, Manley P, Trussell C, Schmitt-Graeff A, Landwerlin K, Veelken H, Warmuth M. Expansion of Bcr-Abl-positive leukemic stem cells is dependent on Hedgehog pathway activation. *Cancer Cell*. 2008 Sep 9;14(3):238-49.

Dons EM, Raimondi G, Cooper DK, Thomson AW. Induced regulatory T cells: mechanisms of conversion and suppressive potential. *Hum Immunol*. 2012 Apr;73(4):328-34.

Drakopoulou E, Outram SV, Rowbotham NJ, Ross SE, Furmanski AL, Saldana JI, Hager-Theodorides AL, Crompton T. Non-redundant role for the transcription factor *Gli1* at multiple stages of thymocyte development. *Cell Cycle*. 2010 Oct 15;9(20):4144-52.

Dufour E, Carcelain G, Gaudin C, Flament C, Avril MF, Faure F. Diversity of the cytotoxic melanoma-specific immune response: some CTL clones recognize autologous fresh tumor cells and not tumor cell lines. *J Immunol*. 1997 Apr 15;158(8):3787-95.

Duran-Struuck R, Tawara I, Lowler K, Clouthier SG, Weisiger E, Rogers C, Luker G, Kumanogoh A, Liu C, Ferrara JL, Reddy P. A novel role for the semaphorin *Sema4D* in the induction of allo-responses. *Biol Blood Marrow Transplant*. 2007 Nov;13(11):1294-1303.

Earle W.R., Schilling E.L., Stark T.H., Straus N.P., Brown M.F., Shelton E., 1943. Production of malignancy in vitro. The mouse fibroblast cultures and changes seen in the living cells. *J Nat Cancer Inst* 4: 165-212.

Edinger M, Hoffmann P, Ermann J, Drago K, Fathman CG, Strober S, Negrin RS. CD4+CD25+ regulatory T cells preserve graft-versus-tumor activity while inhibiting graft-versus-host disease after bone marrow transplantation. *Nat Med*. 2003 Sep;9(9):1144-50.

El Andaloussi A, Graves S, Meng F, Mandal M, Mashayekhi M, Aifantis I. Hedgehog signaling controls thymocyte progenitor homeostasis and differentiation in the thymus. *Nat Immunol*. 2006 Apr;7(4):418-26.

Endoh-Yamagami S, Evangelista M, Wilson D, Wen X, Theunissen JW, Phamluong K, Davis M, Scales SJ, Solloway MJ, de Sauvage FJ, Peterson AS. The mammalian Cos2 homolog Kif7 plays an essential role in modulating Hh signal transduction during development. *Curr Biol*. 2009 Aug 11;19(15):1320-6.

Erlacher M, Labi V, Manzl C, Böck G, Tzankov A, Häcker G, Michalak E, Strasser A, Villunger A. Puma cooperates with Bim, the rate-limiting BH3-only protein in cell death during lymphocyte development, in apoptosis induction. *J Exp Med*. 2006 Dec 25;203(13):2939-51.

Fehling HJ, Gilfillan S, Ceredig R. Alpha beta/gamma delta lineage commitment in the thymus of normal and genetically manipulated mice. *Adv Immunol*. 1999;71:1-76.

Fidler IJ. Selection of successive tumour lines for metastasis. *Nat New Biol*. 1973 Apr 4;242(118):148-9.

Fliegauf M, Benzing T, Omran H. When cilia go bad: cilia defects and ciliopathies. *Nat Rev Mol Cell Biol*. 2007 Nov;8(11):880-93.

Fontenot JD, Gavin MA, Rudensky AY. Foxp3 programs the development and function of CD4+CD25+ regulatory T cells. *Nat Immunol*. 2003 Apr;4(4):330-6.

Forbes AJ, Nakano Y, Taylor AM, Ingham PW. Genetic analysis of hedgehog signalling in the *Drosophila* embryo. *Dev Suppl*. 1993:115-24.

Furmanski AL, Saldana JI, Rowbotham NJ, Ross SE, Crompton T. Role of Hedgehog signalling at the transition from double-positive to single-positive thymocyte. *Eur J Immunol*. 2012 Feb;42(2):489-99.

Gajewski TF. Failure at the effector phase: immune barriers at the level of the melanoma tumor microenvironment. *Clin Cancer Res*. 2007 Sep 15;13(18 Pt 1):5256-61.

Gao J, Graves S, Koch U, Liu S, Jankovic V, Buonamici S, El Andaloussi A, Nimer SD, Kee BL, Taichman R, Radtke F, Aifantis I. Hedgehog signaling is dispensable for adult hematopoietic stem cell function. *Cell Stem Cell*. 2009 Jun 5;4(6):548-58.

Georas SN, Guo J, De Fanis U, Casolaro V. T-helper cell type-2 regulation in allergic disease. *Eur Respir J*. 2005 Dec;26(6):1119-37.

Ghiringhelli F, Puig PE, Roux S, Parcellier A, Schmitt E, Solary E, Kroemer G, Martin F, Chauffert B, Zitvogel L. Tumor cells convert immature myeloid dendritic cells into TGF-beta-secreting cells inducing CD4+CD25+ regulatory T cell proliferation. *J Exp Med*. 2005 Oct 3;202(7):919-29.

Gobert M, Treilleux I, Bendriss-Vermare N, Bachelot T, Goddard-Leon S, Arfi V, Biota C, Doffin AC, Durand I, Olive D, Perez S, Pasqual N, Faure C, Ray-Coquard I, Puisieux A, Caux C, Blay JY, Ménétrier-Caux C. Regulatory T cells recruited through CCL22/CCR4 are selectively activated in lymphoid infiltrates surrounding primary breast tumors and lead to an adverse clinical outcome. *Cancer Res*. 2009 Mar 1;69(5):2000-9.

Godfrey DI, Kennedy J, Suda T, Zlotnik A. A developmental pathway involving four phenotypically and functionally distinct subsets of CD3-CD4-CD8- triple-negative adult mouse thymocytes defined by CD44 and CD25 expression. *J Immunol*. 1993 May 15;150(10):4244-52.

Goodrich LV, Milenković L, Higgins KM, Scott MP. Altered neural cell fates and medulloblastoma in mouse patched mutants. *Science*. 1997 Aug 22;277(5329):1109-13.

Goodrich LV, Johnson RL, Milenkovic L, McMahon JA, Scott MP. Conservation of the hedgehog/patched signaling pathway from flies to mice: induction of a mouse patched gene by Hedgehog. *Genes Dev*. 1996 Feb 1;10(3):301-12.

Goodrich LV, Jung D, Higgins KM, Scott MP. Overexpression of *ptc1* inhibits induction of Shh target genes and prevents normal patterning in the neural tube. *Dev Biol.* 1999 Jul 15;211(2):323-34.

Goetz SC, Ocbina PJ, Anderson KV. The primary cilium as a Hedgehog signal transduction machine. *Methods Cell Biol.* 2009;94:199-222.

Greenwald RJ, Freeman GJ, Sharpe AH. The B7 family revisited. *Annu Rev Immunol.* 2005;23:515-48.

Hager-Theodorides AL, Dessens JT, Outram SV, Crompton T. The transcription factor Gli3 regulates differentiation of fetal CD4⁻ CD8⁻ double-negative thymocytes. *Blood.* 2005 Aug 15;106(4):1296-304.

Hahn H, Wicking C, Zaphiropoulos PG, Gailani MR, Shanley S, Chidambaram A, Vorechovsky I, Holmberg E, Uden AB, Gillies S, Negus K, Smyth I, Pressman C, Leffell DJ, Gerrard B, Goldstein AM, Dean M, Toftgard R, Chenevix-Trench G, Wainwright B, Bale AE. Mutations of the human homolog of *Drosophila* patched in the nevoid basal cell carcinoma syndrome. *Cell.* 1996 Jun 14;85(6):841-51.

Hahn H, Wojnowski L, Zimmer AM, Hall J, Miller G, Zimmer A. Rhabdomyosarcomas and radiation hypersensitivity in a mouse model of Gorlin syndrome. *Nat Med.* 1998 May;4(5):619-22.

Haks MC, Oosterwegel MA, Blom B, Spits HM, Kruisbeek AM. Cell-fate decisions in early T cell development: regulation by cytokine receptors and the pre-TCR. *Semin Immunol.* 1999 Feb;11(1):23-37.

Hallahan AR, Pritchard JI, Hansen S, Benson M, Stoeck J, Hatton BA, Russell TL, Ellenbogen RG, Bernstein ID, Beachy PA, Olson JM. The *SmoA1* mouse model reveals that notch signaling is critical for the growth and survival of sonic hedgehog-induced medulloblastomas. *Cancer Res.* 2004 Nov 1;64(21):7794-800.

Hallikas O, Palin K, Sinjushina N, Rautiainen R, Partanen J, Ukkonen E, Taipale J. Genome-wide prediction of mammalian enhancers based on analysis of transcription-factor binding affinity. *Cell.* 2006 Jan 13;124(1):47-59.

Hammerschmidt M, Brook A, McMahon AP. The world according to hedgehog. *Trends Genet.* 1997 Jan;13(1):14-21.

Harrington LE, Hatton RD, Mangan PR, Turner H, Murphy TL, Murphy KM, Weaver CT. Interleukin 17-producing CD4⁺ effector T cells develop via a lineage distinct from the T helper type 1 and 2 lineages. *Nat Immunol.* 2005 Nov;6(11):1123-32.

Haycraft CJ, Banizs B, Aydin-Son Y, Zhang Q, Michaud EJ, Yoder BK. Gli2 and Gli3 localize to cilia and require the intraflagellar transport protein polaris for processing and function. *PLoS Genet.* 2005 Oct;1(4):e53.

Hayes SM, Love PE. Strength of signal: a fundamental mechanism for cell fate specification. *Immunol Rev.* 2006 Feb;209:170-5.

Henkart PA. Lymphocyte-mediated cytotoxicity: two pathways and multiple effector molecules. *Immunity.* 1994 Aug;1(5):343-6.

Hoffmann MW, Allison J, Miller JF. Tolerance induction by thymic medullary epithelium. *Proc Natl Acad Sci U S A.* 1992 Apr 1;89(7):2526-30.

Hofmann I, Stover EH, Cullen DE, Mao J, Morgan KJ, Lee BH, Kharas MG, Miller PG, Cornejo MG, Okabe R, Armstrong SA, Ghilardi N, Gould S, de Sauvage FJ, McMahon AP, Gilliland DG. Hedgehog signaling is dispensable for adult murine hematopoietic stem cell function and hematopoiesis. *Cell Stem Cell.* 2009 Jun 5;4(6):559-67.

Hogan SP, Matthaei KI, Young JM, Koskinen A, Young IG, Foster PS. A novel T cell-regulated mechanism modulating allergen-induced airways hyperreactivity in BALB/c mice independently of IL-4 and IL-5. *J Immunol.* 1998 Aug 1;161(3):1501-9.

Hooper JE, Scott MP. The *Drosophila* patched gene encodes a putative membrane protein required for segmental patterning. *Cell.* 1989 Nov 17;59(4):751-65.

Huang P, Schier AF. Dampened Hedgehog signaling but normal Wnt signaling in zebrafish without cilia. *Development.* 2009 Sep;136(18):3089-98.

Huangfu D, Liu A, Rakeman AS, Murcia NS, Niswander L, Anderson KV. Hedgehog signalling in the mouse requires intraflagellar transport proteins. *Nature*. 2003 Nov 6;426(6962):83-7.

Humke EW, Dorn KV, Milenkovic L, Scott MP, Rohatgi R. The output of Hedgehog signaling is controlled by the dynamic association between Suppressor of Fused and the Gli proteins. *Genes Dev*. 2010 Apr 1;24(7):670-82.

Hwang PH, Yi HK, Kim DS, Nam SY, Kim JS, Lee DY. Suppression of tumorigenicity and metastasis in B16F10 cells by PTEN/MMAC1/TEP1 gene. *Cancer Lett*. 2001 Oct 22;172(1):83-91.

Ingham PW, McMahon AP. Hedgehog signaling in animal development: paradigms and principles. *Genes Dev*. 2001 Dec 1;15(23):3059-87.

Ingham PW, Nakano Y, Seger C. Mechanisms and functions of Hedgehog signalling across the metazoa. *Nat Rev Genet*. 2011 Jun;12(6):393-406.

Ishida T, Ishii T, Inagaki A, Yano H, Komatsu H, Iida S, Inagaki H, Ueda R. Specific recruitment of CC chemokine receptor 4-positive regulatory T cells in Hodgkin lymphoma fosters immune privilege. *Cancer Res*. 2006 Jun 1;66(11):5716-22.

Itoh M, Takahashi T, Sakaguchi N, Kuniyasu Y, Shimizu J, Otsuka F, Sakaguchi S. Thymus and autoimmunity: production of CD25+CD4+ naturally anergic and suppressive T cells as a key function of the thymus in maintaining immunologic self-tolerance. *J Immunol*. 1999 May 1;162(9):5317-26.

Ivanov II, McKenzie BS, Zhou L, Tadokoro CE, Lepelley A, Lafaille JJ, Cua DJ, Littman DR. The orphan nuclear receptor ROR γ directs the differentiation program of proinflammatory IL-17+ T helper cells. *Cell*. 2006 Sep 22;126(6):1121-33.

Jäger E, Bernhard H, Romero P, Ringhoffer M, Arand M, Karbach J, Ilsemann C, Hagedorn M, Knuth A. Generation of cytotoxic T-cell responses with synthetic melanoma-associated peptides in vivo: implications for tumor vaccines with melanoma-associated antigens. *Int J Cancer*. 1996 Apr 10;66(2):162-9.

Jenkins D. Hedgehog signalling: emerging evidence for non-canonical pathways. *Cell Signal*. 2009 Jul;21(7):1023-34.

Jiang J. Regulation of Hh/Gli signaling by dual ubiquitin pathways. *Cell Cycle*. 2006 Nov 1;5(21):2457-63.

Jiang X, Yang P, Ma L. Kinase activity-independent regulation of cyclin pathway by GRK2 is essential for zebrafish early development. *Proc Natl Acad Sci U S A*. 2009 Jun 23;106(25):10183-8.

Jordan MS, Boesteanu A, Reed AJ, Petrone AL, Holenbeck AE, Lerman MA, Najj A, Caton AJ. Thymic selection of CD4+CD25+ regulatory T cells induced by an agonist self-peptide. *Nat Immunol*. 2001 Apr;2(4):301-6.

Kappel LW, Goldberg GL, King CG, Suh DY, Smith OM, Ligh C, Holland AM, Grubin J, Mark NM, Liu C, Iwakura Y, Heller G, van den Brink MR. IL-17 contributes to CD4-mediated graft-versus-host disease. *Blood*. 2009 Jan 22;113(4):945-52.

Kappes DJ, He X, He X. CD4-CD8 lineage commitment: an inside view. *Nat Immunol*. 2005 Aug;6(8):761-6.

Keller G, Lacaud G, Robertson S. Development of the hematopoietic system in the mouse. *Exp Hematol*. 1999 May;27(5):777-87.

Kim J, Kato M, Beachy PA. Gli2 trafficking links Hedgehog-dependent activation of Smoothed in the primary cilium to transcriptional activation in the nucleus. *Proc Natl Acad Sci U S A*. 2009 Dec 22;106(51):21666-71.

Kiprilov EN, Awan A, Desprat R, Velho M, Clement CA, Byskov AG, Andersen CY, Satir P, Bouhassira EE, Christensen ST, Hirsch RE. Human embryonic stem cells in culture possess primary cilia with hedgehog signaling machinery. *J Cell Biol*. 2008 Mar 10;180(5):897-904.

Kise Y, Morinaka A, Teglund S, Miki H. Sufu recruits GSK3beta for efficient processing of Gli3. *Biochem Biophys Res Commun*. 2009 Sep 25;387(3):569-74.

Kondo M, Weissman IL, Akashi K. Identification of clonogenic common lymphoid progenitors in mouse bone marrow. *Cell*. 1997 Nov 28;91(5):661-72.

Korngold R, Sprent J. Lethal graft-versus-host disease after bone marrow transplantation across minor histocompatibility barriers in mice. Prevention by removing mature T cells from marrow. *J Exp Med*. 1978 Dec 1;148(6):1687-98.

Kovacs JJ, Whalen EJ, Liu R, Xiao K, Kim J, Chen M, Wang J, Chen W, Lefkowitz RJ. Beta-arrestin-mediated localization of smoothed to the primary cilium. *Science*. 2008 Jun 27;320(5884):1777-81.

Kovalik JP, Singh N, Mendiratta SK, Martin WD, Ignatowicz L, Van Kaer L. The alloreactive and self-restricted CD4+ T cell response directed against a single MHC class II/peptide combination. *J Immunol*. 2000 Aug 1;165(3):1285-93.

Krauss S, Concordet JP, Ingham PW. A functionally conserved homolog of the *Drosophila* segment polarity gene *hh* is expressed in tissues with polarizing activity in zebrafish embryos. *Cell*. 1993 Dec 31;75(7):1431-44.

Krenger W, Ferrara JL. Graft-versus-host disease and the Th1/Th2 paradigm. *Immunol Res*. 1996;15(1):50-73.

Kristiansen K. Molecular mechanisms of ligand binding, signaling, and regulation within the superfamily of G-protein-coupled receptors: molecular modeling and mutagenesis approaches to receptor structure and function. *Pharmacol Ther*. 2004 Jul;103(1):21-80.

Kroczek RA, Mages HW, Hutloff A. Emerging paradigms of T-cell co-stimulation. *Curr Opin Immunol*. 2004 Jun;16(3):321-7.

Kuppers RC, Henney CS. Studies on the mechanism of lymphocyte-mediated cytotoxicity. IX. Relationships between antigen recognition and lytic expression in killer T cells. *J Immunol*. 1977 Jan;118(1):71-6.

Ladner MB, Martin GA, Noble JA, Wittman VP, Warren MK, McGrogan M, Stanley ER. cDNA cloning and expression of murine macrophage colony-stimulating factor from L929 cells. *Proc Natl Acad Sci U S A*. 1988 Sep;85(18):6706-10.

Lai K, Kaspar BK, Gage FH, Schaffer DV. Sonic hedgehog regulates adult neural progenitor proliferation in vitro and in vivo. *Nat Neurosci*. 2003 Jan;6(1):21-7.

Lebedeva T, Dustin ML, Sykulev Y. ICAM-1 co-stimulates target cells to facilitate antigen presentation. *Curr Opin Immunol.* 2005 Jun;17(3):251-8.

Lemischka IR, Raulet DH, Mulligan RC. Developmental potential and dynamic behavior of hematopoietic stem cells. *Cell.* 1986 Jun 20;45(6):917-27.

Lewkowich IP, Herman NS, Schleifer KW, Dance MP, Chen BL, Dienger KM, Sproles AA, Shah JS, Köhl J, Belkaid Y, Wills-Karp M. CD4+CD25+ T cells protect against experimentally induced asthma and alter pulmonary dendritic cell phenotype and function. *J Exp Med.* 2005 Dec 5;202(11):1549-61.

Liem KF Jr, He M, Ocbina PJ, Anderson KV. Mouse Kif7/Costal2 is a cilia-associated protein that regulates Sonic hedgehog signaling. *Proc Natl Acad Sci U S A.* 2009 Aug 11;106(32):13377-82.

Liu S, Dontu G, Mantle ID, Patel S, Ahn NS, Jackson KW, Suri P, Wicha MS. Hedgehog signaling and Bmi-1 regulate self-renewal of normal and malignant human mammary stem cells. *Cancer Res.* 2006 Jun 15;66(12):6063-71.

Lowrey JA, Stewart GA, Lindey S, Hoyne GF, Dallman MJ, Howie SE, Lamb JR. Sonic hedgehog promotes cell cycle progression in activated peripheral CD4(+) T lymphocytes. *J Immunol.* 2002 Aug 15;169(4):1869-75.

Lum L, Yao S, Mozer B, Rovescalli A, Von Kessler D, Nirenberg M, Beachy PA. Identification of Hedgehog pathway components by RNAi in *Drosophila* cultured cells. *Science.* 2003 Mar 28;299(5615):2039-45.

Machold R, Hayashi S, Rutlin M, Muzumdar MD, Nery S, Corbin JG, Gritli-Linde A, Dellovade T, Porter JA, Rubin LL, Dudek H, McMahon AP, Fishell G. Sonic hedgehog is required for progenitor cell maintenance in telencephalic stem cell niches. *Neuron.* 2003 Sep 11;39(6):937-50.

Makino S, Masuya H, Ishijima J, Yada Y, Shiroishi T. A spontaneous mouse mutation, mesenchymal dysplasia (mes), is caused by a deletion of the most C-terminal cytoplasmic domain of patched (ptc). *Dev Biol.* 2001 Nov 1;239(1):95-106.

Marigo V, Davey RA, Zuo Y, Cunningham JM, Tabin CJ. Biochemical evidence that patched is the Hedgehog receptor. *Nature*. 1996 Nov 14;384(6605):176-9.

Marrack P, Bender J, Hildeman D, Jordan M, Mitchell T, Murakami M, Sakamoto A, Schaefer BC, Swanson B, Kappler J. Homeostasis of alpha beta TCR+ T cells. *Nat Immunol*. 2000 Aug;1(2):107-11.

Marrack P, Kappler J. Positive selection of thymocytes bearing alpha beta T cell receptors. *Curr Opin Immunol*. 1997 Apr;9(2):250-5.

Martín V, Carrillo G, Torroja C, Guerrero I. The sterol-sensing domain of Patched protein seems to control Smoothened activity through Patched vesicular trafficking. *Curr Biol*. 2001 Apr 17;11(8):601-7.

Martin-Orozco N, Muranski P, Chung Y, Yang XO, Yamazaki T, Lu S, Hwu P, Restifo NP, Overwijk WW, Dong C. T helper 17 cells promote cytotoxic T cell activation in tumor immunity. *Immunity*. 2009 Nov 20;31(5):787-98.

May SR, Ashique AM, Karlen M, Wang B, Shen Y, Zarbalis K, Reiter J, Ericson J, Peterson AS. Loss of the retrograde motor for IFT disrupts localization of Smo to cilia and prevents the expression of both activator and repressor functions of Gli. *Dev Biol*. 2005 Nov 15;287(2):378-89.

McLellan JS, Zheng X, Hauk G, Ghirlando R, Beachy PA, Leahy DJ. The mode of Hedgehog binding to Ihog homologues is not conserved across different phyla. *Nature*. 2008 Oct 16;455(7215):979-83.

Medvinsky A, Dzierzak E. Definitive hematopoiesis is autonomously initiated by the AGM region. *Cell*. 1996 Sep 20;86(6):897-906.

Mehlen P, Thibert C. Dependence receptors: between life and death. *Cell Mol Life Sci*. 2004 Aug;61(15):1854-66.

Melief CJ. Tumor eradication by adoptive transfer of cytotoxic T lymphocytes. *Adv Cancer Res*. 1992;58:143-75.

Milenkovic L, Scott MP, Rohatgi R. Lateral transport of Smoothed from the plasma membrane to the membrane of the cilium. *J Cell Biol.* 2009 Nov 2;187(3):365-74.

Mille F, Thibert C, Fombonne J, Rama N, Guix C, Hayashi H, Corset V, Reed JC, Mehlen P. The Patched dependence receptor triggers apoptosis through a DRAL-caspase-9 complex. *Nat Cell Biol.* 2009 Jun;11(6):739-46.

Mochizuki M, Bartels J, Mallet AI, Christophers E, Schröder JM. IL-4 induces eotaxin: a possible mechanism of selective eosinophil recruitment in helminth infection and atopy. *J Immunol.* 1998 Jan 1;160(1):60-8.

Mold JE, Venkatasubrahmanyam S, Burt TD, Michaëlsson J, Rivera JM, Galkina SA, Weinberg K, Stoddart CA, McCune JM. Fetal and adult hematopoietic stem cells give rise to distinct T cell lineages in humans. *Science.* 2010 Dec 17;330(6011):1695-9.

Murone M, Rosenthal A, de Sauvage FJ. Sonic hedgehog signaling by the patched-smoothed receptor complex. *Curr Biol.* 1999 Jan 28;9(2):76-84.

Moser R, Fehr J, Bruijnzeel PL. IL-4 controls the selective endothelium-driven transmigration of eosinophils from allergic individuals. *J Immunol.* 1992 Aug 15;149(4):1432-8.

Mosmann TR, Cherwinski H, Bond MW, Giedlin MA, Coffman RL. Two types of murine helper T cell clone. I. Definition according to profiles of lymphokine activities and secreted proteins. *J Immunol.* 1986 Apr 1;136(7):2348-57.

Mosmann TR, Coffman RL. TH1 and TH2 cells: different patterns of lymphokine secretion lead to different functional properties. *Annu Rev Immunol.* 1989;7:145-73.

Motoyama J, Takabatake T, Takeshima K, Hui C. Ptch2, a second mouse Patched gene is co-expressed with Sonic hedgehog. *Nat Genet.* 1998 Feb;18(2):104-6.

Müller B, Basler K. The repressor and activator forms of *Cubitus interruptus* control Hedgehog target genes through common generic gli-binding sites. *Development.* 2000 Jul;127(14):2999-3007.

Murone M, Rosenthal A, de Sauvage FJ. Sonic hedgehog signaling by the patched-smoothed receptor complex. *Curr Biol.* 1999 Jan 28;9(2):76-84.

Nieuwenhuis E, Hui CC. Hedgehog signaling and congenital malformations. *Clin Genet*. 2005 Mar;67(3):193-208.

Nitzki F, Zibat A, Frommhold A, Schneider A, Schulz-Schaeffer W, Braun T, Hahn H. Uncommitted precursor cells might contribute to increased incidence of embryonal rhabdomyosarcoma in heterozygous Patched1-mutant mice. *Oncogene*. 2011 Oct 27;30(43):4428-36

Nüsslein-Volhard C, Wieschaus E. Mutations affecting segment number and polarity in *Drosophila*. *Nature*. 1980 Oct 30;287(5785):795-801.

Ogden SK, Fei DL, Schilling NS, Ahmed YF, Hwa J, Robbins DJ. G protein Galphai functions immediately downstream of Smoothened in Hedgehog signalling. *Nature*. 2008 Dec 18;456(7224):967-70.

Ohkawara Y, Lei XF, Stämpfli MR, Marshall JS, Xing Z, Jordana M. Cytokine and eosinophil responses in the lung, peripheral blood, and bone marrow compartments in a murine model of allergen-induced airways inflammation. *Am J Respir Cell Mol Biol*. 1997 May;16(5):510-20.

Oro AE. The primary cilia, a 'Rab-id' transit system for hedgehog signaling. *Curr Opin Cell Biol*. 2007 Dec;19(6):691-6.

Outram SV, Varas A, Pepicelli CV, Crompton T. Hedgehog signaling regulates differentiation from double-negative to double-positive thymocyte. *Immunity*. 2000 Aug;13(2):187-97.

Ouyang W, Kolls JK, Zheng Y. The biological functions of T helper 17 cell effector cytokines in inflammation. *Immunity*. 2008 Apr;28(4):454-67.

Overwijk WW, Restifo NP. B16 as a mouse model for human melanoma. *Curr Protoc Immunol*. 2001 May;Chapter 20:Unit 20.1

Palma V, Ruiz i Altaba A. Hedgehog-Gli signaling regulates the behavior of cells with stem cell properties in the developing neocortex. *Development*. 2004 Jan;131(2):337-45.

Panoskaltzis-Mortari A, Price A, Hermanson JR, Taras E, Lees C, Serody JS, Blazar BR. In vivo imaging of graft-versus-host-disease in mice. *Blood*. 2004 May 1;103(9):3590-8.

Park HL, Bai C, Platt KA, Matisse MP, Beeghly A, Hui CC, Nakashima M, Joyner AL. Mouse Gli1 mutants are viable but have defects in SHH signaling in combination with a Gli2 mutation. *Development*. 2000 Apr;127(8):1593-605.

Park TJ, Haigo SL, Wallingford JB. Ciliogenesis defects in embryos lacking inturned or fuzzy function are associated with failure of planar cell polarity and Hedgehog signaling. *Nat Genet*. 2006 Mar;38(3):303-11.

Parry RV, Rumbley CA, Vandenberghe LH, June CH, Riley JL. CD28 and inducible costimulatory protein Src homology 2 binding domains show distinct regulation of phosphatidylinositol 3-kinase, Bcl-xL, and IL-2 expression in primary human CD4 T lymphocytes. *J Immunol*. 2003 Jul 1;171(1):166-74.

Pazour GJ, Witman GB. The vertebrate primary cilium is a sensory organelle. *Curr Opin Cell Biol*. 2003 Feb;15(1):105-10.

Pelczar P, Zibat A, van Dop WA, Heijmans J, Bleckmann A, Gruber W, Nitzki F, Uhmman A, Guijarro MV, Hernando E, Dittmann K, Wienands J, Dressel R, Wojnowski L, Binder C, Taguchi T, Beissbarth T, Hogendoorn PC, Antonescu CR, Rubin BP, Schulz-Schaeffer W, Aberger F, van den Brink GR, Hahn H. Inactivation of Patched1 in mice leads to development of gastrointestinal stromal-like tumors that express Pdgfra but not kit. *Gastroenterology*. 2013 Jan;144(1):134-144.e6.

Pelletier M, Maggi L, Micheletti A, Lazzeri E, Tamassia N, Costantini C, Cosmi L, Lunardi C, Annunziato F, Romagnani S, Cassatella MA. Evidence for a cross-talk between human neutrophils and Th17 cells. *Blood*. 2010 Jan 14;115(2):335-43.

Persson M, Stamatakis D, te Welscher P, Andersson E, Böse J, Rütger U, Ericson J, Briscoe J. Dorsal-ventral patterning of the spinal cord requires Gli3 transcriptional repressor activity. *Genes Dev*. 2002 Nov 15;16(22):2865-78.

Philipp M, Fralish GB, Meloni AR, Chen W, MacInnes AW, Barak LS, Caron MG. Smoothed signaling in vertebrates is facilitated by a G protein-coupled receptor kinase. *Mol Biol Cell*. 2008 Dec;19(12):5478-89.

Polizio AH, Chinchilla P, Chen X, Kim S, Manning DR, Riobo NA. Heterotrimeric Gi proteins link Hedgehog signaling to activation of Rho small GTPases to promote fibroblast migration. *J Biol Chem*. 2011 Jun 3;286(22):19589-96.

Porter JA, Young KE, Beachy PA. Cholesterol modification of hedgehog signaling proteins in animal development. *Science*. 1996 Oct 11;274(5285):255-9.

Punt JA, Osborne BA, Takahama Y, Sharrow SO, Singer A. Negative selection of CD4+CD8+ thymocytes by T cell receptor-induced apoptosis requires a costimulatory signal that can be provided by CD28. *J Exp Med*. 1994 Feb 1;179(2):709-13.

Puthalakath H, Strasser A. Keeping killers on a tight leash: transcriptional and post-translational control of the pro-apoptotic activity of BH3-only proteins. *Cell Death Differ*. 2002 May;9(5):505-12.

Ramalho-Santos M, Melton DA, McMahon AP. Hedgehog signals regulate multiple aspects of gastrointestinal development. *Development*. 2000 Jun;127(12):2763-72.

Riobo NA, Saucy B, Dilizio C, Manning DR. Activation of heterotrimeric G proteins by Smoothed. *Proc Natl Acad Sci U S A*. 2006 Aug 15;103(33):12607-12

Robbins DJ, Fei DL, Riobo NA. The Hedgehog signal transduction network. *Sci Signal*. 2012 Oct 16;5(246)

Rohatgi R, Milenkovic L, Scott MP. Patched1 regulates hedgehog signaling at the primary cilium. *Science*. 2007 Jul 20;317(5836):372-6.

Rössler E, Belloni E, Gaudenz K, Jay P, Berta P, Scherer SW, Tsui LC, Muenke M. Mutations in the human Sonic Hedgehog gene cause holoprosencephaly. *Nat Genet*. 1996 Nov;14(3):357-60.

Rothoef T, Gonschorek A, Bartz H, Anhenn O, Schauer U. Antigen dose, type of antigen-presenting cell and time of differentiation contribute to the T helper 1/T helper 2 polarization of naive T cells. *Immunology*. 2003 Dec;110(4):430-9.

- Rowbotham NJ, Hager-Theodorides AL, Cebecauer M, Shah DK, Drakopoulou E, Dyson J, Outram SV, Crompton T. Activation of the Hedgehog signaling pathway in T-lineage cells inhibits TCR repertoire selection in the thymus and peripheral T-cell activation. *Blood*. 2007 May 1;109(9):3757-66.
- Rowbotham NJ, Furmanski AL, Hager-Theodorides AL, Ross SE, Drakopoulou E, Koufaris C, Outram SV, Crompton T. Repression of hedgehog signal transduction in T-lineage cells increases TCR-induced activation and proliferation. *Cell Cycle*. 2008 Apr 1;7(7):904-8.
- Rowbotham NJ, Hager-Theodorides AL, Furmanski AL, Ross SE, Outram SV, Dessens JT, Crompton T. Sonic hedgehog negatively regulates pre-TCR-induced differentiation by a Gli2-dependent mechanism. *Blood*. 2009 May 21;113(21):5144-56.
- Rudd CE, Schneider H. Unifying concepts in CD28, ICOS and CTLA4 co-receptor signalling. *Nat Rev Immunol*. 2003 Jul;3(7):544-56.
- Ryan KE, Chiang C. Hedgehog secretion and signal transduction in vertebrates. *J Biol Chem*. 2012 May 25;287(22):17905-13.
- Sacedón R, Varas A, Hernández-López C, Gutiérrez-deFrías C, Crompton T, Zapata AG, Vicente A. Expression of hedgehog proteins in the human thymus. *J Histochem Cytochem*. 2003 Nov;51(11):1557-66.
- Sakaguchi S, Wing K, Onishi Y, Prieto-Martin P, Yamaguchi T. Regulatory T cells: how do they suppress immune responses? *Int Immunol*. 2009 Oct;21(10):1105-11.
- Sasaki N, Kurisu J, Kengaku M. Sonic hedgehog signaling regulates actin cytoskeleton via Tiam1-Rac1 cascade during spine formation. *Mol Cell Neurosci*. 2010 Dec;45(4):335-44.
- Sentman CL, Shutter JR, Hockenbery D, Kanagawa O, Korsmeyer SJ. bcl-2 inhibits multiple forms of apoptosis but not negative selection in thymocytes. *Cell*. 1991 Nov 29;67(5):879-88.
- Shah DK, Hager-Theodorides AL, Outram SV, Ross SE, Varas A, Crompton T. Reduced thymocyte development in sonic hedgehog knockout embryos. *J Immunol*. 2004 Feb 15;172(4):2296-306.

Sherman LA, Chattopadhyay S. The molecular basis of allorecognition. *Annu Rev Immunol.* 1993;11:385-402.

Shevach EM. Mechanisms of foxp3+ T regulatory cell-mediated suppression. *Immunity.* 2009 May;30(5):636-45.

Siggins SL, Nguyen NY, McCormack MP, Vasudevan S, Villani R, Jane SM, Wainwright BJ, Curtis DJ. The Hedgehog receptor Patched1 regulates myeloid and lymphoid progenitors by distinct cell-extrinsic mechanisms. *Blood.* 2009 Jul 30;114(5):995-1004.

Silver DP, Livingston DM. Self-excising retroviral vectors encoding the Cre recombinase overcome Cre-mediated cellular toxicity. *Mol Cell.* 2001 Jul;8(1):233-43.

Sit ST, Manser E. Rho GTPases and their role in organizing the actin cytoskeleton. *J Cell Sci.* 2011 Mar 1;124(Pt 5):679-83.

Slingluff CL Jr, Darrow TL, Seigler HF. Melanoma-specific cytotoxic T cells generated from peripheral blood lymphocytes. Implications of a renewable source of precursors for adoptive cellular immunotherapy. *Ann Surg.* 1989 Aug;210(2):194-202.

So EY, Park HH, Lee CE. IFN-gamma and IFN-alpha posttranscriptionally down-regulate the IL-4-induced IL-4 receptor gene expression. *J Immunol.* 2000 Nov 15;165(10):5472-9.

Steinman RM, Pack M, Inaba K. Dendritic cells in the T-cell areas of lymphoid organs. *Immunol Rev.* 1997 Apr;156:25-37.

Stewart GA, Lowrey JA, Wakelin SJ, Fitch PM, Lindey S, Dallman MJ, Lamb JR, Howie SE. Sonic hedgehog signaling modulates activation of and cytokine production by human peripheral CD4+ T cells. *J Immunol.* 2002 Nov 15;169(10):5451-7.

Stone DM, Hynes M, Armanini M, Swanson TA, Gu Q, Johnson RL, Scott MP, Pennica D, Goddard A, Phillips H, Noll M, Hooper JE, de Sauvage F, Rosenthal A. The tumour-suppressor gene patched encodes a candidate receptor for Sonic hedgehog. *Nature.* 1996 Nov 14;384(6605):129-34.

Strasser A, Harris AW, Cory S. bcl-2 transgene inhibits T cell death and perturbs thymic self-censorship. *Cell.* 1991 Nov 29;67(5):889-99.

Strutt H, Thomas C, Nakano Y, Stark D, Neave B, Taylor AM, Ingham PW. Mutations in the sterol-sensing domain of Patched suggest a role for vesicular trafficking in Smoothed regulation. *Curr Biol*. 2001 Apr 17;11(8):608-13.

Su X, Ye J, Hsueh EC, Zhang Y, Hoft DF, Peng G. Tumor microenvironments direct the recruitment and expansion of human Th17 cells. *J Immunol*. 2010 Feb 1;184(3):1630-41.

Suda T, Takahashi T, Golstein P, Nagata S. Molecular cloning and expression of the Fas ligand, a novel member of the tumor necrosis factor family. *Cell*. 1993 Dec 17;75(6):1169-78.

Sweet HO, Bronson RT, Donahue LR, Davisson MT. Mesenchymal dysplasia: a recessive mutation on chromosome 13 of the mouse. *J Hered*. 1996 Mar-Apr;87(2):87-95.

Szabo SJ, Kim ST, Costa GL, Zhang X, Fathman CG, Glimcher LH. A novel transcription factor, T-bet, directs Th1 lineage commitment. *Cell*. 2000 Mar 17;100(6):655-69.

Taipale J, Cooper MK, Maiti T, Beachy PA. Patched acts catalytically to suppress the activity of Smoothed. *Nature*. 2002 Aug 22;418(6900):892-7.

Tan JT, Ernst B, Kieper WC, LeRoy E, Sprent J, Surh CD. Interleukin (IL)-15 and IL-7 jointly regulate homeostatic proliferation of memory phenotype CD8+ cells but are not required for memory phenotype CD4+ cells. *J Exp Med*. 2002 Jun 17;195(12):1523-32.

Tempé D, Casas M, Karaz S, Blanchet-Tournier MF, Concordet JP. Multisite protein kinase A and glycogen synthase kinase 3beta phosphorylation leads to Gli3 ubiquitination by SCFbetaTrCP. *Mol Cell Biol*. 2006 Jun;26(11):4316-26.

Tenzen T, Allen BL, Cole F, Kang JS, Krauss RS, McMahon AP. The cell surface membrane proteins Cdo and Boc are components and targets of the Hedgehog signaling pathway and feedback network in mice. *Dev Cell*. 2006 May;10(5):647-56.

Thibert C, Teillet MA, Lapointe F, Mazelin L, Le Douarin NM, Mehlen P. Inhibition of neuroepithelial patched-induced apoptosis by sonic hedgehog. *Science*. 2003 Aug 8;301(5634):843-6.

Thompson SD, Pelkonen J, Hurwitz JL. First T cell receptor alpha gene rearrangements during T cell ontogeny skew to the 5' region of the J alpha locus. *J Immunol.* 1990 Oct 1;145(7):2347-52.

Trowbridge JJ, Scott MP, Bhatia M. Hedgehog modulates cell cycle regulators in stem cells to control hematopoietic regeneration. *Proc Natl Acad Sci U S A.* 2006 Sep 19;103(38):14134-9.

Tukachinsky H, Lopez LV, Salic A. A mechanism for vertebrate Hedgehog signaling: recruitment to cilia and dissociation of SuFu-Gli protein complexes. *J Cell Biol.* 2010 Oct 18;191(2):415-28.

Uhmann A, van den Brandt J, Dittmann K, Hess I, Dressel R, Binder C, Lühder F, Christiansen H, Fassnacht M, Bhandoola A, Wienands J, Reichardt HM, Hahn H. T cell development critically depends on prethymic stromal patched expression. *J Immunol.* 2011 Mar 15;186(6):3383-91.

Uhmann A, Dittmann K, Nitzki F, Dressel R, Koleva M, Frommhold A, Zibat A, Binder C, Adham I, Nitsche M, Heller T, Armstrong V, Schulz-Schaeffer W, Wienands J, Hahn H. The Hedgehog receptor Patched controls lymphoid lineage commitment. *Blood.* 2007 Sep 15;110(6):1814-23.

van den Heuvel M, Ingham PW. Smoothed encodes a receptor-like serpentine protein required for hedgehog signalling. *Nature.* 1996 Aug 8;382(6591):547-51.

van Ewijk W. T-cell differentiation is influenced by thymic microenvironments. *Annu Rev Immunol.* 1991;9:591-615.

van Dijk AM, Kessler FL, Stadhouders-Keet SA, Verdonck LF, de Gast GC, Otten HG. Selective depletion of major and minor histocompatibility antigen reactive T cells: towards prevention of acute graft-versus-host disease. *Br J Haematol.* 1999 Oct;107(1):169-75.

Venkayya R, Lam M, Willkom M, Grünig G, Corry DB, Erle DJ. The Th2 lymphocyte products IL-4 and IL-13 rapidly induce airway hyperresponsiveness through direct effects on resident airway cells. *Am J Respir Cell Mol Biol.* 2002 Feb;26(2):202-8.

Vokes SA, Ji H, Wong WH, McMahon AP. A genome-scale analysis of the cis-regulatory circuitry underlying sonic hedgehog-mediated patterning of the mammalian limb. *Genes Dev.* 2008 Oct 1;22(19):2651-63.

von Boehmer H, Kisielow P, Kishi H, Scott B, Borgulya P, Teh HS. The expression of CD4 and CD8 accessory molecules on mature T cells is not random but correlates with the specificity of the alpha beta receptor for antigen. *Immunol Rev.* 1989 Jun;109:143-51.

von Boehmer H, Fehling HJ. Structure and function of the pre-T cell receptor. *Annu Rev Immunol.* 1997;15:433-52.

Vyas N, Goswami D, Manonmani A, Sharma P, Ranganath HA, VijayRaghavan K, Shashidhara LS, Sowdhamini R, Mayor S. Nanoscale organization of hedgehog is essential for long-range signaling. *Cell.* 2008 Jun 27;133(7):1214-27.

Wang J, Saffold S, Cao X, Krauss J, Chen W. Eliciting T cell immunity against poorly immunogenic tumors by immunization with dendritic cell-tumor fusion vaccines. *J Immunol.* 1998 Nov 15;161(10):5516-24.

Wang C, Pan Y, Wang B. Suppressor of fused and Spop regulate the stability, processing and function of Gli2 and Gli3 full-length activators but not their repressors. *Development.* 2010 Jun;137(12):2001-9.

Watanabe N, Gavrieli M, Sedy JR, Yang J, Fallarino F, Loftin SK, Hurchla MA, Zimmerman N, Sim J, Zang X, Murphy TL, Russell JH, Allison JP, Murphy KM. BTLA is a lymphocyte inhibitory receptor with similarities to CTLA-4 and PD-1. *Nat Immunol.* 2003 Jul;4(7):670-9.

Watkins DN, Berman DM, Burkholder SG, Wang B, Beachy PA, Baylin SB. Hedgehog signalling within airway epithelial progenitors and in small-cell lung cancer. *Nature.* 2003 Mar 20;422(6929):313-7.

Weaver CT, Harrington LE, Mangan PR, Gavrieli M, Murphy KM. Th17: an effector CD4 T cell lineage with regulatory T cell ties. *Immunity.* 2006 Jun;24(6):677-88.

Wedemeyer J, Tsai M, Galli SJ. Roles of mast cells and basophils in innate and acquired immunity. *Curr Opin Immunol.* 2000 Dec;12(6):624-31.

Whitelegg A, Barber LD. The structural basis of T-cell allorecognition. *Tissue Antigens*. 2004 Feb;63(2):101-8.

Wilson CW, Nguyen CT, Chen MH, Yang JH, Gacayan R, Huang J, Chen JN, Chuang PT. Fused has evolved divergent roles in vertebrate Hedgehog signalling and motile ciliogenesis. *Nature*. 2009 May 7;459(7243):98-102.

Wolfer A, Bakker T, Wilson A, Nicolas M, Ioannidis V, Littman DR, Lee PP, Wilson CB, Held W, MacDonald HR, Radtke F. Inactivation of Notch 1 in immature thymocytes does not perturb CD4 or CD8T cell development. *Nat Immunol*. 2001 Mar;2(3):235-41.

Wong PM, Chung SW, Chui DH, Eaves CJ. Properties of the earliest clonogenic hemopoietic precursors to appear in the developing murine yolk sac. *Proc Natl Acad Sci U S A*. 1986 Jun;83(11):3851-4.

Xiao Y, Karnati S, Qian G, Nenicu A, Fan W, Tchatalbachev S, Höland A, Hossain H, Guillou F, Lüers GH, Baumgart-Vogt E. Cre-mediated stress affects sirtuin expression levels, peroxisome biogenesis and metabolism, antioxidant and proinflammatory signaling pathways. *PLoS One*. 2012;7(7):e41097.

Yam PT, Langlois SD, Morin S, Charron F. Sonic hedgehog guides axons through a noncanonical, Src-family-kinase-dependent signaling pathway. *Neuron*. 2009 May 14;62(3):349-62.

Yamashita M, Ukai-Tadenuma M, Miyamoto T, Sugaya K, Hosokawa H, Hasegawa A, Kimura M, Taniguchi M, DeGregori J, Nakayama T. Essential role of GATA3 for the maintenance of type 2 helper T (Th2) cytokine production and chromatin remodeling at the Th2 cytokine gene loci. *J Biol Chem*. 2004 Jun 25;279(26):26983-90.

Yang XO, Pappu BP, Nurieva R, Akimzhanov A, Kang HS, Chung Y, Ma L, Shah B, Panopoulos AD, Schluns KS, Watowich SS, Tian Q, Jetten AM, Dong C. T helper 17 lineage differentiation is programmed by orphan nuclear receptors ROR alpha and ROR gamma. *Immunity*. 2008 Jan;28(1):29-39.

Yang XO, Panopoulos AD, Nurieva R, Chang SH, Wang D, Watowich SS, Dong C. STAT3 regulates cytokine-mediated generation of inflammatory helper T cells. *J Biol Chem*. 2007 Mar 30;282(13):9358-63.

Yang Y, Niswander L. Interaction between the signaling molecules WNT7a and SHH during vertebrate limb development: dorsal signals regulate anteroposterior patterning. *Cell*. 1995 Mar 24;80(6):939-47.

Yavari A, Nagaraj R, Owusu-Ansah E, Folick A, Ngo K, Hillman T, Call G, Rohatgi R, Scott MP, Banerjee U. Role of lipid metabolism in smoothed derepression in hedgehog signaling. *Dev Cell*. 2010 Jul 20;19(1):54-65.

Yi T, Zhao D, Lin CL, Zhang C, Chen Y, Todorov I, LeBon T, Kandeel F, Forman S, Zeng D. Absence of donor Th17 leads to augmented Th1 differentiation and exacerbated acute graft-versus-host disease. *Blood*. 2008 Sep 1;112(5):2101-10.

Yin Y, Bangs F, Paton IR, Prescott A, James J, Davey MG, Whitley P, Genikhovich G, Technau U, Burt DW, Tickle C. The *Talpid3* gene (KIAA0586) encodes a centrosomal protein that is essential for primary cilia formation. *Development*. 2009 Feb;136(4):655-64.

Zaphiropoulos PG, Undén AB, Rahnama F, Hollingsworth RE, Toftgård R. *PTCH2*, a novel human patched gene, undergoing alternative splicing and up-regulated in basal cell carcinomas. *Cancer Res*. 1999 Feb 15;59(4):787-92.

Zeng H, Jia J, Liu A. Coordinated translocation of mammalian Gli proteins and suppressor of fused to the primary cilium. *PLoS One*. 2010 Dec 29;5(12):e15900

Zeng X, Goetz JA, Suber LM, Scott WJ Jr, Schreiner CM, Robbins DJ. A freely diffusible form of Sonic hedgehog mediates long-range signalling. *Nature*. 2001 Jun 7;411(6838):716-20.

Zhang L, Zhao Y. The regulation of Foxp3 expression in regulatory CD4(+)CD25(+)T cells: multiple pathways on the road. *J Cell Physiol*. 2007 Jun;211(3):590-7.

Zhang W, Kang JS, Cole F, Yi MJ, Krauss RS. *Cdo* functions at multiple points in the Sonic Hedgehog pathway, and *Cdo*-deficient mice accurately model human holoprosencephaly. *Dev Cell*. 2006 May;10(5):657-65.

Zhang W, Hong M, Bae GU, Kang JS, Krauss RS. *Boc* modifies the holoprosencephaly spectrum of *Cdo* mutant mice. *Dis Model Mech*. 2011 May;4(3):368-80.

REFERENCES

Zheng W, Flavell RA. The transcription factor GATA-3 is necessary and sufficient for Th2 cytokine gene expression in CD4 T cells. *Cell*. 1997 May 16;89(4):587-96.

Zhu J, Paul WE. CD4 T cells: fates, functions, and faults. *Blood*. 2008 Sep 1;112(5):1557-69.

Zibat A, Uhmman A, Nitzki F, Wijgerde M, Frommhold A, Heller T, Armstrong V, Wojnowski L, Quintanilla-Martinez L, Reifenberger J, Schulz-Schaeffer W, Hahn H. Time-point and dosage of gene inactivation determine the tumor spectrum in conditional Ptch knockouts. *Carcinogenesis*. 2009 Jun;30(6):918-26.

7 Appendix

7.1 List of abbreviations

Abbreviation	Full name
7-AAD	7-Aminoactinomycin D
aGvHD	Acute Graft-versus-Host disease
APC	Antigen presenting cell
BALF	Bronchoalveolar lavage fluid
BCC	Basal cell carcinoma
BM	Bone marrow
BMDM	Bone marrow derived macrophage
BOC	Brother of CDO
bp	Base pair
BSA	Bovine serum albumin
BTLA	B- and T-lymphocyte attenuator
β -TrCP	beta-transducin repeat containing protein
cAMP	3',5'-cyclic adenosine monophosphate
CD	Cluster of differentiation
cDNA	Complementary DNA
CDO	Cell adhesion molecule down-regulated by oncogenes
CFA	Complete Freund's adjuvant
cGvHD	Chronic Graft-versus-Host disease
Ck1 α	Casein kinase 1 alpha
CLP	Common lymphoid progenitor
CLR	C-type lectin receptor
ConA	Concanavalin A
cpm	Counts per minute
cTEC	Cortical thymic epithelial cells
CTL	Cytotoxic T lymphocyte
CTLA-4	Cytotoxic T lymphocyte antigen 4
Dex	Dexamethasone
Dhh	Desert hedgehog
di	Deionised
Disp	Dispatched

APPENDIX

DMEM	Dulbecco's modified eagle medium
DN	Double negative
DNA	Deoxyribonucleic acid
dNTP	Deoxynucleotide Triphosphate
DP	Double positive
EDTA	Ethylenediaminetetraacetic acid
EGFR	Epidermal growth factor receptor
ELISA	Enzyme-linked immunosorbent assay
ER	Endoplasmic reticulum
ETP	Early thymocyte progenitor
FACS	Fluorescence-activated cell sorting
FBS	Fetal bovine serum
FGF	Fibroblast growth factor
FITC	Fluorescein isothiocyanate
Fn	Fibronectin
FoxP3	Forkhead box P3
FSC	Forward scatter of light
FTOC	Fetal thymic organ culture
GAS1	Growth arrest-specific gene 1
GATA3	GATA binding protein 3
GEF	Guanine nucleotide exchange factor
G _i	Inhibitory G protein
GITR	glucocorticoid induced tumour necrosis factor receptor family related gene
Gli	glioma-associated oncogene
Gli-A	Activator form of Gli
Gli-FL	Full-length form of Gli
Gli-R	Repressor form of Gli
GM-CSF	Granulocyte macrophage colony-stimulating factor
GPCR	G protein-coupled receptor
GRK2	G protein-coupled receptor kinase 2
GSK-3 β	Glycogen synthase kinase 3 beta
GvHD	Graft-versus-Host disease
Hh	Hedgehog
Hhat	Hedgehog acetyltransferase

HIP	Hedgehog interacting protein
HPRT1	Hypoxanthine-guanine phosphoribosyltransferase one
HRP	Horseradish peroxidase
HSC	Haematopoietic stem cell
i.n.	Intranasal
i.p.	Intraperitoneal
i.v.	Intravenous
IVC	individually ventilated cage
ICOS	Inducible T cell co-stimulator
IFN	Interferon
Ihh	Indian hedgehog
IL	Interleukin
iT _{reg}	Induced regulatory T cell
JAK	Janus kinase
LCCM	L cell conditioned medium
mAb	Monoclonal antibody
MACS	Magnetic activated cell sorting
MB	Medulloblastoma
MFI	Mean fluorescent intensity
MHC	Major histocompatibility complex
MLR	Mixed leukocyte reaction
MPP	Multipotent progenitor
mTEC	medullary thymic epithelial cells
nT _{reg}	Naturally occurring regulatory T cell
OD	Optical density
Ova	Ovalbumin
PAMP	Pathogen-associated molecular pattern
PBS	Phosphate-buffered saline
PCR	Polymerase chain reaction
PD-1	Programmed cell death 1
PE	Phycoerythrin
PI3K	Phosphatidylinositide 3-kinase
PI4P	Phosphatidylinositol-4-phosphate
PKA	Protein kinase A
PLC- γ	Phospholipase C gamma

APPENDIX

PRR	Pattern recognition receptor
PS	Penicillin / Streptomycin
Ptch	Patched1
qRT-PCR	Quantitative reverse transcription polymerase chain reaction
RMS	Rhabdomyosarcoma
RNA	Ribonucleic acid
RND	Resistance-nodulation-division
rShh	Recombinant sonic hedgehog
SDS	Sodium dodecyl sulphate
SEM	Standard error of the mean
Shh	Sonic hedgehog
Smo	Smoothed
SP	Single positive
SPF	Specific pathogen free
SSC	Side scatter of light
SSD	Sterol-sensing domain
STAT	Signal transducer and activator of transcription
Sufu	Suppressor of fused
TAC	Tris ammonium chloride
Taq	<i>Thermus aquaticus</i>
T-bet	T-box expressed in T cells
TCR	T cell receptor
TE	Tris EDTA
TGF- β	Transforming growth factor beta
T _h	T helper cell
Tiam-1	T-lymphoma invasion and metastasis 1
TLR	Toll-like receptor
TNFR	Tumour necrosis factor receptor
TNF- α	Tumour necrosis factor alpha
T _{reg}	Regulatory T cell
VCAM-1	Vascular cell adhesion molecule-1
wt	Wild type

7.2 List of figures

Figure 1. Schematic view of Ptch.....	10
Figure 2. The canonical hedgehog signalling pathway	14
Figure 3. Comparison of thymic morphology and cellularity between <i>Ptch</i> ^{flox/flox} and <i>CD4Cre</i> ^{+/-} <i>Ptch</i> ^{flox/flox} mice.....	57
Figure 4. Flow cytometric analysis of thymocyte development	58
Figure 5. Gene expression analysis of peripheral T cells.....	60
Figure 6. Comparison of splenic morphology and cellularity.....	61
Figure 7. Flow cytometric analysis of peripheral T cell populations	62
Figure 8. Activation state of peripheral T cells	64
Figure 9. Allogeneic stimulation of T cells	65
Figure 10. Proliferation of polyclonally stimulated T cells.....	67
Figure 11. Cytokine secretion of polyclonally stimulated T cells	68
Figure 12. Analysis of naturally occurring T _{reg} cells.....	70
Figure 13. Sensitivity of resting T cells to apoptosis.....	71
Figure 14. Sensitivity of activated T cells to apoptosis.....	73
Figure 15. Lung infiltration in allergic airway inflammation experiments	75
Figure 16. Histologic analysis of lung tissues in allergic airway inflammation experiments	76
Figure 17. Antibody response and T cell function after induction of allergic airway inflammation.....	77
Figure 18. Disease course of aGvHD.....	78
Figure 19. Body temperature and blood glucose levels in aGvHD.....	80
Figure 20. Development of subcutaneous tumours after inoculation of B16F10 melanoma cells	81
Figure 21. Development of subcutaneous tumours after inoculation of B16F10 melanoma cells in immunised mice	82

7.3 Acknowledgements

First and foremost, I would like to thank my supervisor Prof. Dr. Holger Reichardt for the opportunity to work in his group and for his continuous support during this and other projects. I am deeply grateful for the possibility to work independently but still being able to benefit from his broad scientific expertise and guidance whenever I needed it.

Next I wish to thank Prof. Dr. Heidi Hahn for the collaboration, for open-minded discussions about my project during and beyond committee meetings and for her enthusiasm which further encouraged me to perform investigations. I am also very grateful to Prof. Dr. Matthias Dobbelstein for being part of my thesis committee, for his interest in my projects as well as for his valuable scientific input.

Furthermore, I am indebted to several other members of the Institute of Human Genetics who helped me a lot during this project. Firstly, I owe thanks to Dr. Anja Uhmman for the introduction into the topic and for sharing data and information about the mouse model. I am also very thankful to Penelope Pelczar for the maintenance the mouse colony, for sharing experience about the B16 melanoma model and the B16F10 cell line itself. Additionally, my thanks go to Dr. Frauke Nitzki who provided me with several primers for qRT-PCR.

From the Department of Cellular and Molecular Immunology, I need to especially thank Dr. Kai Dittmann and Dr. Johannes Lutz for help getting into the project, for methodological support and for interesting discussions.

I also need to thank our technicians Amina Bassibas for too much to count and Julian Koch for animal transports and small favours.

Finally, my thanks go to current and past members of our lab especially to Jennifer, Anna, Xiao, Katharina, Elena and Carina (in order of appearance) for a good working atmosphere, out-of-lab activities and for keeping everything fun.

7.4 Curriculum vitæ

Personal Details

Name: Kai-David Michel
Date of birth: April 9th, 1980
Place of birth: Bad Kreuznach
Nationality: German
email: Kai.Michel.3@googlemail.com

Education and Employment

05/2009 – 05/2013 Doctoral thesis in the Department of Cellular and Molecular Immunology, University of Göttingen Medical School. Project: “Role of the Hedgehog receptor Patched1 in the development and function of T lymphocytes.”

10/2006 – 04/2008 Scientific employee at the Department of Dermatology, Johannes Gutenberg-University Mainz

12/2005 – 09/2006 Diploma thesis at the Department of Dermatology, Johannes Gutenberg-University Mainz. Project: “Investigations on the modulation of T cell responses with monoclonal antibodies in the humanised NOD/SCID mouse model.”

10/2000 – 11/2005 Study of biology at the Johannes Gutenberg-University Mainz

07/1990 – 05/1999 University entrance qualification at the Paul Schneider Secondary School, Meisenheim.

07/1986 – 05/1990 Primary School, Meisenheim

Stay abroad

04/2008 – 12/2008 Work and language stay in Australia, Southeast Asia and New Zealand

Compulsory military service

09/1999 – 07/2000 310th Maintenance Battalion in Montabaur and Kusel

Publications

Protection from graft-versus-host disease by HIV-1 envelope protein gp120-mediated activation of human CD4+CD25+ regulatory T cells. Becker C, Taube C, Bopp T, Becker C, Michel K, Kubach J, Reuter S, Dehzad N, Neurath MF, Reifenberg K, Schneider FJ, Schmitt E, Jonuleit H. *Blood*. 2009 Aug 6;114(6):1263-9.

Influence of short-term glucocorticoid therapy on regulatory T cells in vivo. Sbiera S, Dexneit T, Reichardt SD, Michel KD, van den Brandt J, Schmull S, Kraus L, Beyer M, Mlynski R, Wortmann S, Allolio B, Reichardt HM, Fassnacht M. *PLoS One*. 2011;6(9):e24345.

The hedgehog receptor Patched1 in T cells is dispensable for adaptive immunity in mice. Michel KD, Uhmann A, Dressel R, van den Brandt J, Hahn H, Reichardt HM. *PLoS One*. 2013;8(4):e61034.